Bioactive Nano-Fibrous Scaffolds for Bone and Cartilage Tissue Engineering

by

Kai Feng

A dissertation submitted in partial fulfillment
of the requirements for the degree of
Doctor of Philosophy
(Macromolecular Science and Engineering)
in The University of Michigan
2012

Doctoral Committee:
Professor Peter X. Ma, Chair
Professor Zhan Chen
Professor William V. Giannobile
Assistant Professor Kenichi Kuroda

To my parents and to myself

Acknowledgements

First of all, I would like to thank my advisor, Dr. Peter X. Ma, for his valuable mentorship, support and encouragement, without which over the years this graduation would not be possible. I would also like to express thanks and gratitude to my other dissertation committee members, Dr. William V. Giannobile, Dr. Zhan Chen, and Dr. Kenichi Kuroda for their contribution to my scientific training and growth.

Numerous thanks also go to past and present members in Ma lab (particularly Jianxiang zhang, Guobao Wei, Jiang Hu, Hongli Sun, zhanpeng zhang, Xiaohua Liu, Xiaobin Jin, Laura Smith, Ian Smith, Melanie Gupte, Jeremy Holzwarth, etc) members in Dr. Giannobile's lab (particularly Qiming Jin, Jim Sugai, Andrei Taut, Alexandra Plonka, etc) and UROP students who have worked for me. Because of all of you, this journal to a doctorate becomes more interesting. I would also like to thank our beloved Macromolecular science secretary Nonna Hamilton and Biological and material science secretary Elizabeth Rodriguiz for their help getting things going.

I am truly grateful to have the love and support that my family and friends have given me over the years. They have made my Ph. D journey a great experience and offered a major balance in my life.

Table of content

List of Figures

Figure

List of Tables

Tables

Abstract

Bioactive Nano-Fibrous Scaffolds for Bone and Cartilage Tissue Engineering

by

Kai Feng

Chair: Peter X. Ma

Scaffolds that can mimic the structural features of natural extracellular matrix and can deliver biomolecules in a controlled fashion may provide cells with a favorable microenvironment to facilitate tissue regeneration. Biodegradable nanofibrous scaffolds with interconnected pore network have previously been developed in our laboratory to mimic collagen matrix and advantageously support both bone and cartilage regeneration. This dissertation project aims to expand both the structural complexity and the biomolecule delivery capacity of such biomimetic scaffolds for tissue engineering.

We first developed a nanofibrous scaffold that can release an antibiotic (doxycycline) with a tunable release rate and a tunable dosage, which was demonstrated to be able to inhibit bacterial growth over a prolonged time period.

We then developed a nanofibrous tissue-engineering scaffold that can release basic fibroblast growth factor (bFGF) in a spatially and temporally controlled fashion. In a mouse subcutaneous implantation model, the bFGF-releasing scaffold was shown to

enhance cell penetration, tissue ingrowth and angiogenesis. It was also found that both the dose and the release rate of bFGF play roles in the biologic function of the scaffold.

After that, we developed a nanofibrous PLLA scaffold that can release both bone morphogenetic protein 7 (BMP-7) and platelet-derived growth factor (PDGF) with distinct dosages and release kinetics. It was demonstrated that BMP-7 and PDGF could synergistically enhance bone regeneration using a mouse ectopic bone formation model and a rat periodontal fenestration defect regeneration model. The regeneration outcome was dependent on the dosage, the ratio and the release kinetics of the two growth factors.

Last, we developed an anisotropic composite scaffold with an upper layer mimicking the superficial zone of cartilage and a lower layer mimicking the middle zone of cartilage. The thin superficial layer was fabricated using an electrospinning technique to support a more parallel ECM orientation to the cartilage surface. The lower layer was fabricated using a phase-separation technique to support a more isotropic ECM distribution. Human bone marrow-derived mesenchymal stem cells (hMSCs) were seeded on this complex scaffold and cultured under chondrogenic conditions. The results showed that the composite scaffold was indeed able to support anisotropic cartilage tissue structure formation.

Chapter 1

Introduction

Background and motivation

Organ failure and tissue loss resulting from trauma and diseases remain major healthcare challenges in the United States. About one half of the national medical spending is attributed to the treatment of organ failure and tissue loss with approximately 8 million surgeries and 40-90 million hospital days per year. [1-3] Although significant advances have been made in medical sciences and technologies, organ failure and tissue loss are still treated with transplantation. In 2008, 27,281 organ transplantation procedures were performed in the United States, while 100,597 patients were on waiting lists for organ transplantation. [4]There is a huge gap between the number of people on the waiting list and the available organ number, and many patients on the waiting list eventually die because of organ shortage. Besides donor shortage, there are additional problems. For example, bone grafts and metallic/ceramic implants are two major treatments to bone loss. In the U.S, approximately 90% of bone grafts are autografts and allografts. [5]Donor site morbidity and pathogen transmission are two major drawbacks associated with autografts and allografts, respectively. [6] Metallic/ceramic implants are different from native bone in structure and mechanical properties, often leading to additional bone damage. [7]

Tissue engineering is an interdisciplinary field that applies the principle of engineering and life science to aim at constructing biological substitutes to repair damaged tissue. In order to achieve satisfactory tissue regeneration, three key issues need to be considered: the isolation and cultivation of cells, the use of tissue-inductive biomolecules and the placement of cells in suitable scaffolds to support 3-D tissue regeneration. [2] In a traditional tissue engineering approach, cells are cultured and seeded on a scaffold and then implanted into the defect site to form new tissue. [2] In this approach, the cells provide the main source for new tissue regeneration. The scaffolds act as three-dimensional matrices for cell growth and degrade away as the tissues are regenerated.[8] Despite the encouraging early results[3, 9], the limited number of donor cells and low quality of regenerated tissues remained two hurdles in tissue engineering approach. [10] Scaffolds are required to provide additional functions besides providing structure support and suitable degradation kinetics. Another approach is to implant acellular scaffold in the defect site with the capability of delivering appropriate biomolecules in a controlled manner, thereby recruiting progenitor cells to the defect site and promoting cell proliferation and differentiation, inducing tissue regeneration. [2] Factor-releasing scaffolds are gaining popularity and have recently been used along with incorporated cells. [11-14]These scaffolds are often called bioactive scaffolds. [15, 16]

The main hypotheses of this thesis are: (1) controlled delivery of appropriate growth factors from nanofibrous scaffold will facilitate angiogenesis and osteogenesis leading to high quality bone regeneration; (2) the development of structural complexity in scaffolds to mimic complicated natural extracelluar matrices in terms of pore

morphology, fiber, size and orientation will facilitate complex tissue regeneration. The specific Aims of this thesis are listed below:

1. To fabricate 3D nanofibrous scaffolds with the capacity of delivering a single biomolecule such as an antibiotic or growth factor, characterize the *in vitro* release profiles, and evaluate the biological function of these released biomolecules both *in vitro* and *in vivo*. Specifically, we focus on doxycycline-delivering scaffold to inhibit bacterial growth *in vitro* and basic fibroblast growth factor (bFGF)-delivering scaffold to promote tissue ingrowth and angiogenesis *in vivo*.

2. To fabricate 3D nanofibrous scaffold with capacity of delivering two growth factors and evaluate the effects on bone tissue regeneration in vivo. Specifically, we focus on scaffolds releasing both bone morphogenetic protein 7 (BMP-7) and platelet-derived growth factor (PDGF). The biological function of these scaffolds in bone regeneration will be first examined in a mouse subcutaneous implantation model. Several scaffolds with different dosage ratios and release rates of BMP-7 and PDGF will be implanted and the *in vivo* bone regeneration will be evaluated to determine the optimal release rate and dosage for each growth factor to achieve the most synergetic effects. Then, the biological effectiveness of the scaffolds with the optimal dosage ratio and release rates of two growth factors will be evaluated using a periodontal bone defect repair model.

3. To fabricate a 3D nanofibrous composite scaffold containing two layers with different fiber and pore morphologies and examine the effect of this novel scaffold on complex tissue regeneration *in vitro*. Specifically, we will focus on the combination of

electrospinning and phase separation techniques to create composite scaffolds and examine the effects on chondrogenesis to zonal structure formation *in vitro*.

Dissertation overview

Chapter 2 provides a general literature review of the nanostructured biomaterials used in tissue regeneration. Emphasis is placed on two aspects: (1) nanofibrous scaffold fabrication techniques including electropsinning, self assembly and temperature induced phase separation, (2) growth factor delivery in various 3-D scaffolds.

Chapter 3 begins the research part of this thesis with the fabrication of novel antibacterial nanofibrous PLLA scaffolds. Here, antibiotic doxycycline is incorporated into PLGA nanospheres and the spheres are immobilized onto nanofibrous PLLA scaffolds. The release profiles of doxycycline from the scaffolds are examined and both short term and long term in vitro bacterial inhibition effect of the scaffolds are demonstrated. This work was published in *Journal of Controlled Release*. [17]

Chapter 4 details the development of basic fibroblast growth factor (bFGF)-containing nanospheres (NS) and their immobilization onto nanofibrous PLLA scaffolds. *In vitro* release profiles of bFGF from different PLGA nanospheres on the scaffolds are determined. Tissue ingrowth and angiogenesis into these scaffolds are studied in a subcutaneous implantation model.

Chapter 5 develops one single nano-fibrous scaffold capable of delivering two different growth factors (BMP-7and PDGF). The fabrication method is described. The

ectopic bone formation in scaffolds with different BMP-7/PDGF dosages and release rates is examined. Two week and five week bone regeneration on these dual release scaffolds is investigated using a rat periodontal defect model.

Chapter 6 creates an anisotropic composite scaffold to mimic zonal structure of cartilage tissue with a combination of electropinning and phase separation methods. *In-vitro* chondrogenesis of human bone marrow-derived mesenchymal stem cells (hMSCs) on this scaffold is studied.

The final chapter, chapter 7, summarizes the thesis work with major conclusions and discusses some possible future directions related to this dissertation.

References

1. Karp JM, Langer R: Development and therapeutic applications of advanced biomaterials. *Curr Opin Biotechnol* 2007, 18(5):454-459.

2. Langer R, Vacanti JP: Tissue Engineering. *Science* 1993, 260(5110):920-926.

3. Lysaght MJ, Hazlehurst AL: Tissue engineering: The end of the beginning. *Tissue Eng* 2004, 10(1-2):309-320.

4. 2009 Annual report of the U.S. organ Procurement and Transplantation network and the Scientific Registry of Transplant Recipients: Transplant Data 1999-2008. *Health resources and Services Administration, Healthcare Systems Bureau, Division of Transplantation: Rockville, MD* 2009.

5. Betz RR: Limitations of autograft and allograft: New synthetic solutions. *Orthopedics* 2002, 25(5):S561-S570.

6. Liu XH, Ma PX: Polymeric scaffolds for bone tissue engineering. *Ann Biomed Eng* 2004, 32(3):477-486.

7. Christenson EM, Anseth KS, van den Beucken L, Chan CK, Ercan B, Jansen JA, Laurencin CT, Li WJ, Murugan R, Nair LS *et al*: Nanobiomaterial applications in orthopedics. *J Orthop Res* 2007, 25(1):11-22.

8. Ma ZW, Kotaki M, Inai R, Ramakrishna S: Potential of nanofiber matrix as tissue-engineering scaffolds. *Tissue Eng* 2005, 11(1-2):101-109.

9. Lysaght MJ, Nguy NAP, Sullivan K: An economic survey of the emerging tissue engineering industry. *Tissue Eng* 1998, 4(3):231-238.

10. Bonassar LJ, Vacanti CA: Tissue engineering: The first decade and beyond. *J Cell Biochem* 1998:297-303.

11. Martins A, Duarte ARC, Faria S, Marques AP, Reis RL, Neves NM: Osteogenic induction of hBMSCs by electrospun scaffolds with dexamethasone release functionality. *Biomaterials* 2010, 31(22):5875-5885.

12. Moioli EK, Clark PA, Xin XJ, Lal S, Mao JJ: Matrices and scaffolds for drug delivery in dental, oral and craniofacial tissue engineering. *Adv Drug Deliv Rev* 2007, 59(4-5):308-324.

13. Murphy WL, Peters MC, Kohn DH, Mooney DJ: Sustained release of vascular endothelial growth factor from mineralized poly(lactide-co-glycolide) scaffolds for tissue engineering. *Biomaterials* 2000, 21(24):2521-2527.

14. Wang F, Li ZQ, Khan M, Tamama K, Kuppusamy P, Wagner WR, Sen CK, Guan JJ: Injectable, rapid gelling and highly flexible hydrogel composites as growth factor and cell carriers. *Acta Biomater* 2010, 6(6):1978-1991.

15. Porter JR, Ruckh TT, Popat KC: Bone Tissue Engineering: A Review in Bone Biomimetics and Drug Delivery Strategies. *Biotechnol Prog* 2009, 25(6):1539-1560.

16. Tabata Y: The importance of drug delivery systems in tissue engineering. *Pharmaceutical Science and Technology Today* 2000, 3(3):80-89.

17. Feng K, Sun HL, Bradley MA, Dupler EJ, Giannobile WV, Ma PX: Novel antibacterial nanofibrous PLLA scaffolds. *Journal of Controlled Release* 2010, 146(3):363-369.

Chapter 2

Nanostructured biomaterials and growth factor delivery scaffold

Introduction

Tissue engineering and Nanotechnology are two exciting science and engineering fields. They are both interdisciplinary among biology, chemistry, physics, material science and medical science, etc. Tissue engineering applies the principles of engineering and the life science to the fabrication and development of biological alternatives for harvested tissues and organ transplantation to restore, maintain or improve tissue function. [1] Three important factors exist in tissue engineering: cells, growth factors and biomaterials (scaffolds). Because cells need anchorage sites and specific environments for growth, biomaterials play a pivotal role in both in-vitro tissue culture and in vivo new tissue formation in tissue engineering. [2] They serve as matrices for cellular ingrowth, proliferation, differentiation into functional form, and new tissue formation in three dimensions and eventually disappear over time. [3, 4]

With the advances of nanotechnology, material design can be exploited into the nanometer scale($1nm=10^{-9}m$) and nano-structured biomaterials begin to emerge.[5] Among them, nano-fibrous biomaterials are exciting because their ability to the extracellular matrix (ECM), which contains abundant fibrous collagen proteins (50-500nm) [6-8] that regulates cell morphology, cytoskeletal structure and functionality. [9, 10] The collagen like fibrillar structure of the nanofibrous biomaterials along with their

high surface to volume ratio enhances cell adhesion,[6, 11-13] which in turn improve cell migration, proliferation, and differentiated function on these biomaterials. [14-16] Therefore, nanostructured biomaterials are becoming increasingly important in tissue engineering.

Various biomolecules have been successfully delivered from tissue engineering scaffolds. Growth factors (GFs) are one important group of such biomolecules. They are polypeptides that can modulate cellular growth, proliferation and cellular differentiation involved in the regeneration of new tissues. [17, 18]. In order to achieve efficient biological functions of GFs, the release of GFs from scaffolds should be in a controlled manner to reach suitable therapeutic dosage and duration. [19] The bioactivity of growth factors should be preserved after the incorporation within the scaffolds. The release should occur over a needed time period and the release should be localized to avoid potential side effects.

In this chapter we will discuss three cutting edge technologies to fabricate nanostructured biomaterials: Self assembly, Electrospinning, Phase separation. We will also discuss inorganic/organic nanocomposite biomaterials. Finally we will summarize current advances in technologies to incorporate growth factor delivery systems into three major types of scaffolds used in tissue engineering application including hydrogel scaffold, electrospun scaffold and three dimension (3D) porous scaffold.

Nanofibrous biomaterials

Self assembly

Molecular self assembly is defined as the spontaneous organization of molecules under thermodynamic equilibrium conditions into structurally well-defined and rather stable arrangements through a number of noncovalent interactions. [20-23] These interactions typically involve secondary bonding.[23]

Fields, Tirrell and co-workers have designed peptide-amphiphiles (PAs) molecules by self assembly to mimic the triple-helix super secondary structure of collagen molecules. The PA consists of a α1 (IV) 1263-1277 collagen sequence head group which is covalently linked to a mono- or di-alkyl ester lipid tail. [24-28] Later, Fields and co-workers also developed a chimeric PA incorporating a 21 residue angiogenesis-inducing peptide sequence (SPARC) to enhance cell proliferation and angiogenesis. [29]

Beyond this single molecular unit, nanofibrous materials can be made by self assembly too. Zhang, and co-workers synthesized ionic self-complementary oligopeptides with regular alternating ionic hydrophilic and hydrophobic residue peptides, which can form stable β-sheets.[30-32] When subjected to monovalent alkaline cations or physiological conditions, these oligopeptides can self assemble into macroscopic hydrogel structures which contain nanofibers about 10-20 nm in diameter. [33-35] It was found out that certain cells can attach to, proliferate and differentiate on this hydrogel. [30, 31]

Stupp and co-workers have synthesized peptide amphiphiles (PA) by living anionic polymerization that can self assemble to form nanofiber structure of a hydrogel. [36-38] The forming nanofibers have diameter approximately 5-8 nm and length up to several micrometers. [36, 37] In these nanofibers, the PA molecules are perpendicular to the fiber

axis, which is different from the natural collagen matrix having collagen molecules parallel to each other. [39]

In summary, self assembly peptide systems can generate nanofibers in the lowest end of natural extracellular matrix collagen fiber diameter range, while they are either single molecules or hydrogels.[39] Some properties need to be improved such as pore structure and material degradation rate control, cell-material interaction, mechanical strengthening.

Electrospinning

"Electrospinning" has existed in the literature for more than 100 years. [40] Recently, it has gained much more attention in biomedical engineering due to its ability to produce fibers whose diameters can be reduced to nanometer range.

The basic experimental setup of electrospinning includes: (1) applied voltage (2) grounded target collector (3) polymer reservoir with a spinneret. Once the applied electrical force overcomes the surface tension of the polymer solution or melt, a charged jet forms from the pendent solution surface called "Taylor's cone" [41] and travels in a straight line for a certain distance. Then, an electrically driven bending instability grows to cause the jet to bend and follow a whipping and spiraling path, which reduces the jet diameter. In the final stage, the solution jet evaporates, solidifies and is collected as a non-woven fiber mats on the stationary grounded collector [42-44]or rotating target if fiber orientation is needed.[45, 46]

Several natural biopolymers[46-49]and synthetic biodegradable polymers[50-56]have been successfully electrospun into nanofibrous scaffolds. The diameters of these

electrospun fibers can be down to nanometer size, while electrospun fibers of FDA approved biodegradable polymers usually have diameters in micrometer range[50, 52-54, 56]. However, the porosity of electrospun matrices is usually not very high and the pore shape is random.[57] A variety of cells were reported to attach and proliferate well on these scaffolds and some have been shown to differentiate into or maintain their functional phenotypes as well.[46, 52, 54, 56, 58-61] As fiber diameter decreases, cell interaction improves and immune response decreases. [62]

Though there are some untamed challenges with electrospinning technology such as difficulty to control pore size and shape and its low porosity, the simplicity makes it widely used to fabricate nanofibrous scaffolds.

Phase separation

As a scaffold fabrication method, phase separation is a process that a homogenous polymer solution system becomes thermodynamically unstable and phase separates into two phases in order to lower the system free energy under certain conditions. One phase is a polymer rich phase while the other is a polymer lean phase. After the solvent is removed, the polymer-rich phase solidifies.

Conventional phase separation process though very useful in fabricating porous membrane for filtration and separation, is not suitable for tissue scaffold fabrication. [63] So, Controlled phase separation, primarily thermally induced phase separation (TIPS) has been used to fabricate polymeric scaffolds for tissue engineering. [4, 64-71] Liquid-liquid phase separation, one of the TIPS, occurs when the crystallization temperature is much lower than the phase separation temperature. Combining liquid-liquid phase separation

with gelation process [72, 73], nanofibrous matrices mimicking natural type I collagen (Fig.2.1) were fabricated in our lab. The fibers diameters are ranged from 50 to 500 nm and the porosity of the matrices can be as high as 98%.[71] The morphology of the matrices is mainly determined by gelation condition, [4] while other processing parameters such as polymer molecular weight, polymer solution concentration, solvent exchange and quenching temperature will also affect the morphology of the matrices. [71] Open macropore (>100 μm) structure can be incorporated into nanofibrous matrices by combining porogen leaching technique or solid Freeform Fabrication techniques (SFF). Five steps are involved in the porogen leaching-phase separation process: Polymer dissolution, porogen assembly, polymer solution casting, phase- separation and gelation, porogen leaching. Porogens used in our lab are salt or sugar particle[71, 74], sugar fibers[71], sugar microspheres[75-77], paraffin microspheres[66]. These matrices have very low density and even higher porosity which contains both open pore structure and nanofibrous wall. (Fig.2.2) These macropores in the matrices facilitate cell seeding, cell migration inside and neovascularization after in vivo scaffold implantation.

Solid freeform fabrication (SFF) is a process that uses a computer aided design (CAD) program to create 3-D structured objects, while reversed SFF is used to design a 3-D negative mold which is then created layer-by-layer on a 3-D printer. Due to its ability to well control the scaffold geometric parameter such as external shape, pore geometries and pore interconnectivity, SFF has become more and more popular in scaffolding fabrication nowadays. [78, 79] Combining SFF and TIPS, nano-fibrous scaffold with complex geometry mimicking human organ can be fabricated. Nanofibrous human ear and mandible segment scaffolds were created from 3-D reconstruction of CT-scans or

histological section in our lab (Fig.2.3). Cell studies of MC3T3-E1 preosteoblasts showed significant better proliferation and higher expression of osteocalcin and bone sialoprotein mRNAs on NF scaffolds. [80]

Nanofibrous scaffolds have been shown to have better cell attachment than solid-walled scaffolds due to more cell adhesion proteins absorbance. [81] Osteoblasts were cultured on both nanofibrous and solid-walled PLLA scaffolds and cells on nanofibrous scaffolds showed higher alkaline phosphatase activity and an earlier and enhanced gene expression of the osteoblast phenotype. Biomineralization was 13-fold enhanced on nanofibrous scaffolds in terms of calcium content assay. Cell seeded on nanofibrous scaffolds sustained expression of α-2 integrin when the formation of collagen fibril by osteoblasts was inhibited, while cells seed on solid-walled scaffolds failed to do so. These results demonstrated that nanofibrous matrices processes some natural collagen fibers property and is a better scaffolding than solid-wall scaffolds for promoting osteoblast differentiation and biomineralization.[82]

In summary, TIPS does not involve complicated PA synthesis and purification processes as in self aasembly, nor does it require any facilities in electrospinning. However, it provides a great deal of control and diversity in the nanofibrous biomaterials fabricated from external shape to macropore structure and to fiber diameter. Their interconnected spherical macro-pore network promotes cell penetration. Their nanofibrous architecture mimics natural extracellular matrix to promote cell attachment, proliferation, differentiation of multiple cell types. [83-86] With these beneficial features, these three dimensional porous scaffolds have found applications in regeneration of various tissues. [86-90]

Nanocomposite biomaterials

The combination of improved mechanical properties and biocompatibility is the goal of nanocomposite biomaterials design. Bone, one of mineralized tissues in human body, is a perfect example of natural nanocomposite with nanometer sized platelike apatite crystals dispersed in collagen nanofibrous network. Its good mechanical property comes from both the nanometer feature of the collagen fiber and apatite crystal and composite organization of these two contents. [91, 92]

To mimic the nanoscale feature of mineral component of the bone, hydroxyaptite nanoparticle(nHAP), which is the major mineral phase in natural bone and has good osteoconductivity and bone bonding ability, was precipitated onto collagen to form a porous composite scaffold. [93, 94] Interfacial new bone formation by osteoblasts and composite degradation were observed on these composite scaffolds. [95, 96] In order to avoid pathogen transmission and immunorejection, synthetic biodegradable polymers were used as the organic component of the composite instead. By using TIPS, nHAP/poly(α -hydroxy acids) composite scaffolds with high porosity (>90%) were fabricated. By varying phase separation parameters, different morphology like tubular and platelet like can be achieved. If a dioxane/water mixture solvent system was used, nHAP-PLLA composite scaffold developed a nanofibrous morphology (shown in Fig 2.4) which greatly improve the mechanical properties and protein adsorption capacity of the scaffolds. [97] Fibronectin and vitronection adsorption was increased which is very important for preventing apatotic cell death in these composite scaffolds. [98] It is believed that nHAP increased hydrophilicity, surface roughness and total surface area which altogether increase protein adsorption and osteoblast adhesion. [99-101] When

macropores were introduced into the scaffold, bone-like apatite deposited onto the composite scaffold in a simulated body fluid (SBF) (Fig.2.5). The resulting composite scaffolds mimics bone matrix and is desirable for bone tissue engineering. [75]

Growth factor delivery scaffold

Growth factor delivery from hydrogel scaffold

Hydrogel scaffold are frequently used to engineer highly metabolic soft tissues, for which the load bearing capacity is less demanding but the high permeability of oxygen and nutrients are desirable. [102, 103]

Four major techniques have been applied to deliver growth factors from hydrogel scaffolds including: direct incorporation, microparticle encapsulation, covalent attachment and enzymatically cleavable tether attachment. [104]

The typical release profile of direct incorporation of growth factors into hydrogels consists of a rapid burst release during hydrogel initial swelling phase followed by an extended release of protein retarded by hydrogel polymer crosslink network. [105] Since a hydrogel contains more than 90% water in weight, the diffusion of incorporated growth factors is mainly determined by the growth factor size relative to chemical or physical crosslink density between polymer chains. [102, 106] Several attempts have been made to adjust crosslink density to alter these release profiles. [107-110] A slower release rate can be achieved by introducing charged polymers such as gelatin to interact with the incorporated growth factor (e.g., vascular endothelial growth factor, VEGF) via oppositely charged functional groups. [111] Concerns for this approach include the denature of growth factors due tochemical cross-linking if they are loaded into a hydrogel

before crosslinking or the uneven distribution of the growth factors if they are loaded into hydrogel after the cross-linking. [104]

Microparticle encapsulation system made from hydrophobic non-swelling polymers[112], solid lipids[113], hydrophilic polymers[105, 114]were incorporated into hydrogel system to further alter the release profile of growth factor from hydrogel scaffold. Transforming growth factor-beta-1 (TGF-β1) was encapsulated into hydrophilic cross-linked gelatin microparticles incorporated into hydrogels. The growth factor release profile depends on the degradation of the used micropartiles, which allow multiple growth factors to be released at distinct release rates by using different gelatin microparticles. [115]

Besides, growth factors can also be incorporated into hydrogels by covalent attachment [116, 117] and enzymatically cleavable tether attachment. [118, 119] In one example, basic fibroblast growth factor (bFGF) was successfully covalent bonded to PEG hydrogel. When covalently immobilized bFGF gradient was introduced, cells on the hydrogel aligned along the direction of increasing bFGF concentration. [116] These designed hydrogels with attached growth factors will be useful in many tissue engineering applications, while concerns about the stability of the attached growth factors remains. [104]

Growth factor delivery from electrospun scaffold

Due to their wide variety of material choices and fabrication simplicity, electrospun scaffolds have been applied in multiple types of tissues regeneration. [120-124]However,

this technique remains difficult to create macro-pore network and complex 3D shapes for large size tissue regeneration. [125-127]

In general, four major techniques have been used to incorporate growth factors into electrospun scaffolds, including physical adsorption [128, 129], blend electrospinning (emulsion electrospinning) [129-132], coaxial electrospinning [131, 133, 134], and covalent immobilization[135].

Physical adsorption is the easiest way to load growth factors into an electrospun scaffold, which is simply dip the scaffold into an aqueous growth factor aqueous solution. Bone morphogenic protein-2 (BMP-2) was incorporated into PLGA scaffolds using this method. [128, 129] The major disadvantage of this approach is the uncontrolled release profile and a very short release duration.

Blending electrospinning approach mixes growth factor within the polymer solution and electrospinning the mixed solution into a hybrid scaffold with growth factors localized within the fibers of the scaffold. This approach is also called " emulsion electrospinning" when growth factor is emulsified into polymer solution by ultra-sonication or homogenization. [136-139]Compared to physical adsorption, blend electrospinning approach usually results in a more sustained growth factor release from scaffold which can last over several weeks. A typical growth factor release profile from blend electrospun scaffold consists of an initial burst release followed a sustained release. [128, 140] BMP-2 and epidermal growth factor (EGF) were incorporated into scaffold using this approach. [129, 130, 132] The major disadvantage of this approach is the loss of bioactivity of the incorporated growth factors due to their conformational changes in the organic solution environment or under harsh mixing conditions. [141] Several

strategies have been applied to address this issue including addition of hydrophilic polymers such as poly(ethylene glyco) (PEG) in the aqueous growth factor solution to improve protein stability [130, 142]and addition of hydrophilic hydroxyapatite (HAP) particle to attach growth factors, reducing the damage of harsh electrospinning process. [129]

Coaxial electrospinning, also called co-electrospinning, can produce growth factor containing composite nano-fibers with core-shell structures by coaxially and simultaneously electrospinning a growth factor solution and a polymer solution through different feeding capillary channels in one needle. [143, 144] The growth factor release profile from coaxial electrospun scaffolds is similar to that from blend electrospun scaffolds, consisting of two stages. [131] However, the burst release is significantly lower and the release duration is prolonged, [145, 146]because the growth factors are mainly incorporated and distributed in the core part. The polymer shell provides a barrier membrane that controls the protein diffusion rate. [145]Introduction of porogens in the polymer shell is able to further adjust the growth factor release profile from the coaxial electrospun scaffold. [147]Platelet-derived growth factor-b (PDGF-bb) [133, 134], nerve growth factor (NGF) [148] and fibroblast growth factor (FGF) [131] have been encapsulated in coaxially electrospun scaffolds.

Covalent immobilization introduces chemical bond to immobilize growth factors on the electrospun fiber surface. Epidermal growth factor (EGF) was delivered from electrospun scaffold using this strategy. [135] Due to its technical complexity and possible loss of scaffold uniformity, it has not been a routine approach to delivery growth factors from electrospun scaffolds.

Besides these four major approaches discussed above, microsphere(MS)/nanosphere (NS) encapsulation were also explored to deliver growth factor from electrospun scaffolds. However, this method is uncommon due to technique difficulty associated with electrospun scaffold's limited pore size. Electrosprying and electrospinning techniques were combined to incorporate insulin-like growth factor-containing MS into an electrospun PLGA nanofibrous scaffold. [149] In another case, a poly(caprolactone) (PCL) jet and a poly(ethylene oxide) (PEO) jet with pre-fabricated MS were both electrospun onto a common mandrel and the MS were entrapped within the PCL scaffold after PEO was removed. [150]

Growth factor delivery from three dimensional (3-D) porous scaffold

Several techniques have been applied to incorporate and deliver growth factor from three dimensional (3-D) porous scaffolds, including direct encapsulation, passive absorption, coating and microsphere (MS)/nanosphere (NS) encapsulation.

Osteotropic factors were mixed with PLGA emulsion and directly encapsulated inside PLGA porous scaffold walls during an emulsion freeze-drying scaffold fabrication process. [151] Bone morphogenetic protein-2 released from such scaffold enhanced ectopic bone formation in rats. [152] While it combined the scaffold fabrication and growth factor incorporation into one single step, however, the scaffolds' structure, mechanical properties are altered and growth factor release rate depends on scaffold bulk degradation rates which may not be ideal for some tissue engineering applications. In an alternative method, pre-fabricated porous scaffold was immersed in a protein solution to passively absorb the proteins on the surface of scaffold. [153] However, the release

profile of growth factor from a scaffold is not controlled, resulting in a very short release period. The growth factors are not protected, resulting in their denaturation and failure to achieve the desired biological effects. [153] Polymer emulsion coating method is also used to coat growth factors on the surface of pre-fabricated porous scaffold. The bioactivity of the growth factor is protected and the release time period is extended by the introduction of a protective polymer layer. However, the porous structure of the scaffold is altered by the coating process. [154, 155]

In order to overcome these shortcomings associated with the above discussed methods of growth factor incorporation into scaffolds, our lab developed techniques to encapsulate growth factors into polymer microsphere (MS)/nanosphere (NS) and then to immobilize these spheres onto the nanofibrous pore surface of pre-fabricated scaffolds.[156, 157] The typical procedures contain two steps: First, an aqueous growth factor solution is mixed with a PLGA polymer solution to encapsulate growth factor domains into PLGA spheres using a water-in-oil-in-water double emulsion process. [158, 159] The sphere size ranges from nanometers to micrometer depending on the emulsion process parameters such as surfactant concentration and emulsion strength applied. [160] Then these obtained growth factor-containing PLGA MS/NS are immobilized onto the inner nanofibrous pore surface of a pre-fabricated scaffold using a post-seeding method.[156, 157] This novel MS/NS encapsulation method offers several advantages over other scaffold growth factor delivery systems. First, the scaffold fabrication process is separated from the growth factor incorporation process. Thus, the macro-porous architecture, the mechanical and degradation properties of the scaffold are not altered. The release of growth factors and the degradation of the scaffold can be individually

optimized. Second, polymeric MS/NS have been widely applied to encapsulate bioactive molecules and their ability to protect the encapsulated bioactive molecules from denaturation and degradation has been demonstrated. [161, 162] Third, the release of growth factors released from the scaffolds are in a temporally controlled fashion, which is primarily determined by the chemical and degradation properties of MS/NS polymer formulation. The release of the encapsulated proteins takes two phases, with the first phase mainly controlled by diffusion and the second phase mainly controlled by polymer degradation. Various release duration from several days to months can be easily achieved by adjusting polymer formulations such as PLGA copolymer LA/GA ratio or/and the molecular weight of the copolymer, showed in Fig.2.6. Fourth, the immobilization of MS/NS on porous NF scaffolds can reduce the burst release of growth factors and prolong the release duration. [156]

Summary

Although nanostructured biomaterials are relatively new scientific and engineering field, they have developed rapidly over recent years. Nanofibrous biomaterials, nanocomposite biomaterials, micro- and nanospheres discussed herein and have had significant impacts on the tissue engineering and regenerative medicine fields. In literature, electrospinning and phase separation techniques have been used individually to fabricate nanofibrous scaffolds. In this thesis, a new nanofibrous scaffold will be fabricated using the combination of these two techniques to mimic more complex tissue structure, which will be discussed in Chapter 6. In literature, single growth factor has been released from nanofibrous PLLA nanofibrous scaffold. In this thesis, release of

small molecule drugs from nanofibrous scaffold will be discussed in Chapter 3 and dual release of growth factors from nanofibrous scaffold will be discussed in Chapter5.

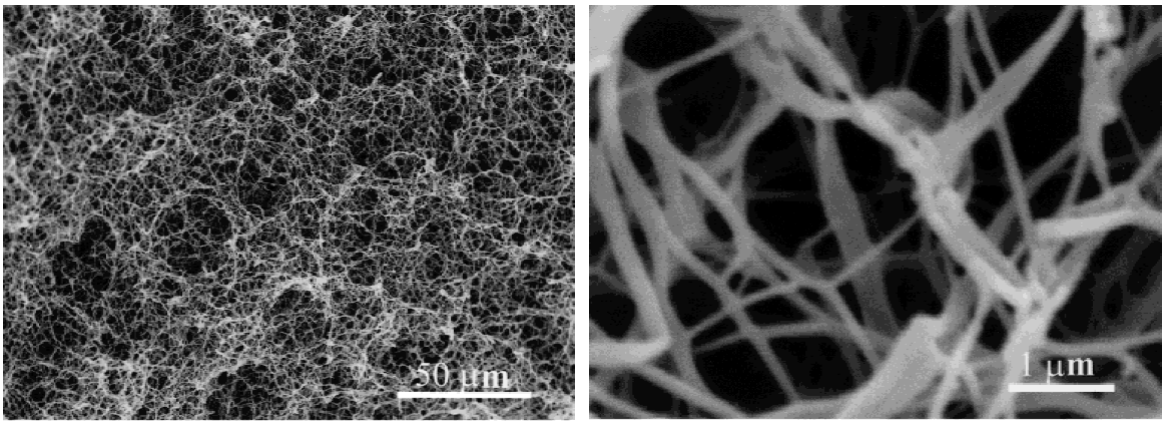

Fig.2.1. SEM micrographs of a PLLA fibrous matrix SEM micrographs of a PLLA fibrous matrix prepared from 2.5% (wt/v) PLLA/THF solution at a gelation temperature of 8°C: (a) ×500; (b) ×20K. Ma and Zhang, J. Biomed.Mater.Res.46,66(1999). © 1999, John Wiley & Sons.

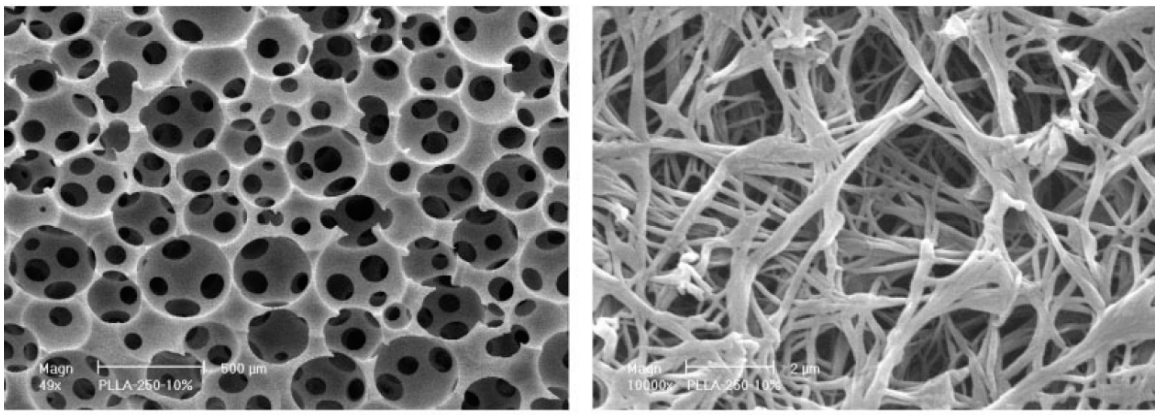

(e) (f)

Fig.2.2. Fabrication process of sugar sphere template leaching and thermally induced phase separation technique, shown by SEM micrographs: (e, f) 3D macroporous and nanofibrous scaffold at low (×50) and high (×10,000) magnifications. Wei and Ma, J. Biomed.Mater.Res.78,307(2006). © 2006, John Wiley & Sons.

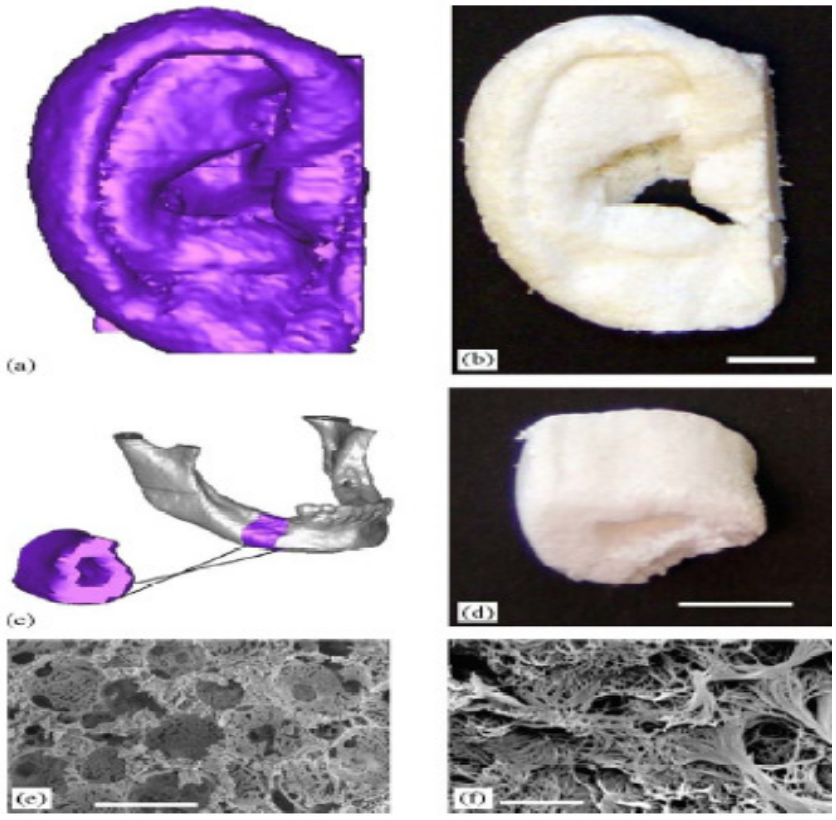

Fig.2.3. Scaffolds created from 3-D reconstructions of CT-scans or histological sections. (a) Human ear reconstruction from histological sections and (b) the resulting NF scaffold (scale bar; 10 mm), (c) human mandible reconstruction from CT-scans. Purple segment shows the reversed image of the bone fragment to be engineered, (d) resulting NFscaffold of the mandible segment (scale bar; 10 mm), (e) SEM micrographs of the interconnected spherical pores within the mandible segment (scale bar; 500 mm), and (f) the NF pore morphology of a spherical pore (scale bar; 5 mm). Chen,Smith and Ma, Biomaterials 27,3976(2006). © 2006,Elsevier Ltd.

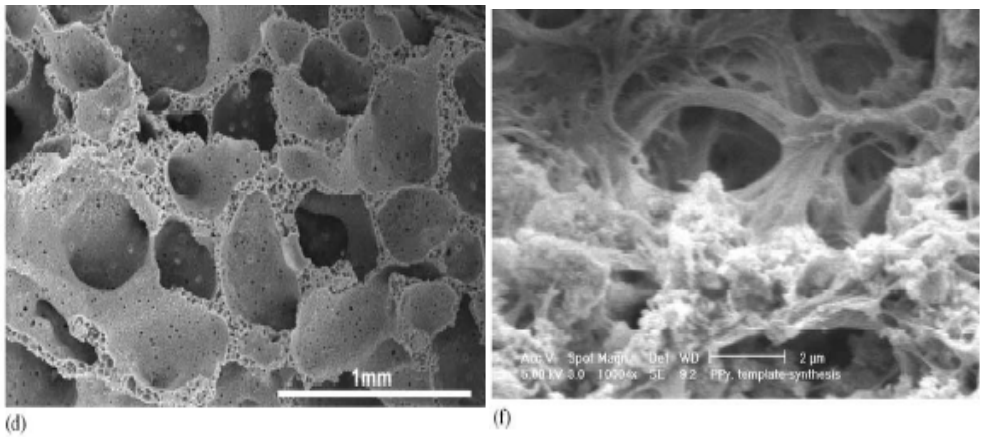

Fig.2.4. SEM micrographs of NHAP/PLLA (30:70) scaffolds fabricated using dioxane/water mixture solvents. (d,f) Dioxane:water=87:13, ×45, ×10000. Guo, Ma, Biomaterials 25,4749(2004). © 2006, Elsevier Ltd.

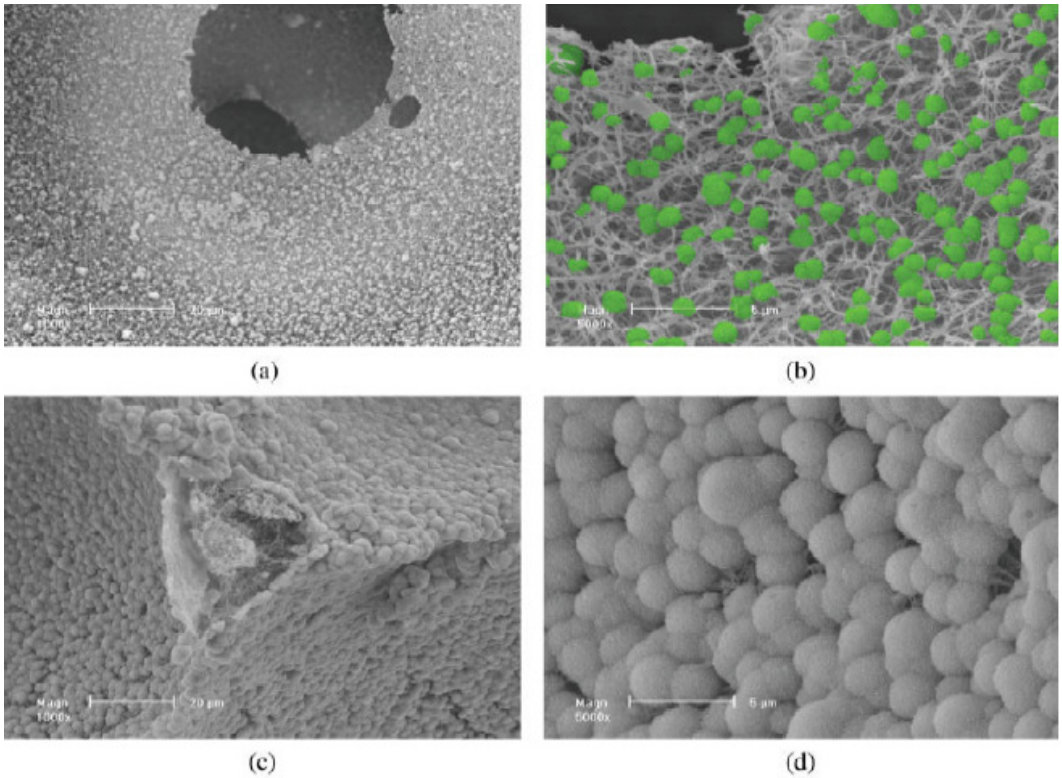

Fig. 2.5. SEM micrographs of nanofibrous PLLA/nHAP (90:10) composite scaffolds incubated in ×1.5 SBF for varying times. (a, b) 4 days [(b) is a portion of (a) at a higher magnification in which the newly formed bone-like apatite is colored green]; (c, d) 30 days. Guo, Ma, J.Biomed Mater Res 78A,306(2006). © 2006,Wiley Periodicals, Ltd.

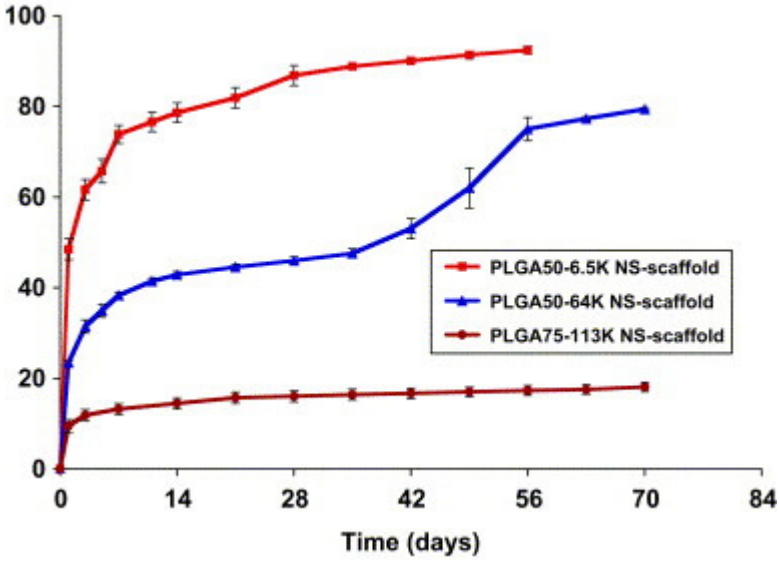

Fig. 2.6. *In vitro* release kinetics of rhBMP-7 from nanospheres immobilized on nanofibrous scaffolds in 10 mM PBS. Three distinct rhBMP-7 release profiles were achieved with NS composed of different PLGA formulations. (PLGA50-6.5K: LA/GA ratio: 50/50, Mw:6.5K; PLGA50-64K: LA/GA ratio: 50/50, Mw:64K; PLGA75-113K; LA/GA ratio:75/25, Mw:113K) [157] Reproduced with permission from Elsevier.

References

1. Langer R, Vacanti JP: Tissue engineering. *Science (Washington, DC, United States)* 1993, 260(5110):920-926.

2. Griffith LG, Naughton G: Bodybuilding: The bionic human: Tissue engineering - current challenges and expanding opportunities. *Science (Washington, DC, United States)* 2002, 295(5557):1009-1010, 1012-1014.

3. Hubbell JA: Biomaterials in tissue engineering. *Bio/technology (Nature Publishing Company)* 1995, 13(6):565-576.

4. Ma PX, Zhang R: Synthetic nanoscale fibrous extracellular matrix. *Journal of Biomedical Materials Research* 1999, 46(1):60-72.

5. Thomas V, Dean DR, Vohra YK: Nanostructured biomaterials for regenerative medicine. *Current Nanoscience* 2006, 2(3):155-177.

6. Elsdale T, Bard J: Collagen substrata for studies on cell behavior. *Journal of Cell Biology* 1972, 54(3):626-637.

7. E.D.Hay: Cell Biology of Extracellular Matrix, Secon ed. New York: Plenum Press; 1991.

8. Tan W, Krishnaraj R, Desai TA: Evaluation of nanostructured composite collagen-chitosan matrices for tissue engineering. *Tissue Engineering* 2001, 7(2):203-210.

9. Desai TA: Micro- and nanoscale structures for tissue engineering constructs. *Medical engineering & physics* 2000, 22(9):595-606.

10. B.Alberts AJ, J.Lewis, M.Raff, K. Roberts, and P.Walter: Molecular Biology of the cell. Garland, New York; 2002.

11. Strom SC, Michalopoulos G: Collagen as a substrate for cell growth and differentiation. *Methods in Enzymology* 1982, 82(Struct. Contract. Proteins, Pt. A):544-555.

12. Grinnell F, Bennett MH: Ultrastructural studies of cell--collagen interactions. *Methods in enzymology* 1982, 82 Pt A:535-544.

13. P.X.Ma RL, in: M. Yarmush, J. Morgan (Eds.). In: *Tissue Engineering Methods and Protocols.* Totowa, NJ: Humana Press, Inc; 1999: 47-56.

14. Folkman J, Moscona A: Role of cell shape in growth control. *Nature* 1978, 273(5661):345-349.

15. Palecek SP, Loftus JC, Ginsberg MH, Lauffenburger DA, Horwitz AF: Integrin-ligand binding properties govern cell migration speed through cell-substratum adhesiveness. *Nature* 1997, 385(6616):537-540.

16. Benya PD, Shaffer JD: Dedifferentiated chondrocytes reexpress the differentiated collagen phenotype when cultured in agarose gels. *Cell* 1982, 30(1):215-224.

17. Babensee JE, McIntire LV, Mikos AG: Growth factor delivery for tissue engineering. *Pharm Res* 2000, 17(5):497-504.

18. Chen FM, Zhang M, Wu ZF: Toward delivery of multiple growth factors in tissue engineering. *Biomaterials* 2010, 31(24):6279-6308.

19. Luginbuehl V, Meinel L, Merkle HP, Gander B: Localized delivery of growth factors for bone repair. *Eur J Pharm Biopharm* 2004, 58(2):197-208.

20. Ball P: Materials science. Polymers made to measure. *Nature* 1994, 367(6461):323-324.

21. Lehn JM: Supramolecular chemistry. *Science (Washington, DC, United States)* 1993, 260(5115):1762-1763.

22. Whitesides GM, Mathias JP, Seto CT: Molecular self-assembly and nanochemistry: a chemical strategy for the synthesis of nanostructures. *Science (Washington, DC, United States)* 1991, 254(5036):1312-1319.

23. Zhang S: Emerging biological materials through molecular self-assembly. *Biotechnology Advances* 2002, 20(5-6):321-339.

24. Berndt P, Fields GB, Tirrell M: Synthetic lipidation of peptides and amino acids: monolayer structure and properties. *Journal of the American Chemical Society* 1995, 117(37):9515-9522.

25. Fields GB, Lauer JL, Dori Y, Forns P, Yu Y-C, Tirrell M: Proteinlike molecular architecture: biomaterial applications for inducing cellular receptor binding and signal transduction. *Biopolymers* 1998, 47(2):143-151.

26. Haverstick K, Pakalns T, Yu Y-C, McCarthy JB, Fields GB, Tirrell M: Targeted cell interactions with surfaces incorporating synthetic peptide amphiphiles. *Polymeric Materials Science and Engineering* 1997, 77:584-585.

27. Yu YC, Roontga V, Daragan VA, Mayo KH, Tirrell M, Fields GB: Structure and dynamics of peptide-amphiphiles incorporating triple-helical proteinlike molecular architecture. *Biochemistry* 1999, 38(5):1659-1668.

28. Yu Y-C, Tirrell M, Fields GB: Minimal Lipidation Stabilizes Protein-Like Molecular Architecture. *Journal of the American Chemical Society* 1998, 120(39):9979-9987.

29. Malkar NB, Lauer-Fields JL, Juska D, Fields GB: Characterization of Peptide-Amphiphiles Possessing Cellular Activation Sequences. *Biomacromolecules* 2003, 4(3):518-528.

30. Holmes TC, De Lacalle S, Su X, Liu G, Rich A, Zhang S: Extensive neurite outgrowth and active synapse formation on self-assembling peptide scaffolds. *Proceedings of the National Academy of Sciences of the United States of America* 2000, 97(12):6728-6733.

31. Zhang S, Holmes TC, DiPersio CM, Hynes RO, Su X, Rich A: Self-complementary oligopeptide matrixes support mammalian cell attachment. *Biomaterials* 1995, 16(18):1385-1393.

32. Zhang S, Holmes T, Lockshin C, Rich A: Spontaneous assembly of a self-complementary oligopeptide to form a stable macroscopic membrane. *Proceedings of the National Academy of Sciences of the United States of America* 1993, 90(8):3334-3338.

33. Marini DM, Hwang W, Lauffenburger DA, Zhang S, Kamm RD: Left-Handed Helical Ribbon Intermediates in the Self-Assembly of a b-Sheet Peptide. *Nano Letters* 2002, 2(4):295-299.

34. Leon EJ, Verma N, Zhang S, Lauffenburger DA, Kamm RD: Mechanical properties of a self-assembling oligopeptide matrix. *Journal of Biomaterials Science, Polymer Edition* 1998, 9(3):297-312.

35. Caplan MR, Moore PN, Zhang S, Kamm RD, Lauffenburger DA: Self-Assembly of a b-Sheet Protein Governed by Relief of Electrostatic Repulsion Relative to van der Waals Attraction. *Biomacromolecules* 2000, 1(4):627-631.

36. Hartgerink JD, Beniash E, Stupp SI: Peptide-amphiphile nanofibers: a versatile scaffold for the preparation of self-assembling materials. *Proceedings of the National Academy of Sciences of the United States of America* 2002, 99(8):5133-5138.

37. Hartgerink JD, Beniash E, Stupp SI: Self-assembly and mineralization of peptide-amphiphile nanofibers. *Science (Washington, DC, United States)* 2001, 294(5547):1684-1688.

38. Stupp SI, LeBonheur V, Walker K, Li LS, Huggins KE, Keser M, Amstutz A: Supramolecular materials: self-organized nanostructures. *Science (Washington, D C)* 1997, 276(5311):384-389.

39. Smith LA, Ma PX: Nano-fibrous scaffolds for tissue engineering. *Colloids and Surfaces, B: Biointerfaces* 2004, 39(3):125-131.

40. Morton WJ: Method of Dispersing Fluids. In. US; 1902.

41. Taylor GI: Electrically driven jets. *Proc R Soc London,Ser A* 1969(313):453-475.

42. Deitzel JM, Kosik W, McKnight SH, Beck Tan NC, DeSimone JM, Crette S: Electrospinning of polymer nanofibers with specific surface chemistry. *Polymer* 2001, 43(3):1025-1029.

43. Jaeger R, Bergshoef MM, Martin i Batlle C, Schoenherr H, Vancso GJ: Electrospinning of ultrathin polymer fibers. *Macromolecular Symposia* 1998, 127(Rolduc Polymer Meeting 10: \"Petro\" Polymers vs. \"Green\" Polymers, 1997):141-150.

44. Reneker DH, Chun I: Nanometer diameter fibers of polymer, produced by electrospinning. *Nanotechnology* 1996, 7(3):216-223.

45. A Theron EZaALY: Electrostatic field-assisted alignment of electrospun nanofibres. *Nanotechnology* 2001, 12(3):384-390.

46. Matthews JA, Wnek GE, Simpson DG, Bowlin GL: Electrospinning of Collagen Nanofibers. *Biomacromolecules* 2002, 3(2):232-238.

47. Jin H-J, Fridrikh SV, Rutledge GC, Kaplan DL: Electrospinning Bombyx mori Silk with Poly(ethylene oxide). *Biomacromolecules* 2002, 3(6):1233-1239.

48. Li M, Mondrinos MJ, Gandhi MR, Ko FK, Weiss AS, Lelkes PI: Electrospun protein fibers as matrices for tissue engineering. *Biomaterials* 2005, 26(30):5999-6008.

49. Wnek GE, Carr ME, Simpson DG, Bowlin GL: Electrospinning of Nanofiber Fibrinogen Structures. *Nano Letters* 2003, 3(2):213-216.

50. Inai R, Kotaki M, Ramakrishna S: Structure and properties of electrospun PLLA single nanofibres. *Nanotechnology* 2005, 16(2):208-213.

51. Osanai Y, Kwon OH, Uyama H: Preparation of rapidly degradable poly(L-lactic acid) nanofiber non-woven mat via electrospinning. *Abstracts of Papers, 229th ACS National Meeting, San Diego, CA, United States, March 13-17, 2005* 2005:POLY-266.

52. Yang F, Murugan R, Wang S, Ramakrishna S: Electrospinning of nano/micro scale poly(L-lactic acid) aligned fibers and their potential in neural tissue engineering. *Biomaterials* 2005, 26(15):2603-2610.

53. Boland ED, Wnek GE, Simpson DG, Pawlowski KJ, Bowlin GL: Tailoring tissue engineering scaffolds using electrostatic processing techniques: a study of poly(glycolic acid) electrospinning. *Journal of Macromolecular Science, Pure and Applied Chemistry* 2001, A38(12):1231-1243.

54. Li W-J, Laurencin CT, Caterson EJ, Tuan RS, Ko FK: Electrospun nanofibrous structure: A novel scaffold for tissue engineering. *Journal of Biomedical Materials Research* 2002, 60(4):613-621.

55. Zong X, Ran S, Kim K-S, Fang D, Hsiao BS, Chu B: Structure and Morphology Changes during in Vitro Degradation of Electrospun Poly(glycolide-co-lactide) Nanofiber Membrane. *Biomacromolecules* 2003, 4(2):416-423.

56. Yoshimoto H, Shin YM, Terai H, Vacanti JP: A biodegradable nanofiber scaffold by electrospinning and its potential for bone tissue engineering. *Biomaterials* 2003, 24(12):2077-2082.

57. Boland Eugene D, Coleman Branch D, Barnes Catherine P, Simpson David G, Wnek Gary E, Bowlin Gary L: Electrospinning polydioxanone for biomedical applications. *Acta biomaterialia* 2005, 1(1):115-123.

58. Sanders EH, Kloefkorn R, Bowlin GL, Simpson DG, Wnek GE: Two-Phase Electrospinning from a Single Electrified Jet: Microencapsulation of Aqueous Reservoirs in Poly(ethylene-co-vinyl acetate) Fibers. *Macromolecules* 2003, 36(11):3803-3805.

59. Shin M, Ishii O, Sueda T, Vacanti JP: Contractile cardiac grafts using a novel nanofibrous mesh. *Biomaterials* 2004, 25(17):3717-3723.

60. Shields KJ, Beckman MJ, Bowlin GL, Wayne JS: Mechanical Properties and Cellular Proliferation of Electrospun Collagen Type II. *Tissue Engineering* 2004, 10(9/10):1510-1517.

61. Jin H-J, Chen J, Karageorgiou V, Altman Gregory H, Kaplan David L: Human bone marrow stromal cell responses on electrospun silk fibroin mats. *Biomaterials* 2004, 25(6):1039-1047.

62. Sanders JE, Stiles CE, Hayes CL: Tissue response to single-polymer fibers of varying diameters: evaluation of fibrous encapsulation and macrophage density. *Journal of Biomedical Materials Research* 2000, 52(1):231-237.

63. Ma PX: Scaffolds for tissue fabrication. *Materials Today (Oxford, United Kingdom)* 2004, 7(5):30-40.

64. Lo H, Ponticiello MS, Leong KW: Fabrication of controlled release biodegradable foams by phase separation. *Tissue Engineering* 1995, 1(1):15-28.

65. Ma PX, Zhang R: Microtubular architecture of biodegradable polymer scaffolds. *Journal of Biomedical Materials Research* 2001, 56(4):469-477.

66. Chen VJ, Ma PX: Nano-fibrous poly(l-lactic acid) scaffolds with interconnected spherical macropores. *Biomaterials* 2004, 25(11):2065-2073.

67. Zhang R, Ma PX: Poly(a-hydroxy acids)/hydroxyapatite porous composites for bone-tissue engineering. I. Preparation and morphology. *Journal of Biomedical Materials Research* 1999, 44(4):446-455.

68. Schugens C, Maquet V, Grandfils C, Jerome R, Teyssie P: Polylactide macroporous biodegradable implants for cell transplantation. II. Preparation of polylactide foams by liquid-liquid phase separation. *Journal of Biomedical Materials Research* 1996, 30(4):449-461.

69. Nam YS, Park TG: Porous biodegradable polymeric scaffolds prepared by thermally induced phase separation. *Journal of Biomedical Materials Research* 1999, 47(1):8-17.

70. Zhang R, Ma PX: Porous poly(L-lactic acid)/apatite composites created by biomimetic process. *Journal of Biomedical Materials Research* 1999, 45(4):285-293.

71. Zhang R, Ma PX: Synthetic nano-fibrillar extracellular matrixes with predesigned macroporous architectures. *Journal of Biomedical Materials Research* 2000, 52(2):430-438.

72. van de Witte P, Dijkstra PJ, van den Berg JWA, Feijen J: Phase separation processes in polymer solutions in relation to membrane formation. *Journal of Membrane Science* 1996, 117(1-2):1-31.

73. J.M.Guenet: Thermoreversible Gelation of Polymers and Biopolymers. London, San diego: Academic Press; 1992.

74. Mikos AG, Thorsen AJ, Czerwonka LA, Bao Y, Langer R, Winslow DN, Vacanti JP: Preparation and characterization of poly(L-lactic acid) foams. *Polymer* 1994, 35(5):1068-1077.

75. Wei G, Ma PX: Macroporous and nanofibrous polymer scaffolds and polymer/bone-like apatite composite scaffolds generated by sugar spheres. *Journal of Biomedical Materials Research, Part A* 2006, 78A(2):306-315.

76. Wei G, Jin Q, Giannobile WV, Ma PX: Nano-fibrous scaffold for controlled delivery of recombinant human PDGF-BB. *Journal of Controlled Release* 2006, 112(1):103-110.

77. Liu X, Smith L, Wei G, Won Y, Ma PX: Surface engineering of nano-fibrous poly(L-lactic acid) scaffolds via self-assembly technique for bone tissue engineering. *Journal of Biomedical Nanotechnology* 2005, 1(1):54-60.

78. Chu TMG, Halloran JW, Hollister SJ, Feinberg SE: Hydroxyapatite implants with designed internal architecture. *Journal of Materials Science: Materials in Medicine* 2001, 12(6):471-478.

79. Yang S, Leong K-F, Du Z, Chua C-K: The design of scaffolds for use in tissue engineering. Part II. Rapid prototyping techniques. *Tissue Engineering* 2002, 8(1):1-11.

80. Chen VJ, Smith LA, Ma PX: Bone regeneration on computer-designed nano-fibrous scaffolds. *Biomaterials* 2006, 27(21):3973-3979.

81. Woo KM, Chen VJ, Ma PX: Nano-fibrous scaffolding architecture selectively enhances protein adsorption contributing to cell attachment. *Journal of Biomedical Materials Research, Part A* 2003, 67A(2):531-537.

82. Woo KM, Jun J-H, Chen VJ, Seo J, Back J-H, Ryoo H-M, Kim G-S, Somerman MJ, Ma PX: Nano-fibrous scaffolding promotes osteoblast differentiation and biomineralization. *Biomaterials* 2007, 28:335-343.

83. Chen VJ, Ma PX: The effect of surface area on the degradation rate of nano-fibrous poly(L-lactic acid) foams. *Biomaterials* 2006, 27(20):3708-3715.

84. Woo KM, Chen VJ, Jung HM, Kim TI, Shin HI, Baek JH, Ryoo HM, Ma PX: Comparative Evaluation of Nanofibrous Scaffolding for Bone Regeneration in Critical-Size Calvarial Defects. *Tissue Eng Part A* 2009, 15(8):2155-2162.

85. Woo KM, Chen VJ, Ma PX: Nano-fibrous scaffolding architecture selectively enhances protein adsorption contributing to cell attachment. *J Biomed Mater Res Part A* 2003, 67A(2):531-537.

86. Woo KM, Jun JH, Chen VJ, Seo JY, Baek JH, Ryoo HM, Kim GS, Somerman MJ, Ma PX: Nano-fibrous scaffolding promotes osteoblast differentiation and biomineralization. *Biomaterials* 2007, 28(2):335-343.

87. Hu J, Feng K, Liu XH, Ma PX: Chondrogenic and osteogenic differentiations of human bone marrow-derived mesenchymal stem cells on a nanofibrous scaffold with designed pore network. *Biomaterials* 2009, 30(28):5061-5067.

88. Smith LA, Liu XH, Hu J, Ma PX: The influence of three-dimensional nanofibrous scaffolds on the osteogenic differentiation of embryonic stem cells. *Biomaterials* 2009, 30(13):2516-2522.

89. Smith LA, Liu XH, Hu J, Wang P, Ma PX: Enhancing Osteogenic Differentiation of Mouse Embryonic Stem Cells by Nanofibers. *Tissue Eng Part A* 2009, 15(7):1855-1864.

90. Sun HL, Feng K, Hu J, Soker S, Atala A, Ma PX: Osteogenic differentiation of human amniotic fluid-derived stem cells induced by bone morphogenetic protein-7 and enhanced by nanofibrous scaffolds. *Biomaterials* 2010, 31(6):1133-1139.

91. Rho JY, Kuhn-Spearing L, Zioupos P: Mechanical properties and the hierarchical structure of bone. *Medical engineering & physics* 1998, 20(2):92-102.

92. Landis WJ: The strength of a calcified tissue depends in part on the molecular structure and organization of its constituent mineral crystals in their organic matrix. *Bone (New York, NY, United States)* 1995, 16(5):533-544.

93. Wang RZ, Cui FZ, Lu HB, Wen HB, Ma CL, Li HD: Synthesis of nanophase hydroxyapatite/collagen composite. *Journal of Materials Science Letters* 1995, 14(7):490-492.

94. Du C, Cui FZ, Zhu XD, De Groot K: Three-dimensional nano-HAp/collagen matrix loading with osteogenic cells in organ culture. *Journal of Biomedical Materials Research* 1999, 44(4):407-415.

95. Du C, Cui FZ, Feng QL, Zhu XD, de Groot K: Tissue response to nano-hydroxyapatite/collagen composite implants in marrow cavity. *Journal of Biomedical Materials Research* 1998, 42(4):540-548.

96. Cui FZ, Du C, Su XW, Zhu XD, Zhao NM: Biodegradation of a nano-hydroxyapatite/collagen composite by peritoneal monocyte-macrophages. *Cells and Materials* 1996, 6(1-3):31-44.

97. Wei G, Ma PX: Structure and properties of nano-hydroxyapatite/polymer composite scaffolds for bone tissue engineering. *Biomaterials* 2004, 25(19):4749-4757.

98. Woo KM, Zhang R, Deng H, Ma PX: Highly porous biodegradable polymer/hydroxyapatite composite scaffolds enhance protein adsorption and osteoblast survival. *Abstracts of Papers, 222nd ACS National Meeting, Chicago, IL, United States, August 26-30, 2001* 2001:MACR-030.

99. Webster TJ, Schadler LS, Siegel RW, Bizios R: Mechanisms of enhanced osteoblast adhesion on nanophase alumina involve vitronectin. *Tissue engineering* 2001, 7(3):291-301.

100. Webster TJ, Ergun C, Doremus RH, Siegel RW, Bizios R: Specific proteins mediate enhanced osteoblast adhesion on nanophase ceramics. *Journal of biomedical materials research* 2000, 51(3):475-483.

101. Webster TJ, Siegel RW, Bizios R: Osteoblast adhesion on nanophase ceramics. *Biomaterials* 1999, 20(13):1221-1227.

102. Lee KY, Mooney DJ: Hydrogels for tissue engineering. *Chem Rev* 2001, 101(7):1869-1879.

103. Nguyen KT, West JL: Photopolymerizable hydrogels for tissue engineering applications. *Biomaterials* 2002, 23(22):4307-4314.

104. Tessmar JK, Gopferich AM: Matrices and scaffolds for protein delivery in tissue engineering. *Adv Drug Deliv Rev* 2007, 59(4-5):274-291.

105. Holland TA, Tabata Y, Mikos AG: In vitro release of transforming growth factor-beta 1 from gelatin microparticles encapsulated in biodegradable, injectable oligo(poly(ethylene glycol) fumarate) hydrogels. *J Control Release* 2003, 91(3):299-313.

106. Peppas NA, Khare AR: Preparation, Structure and Diffusional Behavior of Hydrogels in Controlled-Release. *Adv Drug Deliv Rev* 1993, 11(1-2):1-35.

107. Bhattarai N, Ramay HR, Gunn J, Matsen FA, Zhang MQ: PEG-grafted chitosan as an injectable thermosensitive hydrogel for sustained protein release. *J Control Release* 2005, 103(3):609-624.

108. Cadee JA, de Groot CJ, Jiskoot W, den Otter W, Hennink WE: Release of recombinant human interleukin-2 from dextran-based hydrogels. *J Control Release* 2002, 78(1-3):1-13.

109. Mellott MB, Searcy K, Pishko MV: Release of protein from highly cross-linked hydrogels of poly(ethylene glycol) diacrylate fabricated by UV polymerization. *Biomaterials* 2001, 22(9):929-941.

110. Temenoff JS, Athanasiou KA, LeBaron RG, Mikos AG: Effect of poly(ethylene glycol) molecular weight on tensile and swelling properties of oligo(poly(ethylene glycol) fumarate) hydrogels for cartilage tissue engineering. *J Biomed Mater Res* 2002, 59(3):429-437.

111. Tabata Y, Miyao M, Ozeki M, Ikada Y: Controlled release of vascular endothelial growth factor by use of collagen hydrogels. *J Biomater Sci-Polym Ed* 2000, 11(9):915-930.

112. Ungaro F, Biondi M, d'Angelo I, Indolfi L, Quaglia F, Netti PA, La Rotonda MI: Microsphere-integrated collagen scaffolds for tissue engineering: Effect of microsphere formulation and scaffold properties on protein release kinetics. *J Control Release* 2006, 113(2):128-136.

113. Maschke A, Becker C, Eyrich D, Kiermaier J, Blunk T, Gopferich A: Development of a spray congealing process for the preparation of insulin-loaded lipid microparticles and characterization thereof. *Eur J Pharm Biopharm* 2007, 65(2):175-187.

114. Holland TA, Tessmar JKV, Tabata Y, Mikos AG: Transforming growth factor-beta 1 release from oligo(poly(ethylene glycol) fumarate) hydrogels in conditions that model the cartilage wound healing environment. *J Control Release* 2004, 94(1):101-114.

115. Holland TA, Tabata Y, Mikos AG: Dual growth factor delivery from degradable oligo(poly(ethylene glycol) fumarate) hydrogel scaffolds for cartilage tissue engineering. *J Control Release* 2005, 101(1-3):111-125.

116. DeLong SA, Moon JJ, West JL: Covalently immobilized gradients of bFGF on hydrogel scaffolds for directed cell migration. *Biomaterials* 2005, 26(16):3227-3234.

117. Mann BK, Schmedlen RH, West JL: Tethered-TGF-beta increases extracellular matrix production of vascular smooth muscle cells. *Biomaterials* 2001, 22(5):439-444.

118. Rizzi SC, Ehrbar M, Halstenberg S, Raeber GP, Schmoekel HG, Hagenmuller H, Muller R, Weber FE, Hubbell JA: Recombinant protein-co-PEG networks as cell-adhesive and proteolytically degradable hydrogel matrixes. Part II: Biofunctional characteristics. *Biomacromolecules* 2006, 7(11):3019-3029.

119. Rizzi SC, Hubbell JA: Recombinant protein-co-PEG networks as cell-adhesive and proteolytically degradable hydrogel matrixes. Part 1: Development and physicochernical characteristics. *Biomacromolecules* 2005, 6(3):1226-1238.

120. Janjanin S, Li WJ, Morgan MT, Shanti RA, Tuan RS: Mold-shaped, nanofiber scaffold-based cartilage engineering using human mesenchymal stem cells and bioreactor. *J Surg Res* 2008, 149(1):47-56.

121. Nieponice A, Soletti L, Guan JJ, Hong Y, Gharaibeh B, Maul TM, Huard J, Wagner WR, Vorp DA: In Vivo Assessment of a Tissue-Engineered Vascular Graft Combining a Biodegradable Elastomeric Scaffold and Muscle-Derived Stem Cells in a Rat Model. *Tissue Eng Part A* 2010, 16(4):1215-1223.

122. Pritchard CD, Arner KM, Neal RA, Neeley WL, Bojo P, Bachelder E, Holz J, Watson N, Botchwey EA, Langer RS *et al*: The use of surface modified poly(glycerol-co-sebacic acid) in retinal transplantation. *Biomaterials* 2010, 31(8):2153-2162.

123. Shin M, Yoshimoto H, Vacanti JP: In vivo bone tissue engineering using mesenchymal stem cells on a novel electrospun nanofibrous scaffold. *Tissue Eng* 2004, 10(1-2):33-41.

124. Xu CY, Inai R, Kotaki M, Ramakrishna S: Aligned biodegradable nanotibrous structure: a potential scaffold for blood vessel engineering. *Biomaterials* 2004, 25(5):877-886.

125. Balguid A, Mol A, van Marion MH, Bank RA, Bouten CVC, Baaijens FPT: Tailoring Fiber Diameter in Electrospun Poly(epsilon-Caprolactone) Scaffolds for Optimal Cellular Infiltration in Cardiovascular Tissue Engineering. *Tissue Eng Part A* 2009, 15(2):437-444.

126. Guimaraes A, Martins A, Pinho ED, Faria S, Reis RL, Neves NM: Solving cell infiltration limitations of electrospun nanofiber meshes for tissue engineering applications. *Nanomedicine* 2010, 5(4):539-554.

127. Telemeco TA, Ayres C, Bowlin GL, Wnek GE, Boland ED, Cohen N, Baumgarten CM, Mathews J, Simpson DG: Regulation of cellular infiltration into tissue engineering scaffolds composed of submicron diameter fibrils produced by electrospinning. *Acta Biomater* 2005, 1(4):377-385.

128. Fu YC, Nie H, Ho ML, Wang CK, Wang CH: Optimized bone regeneration based on sustained release from three-dimensional fibrous PLGA/HAp composite scaffolds loaded with BMP-2. *Biotechnol Bioeng* 2008, 99(4):996-1006.

129. Nie H, Soh BW, Fu YC, Wang CH: Three-dimensional fibrous PLGA/HAp composite scaffold for BMP-2 delivery. *Biotechnol Bioeng* 2008, 99(1):223-234.

130. Li CM, Vepari C, Jin HJ, Kim HJ, Kaplan DL: Electrospun silk-BMP-2 scaffolds for bone tissue engineering. *Biomaterials* 2006, 27(16):3115-3124.

131. Sahoo S, Ang LT, Goh JCH, Toh SL: Growth factor delivery through electrospun nanofibers in scaffolds for tissue engineering applications. *J Biomed Mater Res Part A* 2009, 93A(4):1539-1550.

132. Schneider A, Wang XY, Kaplan DL, Garlick JA, Egles C: Biofunctionalized electrospun silk mats as a topical bioactive dressing for accelerated wound heating. *Acta Biomater* 2009, 5(7):2570-2578.

133. Li H, Zhao CG, Wang ZX, Zhang H, Yuan XY, Kong DL: Controlled Release of PDGF-bb by Coaxial Electrospun Dextran/Poly(L-lactide-co-epsilon-caprolactone) Fibers with an Ultrafine Core/Shell Structure. *J Biomater Sci-Polym Ed* 2010, 21(6-7):803-819.

134. Liao IC, Chew SY, Leong KW: Aligned core-shell nanofibers delivering bioactive proteins. *Nanomedicine* 2006, 1(4):465-471.

135. Choi JS, Leong KW, Yoo HS: In vivo wound healing of diabetic ulcers using electrospun nanofibers immobilized with human epidermal growth factor (EGF). *Biomaterials* 2008, 29(5):587-596.

136. Li XQ, Su Y, Liu SP, Tan LJ, Mo XM, Ramakrishna S: Encapsulation of proteins in poly(L-lactide-co-caprolactone) fibers by emulsion electrospinning. *Colloid Surf B-Biointerfaces* 2010, 75(2):418-424.

137. Su Y, Li XQ, Liu SP, Mo XM, Ramakrishna S: Controlled release of dual drugs from emulsion electrospun nanofibrous mats. *Colloid Surf B-Biointerfaces* 2009, 73(2):376-381.

138. Valmikinathan CM, Defroda S, Yu XJ: Polycaprolactone and Bovine Serum Albumin Based Nanofibers for Controlled Release of Nerve Growth Factor. *Biomacromolecules* 2009, 10(5):1084-1089.

139. Yang Y, Li XH, Qi MB, Zhou SB, Weng J: Release pattern and structural integrity of lysozyme encapsulated in core-sheath structured poly(DL-lactide) ultrafine fibers prepared by emulsion electrospinning. *Eur J Pharm Biopharm* 2008, 69(1):106-116.

140. Chew SY, Wen J, Yim EKF, Leong KW: Sustained release of proteins from electrospun biodegradable fibers. *Biomacromolecules* 2005, 6(4):2017-2024.

141. Kim BS, Oh JM, Kim KS, Seo KS, Cho JS, Khang G, Lee HB, Park K, Kim MS: BSA-FITC-loaded microcapsules for in vivo delivery. *Biomaterials* 2009, 30(5):902-909.

142. Casper CL, Yamaguchi N, Kiick KL, Rabolt JF: Functionalizing electrospun fibers with biologically relevant macromolecules. *Biomacromolecules* 2005, 6(4):1998-2007.

143. McCann JT, Li D, Xia YN: Electrospinning of nanofibers with core-sheath, hollow, or porous structures. *J Mater Chem* 2005, 15(7):735-738.

144. Sun ZC, Zussman E, Yarin AL, Wendorff JH, Greiner A: Compound core-shell polymer nanofibers by co-electrospinning. *Adv Mater* 2003, 15(22):1929-+.

145. Ji W, Yang F, van den Beucken J, Bian ZA, Fan MW, Chen Z, Jansen JA: Fibrous scaffolds loaded with protein prepared by blend or coaxial electrospinning. *Acta Biomater* 2010, 6(11):4199-4207.

146. Jiang HL, Hu YQ, Li Y, Zhao PC, Zhu KJ, Chen WL: A facile technique to prepare biodegradable coaxial electrospun nanofibers for controlled release of bioactive agents. *J Control Release* 2005, 108(2-3):237-243.

147. Jiang HL, Hu YQ, Zhao PC, Li Y, Zhu KJ: Modulation of protein release from biodegradable core-shell structured fibers prepared by coaxial electrospinning. *J Biomed Mater Res Part B* 2006, 79B(1):50-57.

148. Liu JJ, Wang CY, Wang JG, Ruan HJ, Fan CY: Peripheral nerve regeneration using composite poly(lactic acid-caprolactone)/nerve growth factor conduits prepared by coaxial electrospinning. *J Biomed Mater Res Part A* 2011, 96A(1):13-20.

149. Wang F, Li ZQ, Tamama K, Sen CK, Guan JJ: Fabrication and Characterization of Prosurvival Growth Factor Releasing, Anisotropic Scaffolds for Enhanced Mesenchymal Stem Cell Survival/Growth and Orientation. *Biomacromolecules* 2009, 10(9):2609-2618.

150. Ionescu LC, Lee GC, Sennett BJ, Burdick JA, Mauck RL: An anisotropic nanofiber/microsphere composite with controlled release of biomolecules for fibrous tissue engineering. *Biomaterials* 2010, 31(14):4113-4120.

151. Whang K, Goldstick TK, Healy KE: A biodegradable polymer scaffold for delivery of osteotropic factors. *Biomaterials* 2000, 21(24):2545-2551.

152. Whang K, Tsai DC, Nam EK, Aitken M, Sprague SM, Patel PK, Healy KE: Ectopic bone formation via rhBMP-2 delivery from porous bioabsorbable polymer scaffolds. *J Biomed Mater Res* 1998, 42(4):491-499.

153. Ziegler J, Mayr-Wohlfart U, Kessler S, Breitig D, Gunther KP: Adsorption and release properties of growth factors from biodegradable implants. *J Biomed Mater Res* 2002, 59(3):422-428.

154. Sohier J, Haan RE, de Groot K, Bezemer JM: A novel method to obtain protein release from porous polymer scaffolds: emulsion coating. *J Control Release* 2003, 87(1-3):57-68.

155. Sohier J, Vlugt TJH, Cabrol N, Van Blitterswijk C, de Groot K, Bezemer JM: Dual release of proteins from porous polymeric scaffolds. *J Control Release* 2006, 111(1-2):95-106.

156. Wei GB, Jin QM, Giannobile WV, Ma PX: Nano-fibrous scaffold for controlled delivery of recombinant human PDGF-BB. *J Control Release* 2006, 112(1):103-110.

157. Wei GB, Jin QM, Giannobile WV, Ma PX: The enhancement of osteogenesis by nano-fibrous scaffolds incorporating rhBMP-7 nanospheres. *Biomaterials* 2007, 28(12):2087-2096.

158. Sinha VR, Trehan A: Biodegradable microspheres for protein delivery. *J Control Release* 2003, 90(3):261-280.

159. Vauthier C, Bouchemal K: Methods for the Preparation and Manufacture of Polymeric Nanoparticles. *Pharm Res* 2009, 26(5):1025-1058.

160. Wei GB, Pettway GJ, McCauley LK, Ma PX: The release profiles and bioactivity of parathyroid hormone from poly(lactic-co-glycolic acid) microspheres. *Biomaterials* 2004, 25(2):345-352.

161. Langer R: New Methods of Drug Delivery. *Science* 1990, 249(4976):1527-1533.

162. Woodrow KA, Cu Y, Booth CJ, Saucier-Sawyer JK, Wood MJ, Saltzman WM: Intravaginal gene silencing using biodegradable polymer nanoparticles densely loaded with small-interfering RNA. *Nat Mater* 2009, 8(6):526-533.

Chapter 3

Novel antibacterial nanofibrous PLLA scaffold

Introduction

Chronic inflammation diseases caused by bacterial infection such as periodontitis and septic arthritis remain common in the United States and throughout the world. For example, approximately half of the adult population in the US suffers chronic periodontitis. This disease is initiated by pathogenic infection on the tooth's surface as a microbial biofilm which gradually leads to the destruction of the periodontal tissue, supporting alveolar bone, and eventually leading to tooth loss. [1] In the treatment of periodontitis, antibiotics such as tetracycline (TCL) and metronidazole have been frequently used.

Doxycycline (DOXY) is a well known broad-spectrum antibiotic, which is effective against both gram-positive and gram-negative bacteria, protozoa, and various anaerobes. [2] As a tetracycline analogue, it can work as a bacteriostatic which is capable of inhibiting the bacterial protein synthesis at the ribosomal sites. [3] Compared to TCL, DOXY has certain advantages such as a longer half-life, higher lipid solubility, and greater oral absorption. [4] It also shows strong inhibition of matrix metalloproteinases (MMPs) both *in vitro* and in clinical studies. [5-9] After being introduced to the clinical area in 1967[10], DOXY has been frequently used in treating destructive periodontal diseases such as juvenile periodontitis and acute periodontal abscesses. It has been used

against periodontal infection and enhancing bone regeneration after periodontal disease. [11] It has also been used to prevent bacterial infection related to septic arthritis. [10, 12] However, there are some concerns over possible side effects such as gastro-intestinal disturbance, esophageal erosion, and photosensitivity when administrated orally [4, 13-17]. Therefore, in order to reach the site of infection in deep tissues with an effective drug concentration and to cirmvent the systemic side effects, controlled localized delivery of DOXY is desired.

Many attempts have been made in the area of controlled delivery of the DOXY/TCL family and certain progress has been achieved. Drug encapsulation methods such as mixing, emulsification, and electrospinning have been used. Delivery systems in the forms of particles, stripes, hollow fibers, gels, and cements have been fabricated. [18-24]However, most systems release all the encapsulated DOXY from hours up to 2 weeks. While a high initial burst release is acceptable for a highly hydrophilic antibiotic such as DOXY/TCL in order to immediately achieve effective concentration, it is also necessary to attain a long term sustained release to fight against chronic infection and avoid repeated local drug administration. How to achieve both reduced initial burst and extended release duration remains a challenge.

Controlled release of proteins has been widely investigated. [25-30] Our laboratory has previously developed a novel growth factor delivery system. The growth factors were encapsulated into PLGA nanospheres and the nanospheres were then incorporated into three dimensional (3-D) macro-porous and nano-fibrous PLLA scaffolds. [31-33] The function of this delivery system is two fold: First, it serves as an osteoconductive scaffold. With its suitable pore structure and nano-fibrous structure similar to collagen, it improves

cell attachment, proliferation and differentiation. [34, 35] Second, it stimulates vascularization or bone formation by localized controlled delivery of a bioactive angiogenic or osteogenic growth factor. [31, 32] In this paper, we incorporated DOXY-containing PLGA nanospheres into the nano-fibrous scaffolds to evaluate their anti-bacterial capacity. The combination of the osteoconductive properties of the macro-porous and the nano-fibrous scaffold with its ability to release antibiotics could be a good candidate for local treatment of oral and periodontal diseases.

Materials and methods

Materials

Doxycycline hyclate, D-fructose, mineral oil, and sorbitanmonooleate (span 80) were obtained from the Sigma-Aldrich Chemical Company (St. Louis, MO). PLGA copolymers with LA/GA ratio of 50:50 (Lakeshore Biomaterials™, PLGA50-6.5K, Mw = 6.5 kDa; PLGA50-64K, Mw = 64KDa); PLGA copolymers with a LA/GA ratio of 75:25 (Lakeshore Biomaterials™, PLGA75-113K, Mw = 113 kDa) and the PLGA copolymers with a LA/GA ratio of 85:15 (Lakeshore Biomaterials™, PLGA85-142K, Mw = 142 kDa) were purchased from SurModics Pharmaceuticals Inc. (Birmingham, AL). Poly(L-lactic acid) (PLLA) with inherent viscosity of 1.6 dl/g was purchased from Boehringer Ingelheim (Ingelheim, Germany). Poly(acrylic acid) (M_W = 5000) and poly(vinyl alcohol) (PVA) (88 mol% hydrolyzed, M_W = 25,000) were obtained from Polysciences Inc. Hexaglyceryl polyricinolate (Hexaglyn PR-15) was provided by the Barnet Products Corp (Englewood Cliffs, NJ). Acetonitrile and petroleum ether (BP 60-

95 °C) were obtained from Acros Organic (Morris Plains, NJ). Dichloromethane (DCM), cyclohexane, hexane, tetrahydrofuran (THF) and Fisherbrand regenerated cellulose dialysis bags (nominal MWCO 3500) were purchased from Fisher Scientific (Pittsburgh, PA).

DOXY containing PLGA nanospheres (NS) and NS-incorporated nano-fibrous scaffold (NS-scaffold) preparation

Doxycycline-containing PLGA NS were fabricated using a modified water-in-oil-in-oil (w/o/o) emulsion method [36, 37]. Briefly, 80 mg PLGA was dissolved in 1 ml solvent mixture of acetonitrile/DMC (3:2 in volume ratio). 100 µl aqueous solution of certain amount of DOXY was added into the above solution and emulsified with a probe sonicator at 50 W (Virsonic 100, Gardiner, NY). This primary w/o emulsion was then emulsified into 30 ml of mineral oil containing 4% hexaglyceryl polyricinolate under sonication at 90 W to form the w/o/o emulsion. The resulting secondary emulsion was magnetically stirred at room temperature for 12 h to evaporate the solvents. The spheres were collected by centrifugation and washed three times with petroleum ether and freeze dried. Four PLGA formulations: PLGA50-6.5K, PLGA50-64K, PLGA75-113K and PLGA85-142K were used for the *in vitro* release study. The macro-porous PLLA nano-fibrous scaffolds with dimensions of 7.2 mm in diameter and 2 mm in thickness were prefabricated by a combination of phase separation and sugar leaching techniques previously described [33]. The PLGA NS were incorporated onto PLLA scaffolds using a post seeding method {Wei, 2006 #6; Wei, 2007 #5}. Briefly, PLGA NS were dispersed in hexane with 0.1% span 80 and were seeded onto NS-scaffolds drop wise. Then, the

scaffolds were subject to vapor of a mixed solvent of hexane/THF (volume ratio 9:1) for 30 min. The scaffolds were vacuum-dried for 3 days to remove the solvent.

Characterization of PLGA NS and NS-scaffolds

The morphology and size of the nanospheres and the scaffolds (before and after NS incorporation) were examined using scanning electron microscopy (Philips XL30 FEG SEM). The nanospheres were dispersed in hexane and deposited onto a metal stub. SEM figures of these spheres were taken after gold coating. Average diameters of all type of PLGA spheres studied were calculated based on the sizes measured from the SEM images using ImageJ software (National Institutes of Health). The sizes of PLGA50-6.5K and PLGA85-142K spheres were also measured by dynamic light scattering (DLS) in an aqueous solution for comparison (Delsa Nano C Particle Size Analyzer, Beckman Coulter Inc). The drug content and encapsulation efficiency were determined by UV spectrophotometric analysis. Briefly, 10 mg DOXY-encapsulated nanospheres (or one NS-scaffold) were dissolved in dichloromethane. Then, 10 ml PBS was added to extract DOXY. The extraction process was repeated several times. The solution was filtered through a 0.45 μm filter to remove polymer debris and then the DOXY concentration was measured using a UV spectrophotometer (Hitachi U2910) at the λ_{max} value of 274 nm. PBS was used as the control.

In vitro drug release studies

The release profiles of DOXY loaded NS or NS-scaffolds with four PLGA formulations were investigated in PBS (0.1 M). 10 mg NS were suspended in 1 ml PBS and placed within a dialysis bag. The dialysis bag was kept in a glass flask containing 20 ml PBS. One NS-scaffold was suspended in 1 ml PBS in a glass vial. Both the glass vial and the glass flask were covered in aluminum foil and shaken at 50 rpm at 37 °C. At designated time points (1, 3, 5, 7, 10, 14, 21, 28, 35, 42 days), the release medium was withdrawn and replaced with pre-warmed fresh PBS. The released amounts of DOXY were analyzed using a UV spectrophotometer at the λ_{max} value of 274 nm [22]. For DOXY release through the dialysis bag from NS alone, PBS was used as the control. For DOXY release from NS-incorporated scaffolds, blank PLGA NS (without DOXY) were immobilized onto the scaffolds and were used as the controls. The absorbance values of the controls were subtracted from those of the DOXY containing samples.

In vitro antibacterial activity of NS-scaffold

The antibacterial assay was performed as previously described [38]. The overnight incubated bacteria solution (*S. aureus* and *E. coli*) was diluted with sterile Müeller–Hinton Broth and reached an absorbance value between 0.1 and 0.2 at 625 nm (equivalent to 0.5 McFarland standard). First, the bacterial clone formation assay was performed using the Müeller–Hinton agar (1.5%) plate. The scaffolds with or without DOXY nanospheres were placed in the center of the melting agar just before solidification. The DOXY was allowed to diffuse from the scaffold into the agar for 4 h before 100 μL

inoculum was spread over the agar plate. The plates were incubated at 37 °C for 5 days. The bacterial growth on plates was visualized directly on the plate. Second, the released drug solutions, collected from different scaffold groups at different time points, were mixed with 2X Müeller–Hinton Broth and overnight inoculum (the bacterial final absorbance value was around 0.1 at 625 nm). All tested solutions were incubated at 37 °C on a shaker (50 rpm). The absorbance at 625 nm was monitored after 12 h of incubation. The percentage of bacterial inhibition was calculated using the following equation.

Bacterial inhibition (%) = abs($I_c - I_s$)/(I_c) × 100, where I_c and I_s are the absorbances of the control bacterial solution without drug and bacterial solutions with released drug respectively at 625 nm after 12 h [38].

Results

PLGA nanospheres loaded PLLA nano-fibrous scaffolds

PLGA NS prepared from a modified w/o/o double emulsion process were of smooth surface (Figure 3.1A). The combination of the phase separation and sugar sphere templating techniques allowed the formation of PLLA scaffolds with a high porosity (98%), multi-level pore structures and nano-fibrous architecture of the pore walls. The scaffolds prepared for this study have regular spherical macro-pores 250–425 μm in diameter with well interconnected inter-pore openings of ~ 100 μm (Figure 3.1B). The scaffold walls are entirely made of the PLLA nanofibers with the diameter range of 50–500 nm (Figure 3.1C), which is similar in size to native collagen fibers. Figure 3.1D and

Figure 3.1E show a cross section of the scaffolds after the DOXY loaded NS incorporation, and the pore wall surface at a higher magnification. From SEM observation, it is clear that the macro-pores and inter-pore opening structure of the scaffolds were well preserved and the nanospheres were uniformly distributed throughout the nano-fibrous pore walls.

Four different PLGA NS formulations were examined for encapsulation efficiency and release behavior. Two of the copolymers had the same LA/GA ratio of 50/50 but different molecular weights, PLGA50-6.5K (Mw: 6.5 K) and PLGA50-64K (Mw: 64 K). The other two had different LA/GA ratios: PLGA75-113K with a LA/GA ratio of 75/25 (Mw: 113 K) and PLGA85-142K with a LA/GA ratio of 85/15 (Mw:142 K). The effects of processing parameters such as polymer concentration, volume ratio of drug solution to inner oil phase (w/o_1), volume ratio of inner oil to outer oil phase (o_1/o_2), the addition of PAA on the DOXY encapsulation efficiency (EE) of PLGA85-142K NS are presented in Table 3.1. It was observed that the EE of DOXY increased with an increase in the polymer concentration from 3% to 8%, no significant difference between 8% and 10%. With the increase of aqueous drug volume, the encapsulation efficiency decreased. The higher polymer concentration may entrap the aqueous DOXY droplets more efficiently (higher EE), while the greater aqueous DOXY volume destabilizes the emulsion (lower EE). The increase in the volume ratio of outer oil phase to inner oil phase did not change EE significantly. It was found that the addition of poly(acrylic acid) (PAA) as a co-encapsulation factor did not have significant effect on the EE of the DOXY.

The diameter and the DOXY encapsulation efficiency of NS of four PLGA formulations with the same other processing parameters are listed in Table 3.2. Based on SEM measurement, the average diameter of the spheres increased with the increase of LA/GA ratio and/or PLGA molecular weight, with PLGA50-6.5K NS had the smallest diameter of 300 nm and PLGA85-142K NS had the largest diameter of 730 nm. Based on DLS measurement, the diameter of PLGA50-6.5K NS and PLGA85-142K NS was 400 nm and 890 nm respectively in aqueous solution, possibly due to some degree of swelling or/and certain discrepancy between the two different methods. The changes in size and shape of similar PLGA spheres in aqueous solution over long-term culture were reported previously by our lab [39] and others [36]. Such PLGA spheres swelled first and then deformed from their original spherical shape into irregular shape with a rough surface texture over time. Eventually, they collapsed and disintegrated as the degradation continued [39]. EE of DOXY was not changed significantly among different PLGA NS formulations. The larger diameter of PLGA85-142K NS was possibly resulted from the higher viscosity of the DOXY/PLGA85-142K polymer emulsion compared to those of other polymers (Table 3.2).

In vitro DOXY release kinetics

In vitro release profiles of DOXY from PLGA NS with four PLGA formulations were displayed in Figure 3.2A and release profiles of DOXY from NS-scaffolds were shown in Figure 3.2B. Compared to release profiles of DOXY from PLGA NS alone, the release from the scaffolds showed a similar release pattern with decreased initial burst

release and prolonged release period. In general, the DOXY release profiles of NS-scaffolds showed two phases: an initial burst release within the first day followed by a slow and sustained release over time. There were also significant differences in both the burst release rate and sustained release rate of different PLGA formulations. Both PLGA50-6.5K NS-scaffold and PLGA50-64K NS-scaffold released approximately 70% of DOXY within the first day and 95% of DOXY within 2 weeks, while the PLGA75-113K NS-scaffold (with a higher LA/GA ratio and higher molecular weight) had a lower burst release (50%) in the first day and a slower sustained release of DOXY (85% within 2 weeks, 95% within 6 weeks). The PLGA85-142K NS-scaffold (with the highest LA/GA ratio and the highest molecular weight) had the lowest burst release (25%) in the first day and kept a continuous slow release for longer than 6 weeks (80% within 6 weeks). This two-phase release profile of PLGA nanospheres, characterized by an initial burst release followed by a sustained slow release, indicated that DOXY was dispersed in a polymeric matrix inside the PLGA nanospheres [40] and [41]. The initial burst release was reduced with the increase of the PLGA LA/GA ratio and the PLGA molecular weight. PLGA85-142K NS-scaffolds with the lowest burst release and the longest release period was selected for *in vitro* antibacterial test.

In vitro antibacterial effect of DOXY NS-scaffolds

The antibacterial activity of the released DOXY was investigated using bacteria inhibition experiments. *S. aureus* and *E. coli* were used in the current study since they represent the most common Gram-positive and Gram-negative bacteria in the human

body. The growth of *S. aureus* and *E. coli* bacteria can be visualized directly from the plate to assess the antibacterial function of all scaffold groups (shown in Figure 3.3). It was observed that the agar plates with the BSA scaffolds were totally covered with *S. aureus* or *E. coli* after 5 days of incubation. In contrast, the growth of *S. aureus* and *E. coli* were both inhibited at regions around the DOXY adsorbed scaffolds and DOXY NS-scaffolds. The bacteria inhibited areas were much larger on the plates with the DOXY NS-scaffolds than DOXY adsorbed scaffolds.

The data from the long-term liquid bacterial culture (*S. aureus* data shown in Figure 3.4 and E. coli data shown in Figure 3.5) demonstrated that the antibacterial activity of DOXY lasted for more than 6 weeks in the NS controlled release group (showed 70% inhibition for *S. aureus* and 40% inhibition for *E. coli* at Day 42), while that of the adsorbed DOXY decreased rapidly after 14 days (showed 18% inhibition for *S. aureus* and 9% inhibition for *E. coli* at Day 42) and the BSA scaffold had no antibacterial effect even from the very beginning (showed less than 20% inhibition for *S. aureus* and less than 10% inhibition for *E. coli*). The antibacterial activity of the scaffold measured over time was the measurement of the overall antibacterial capacity of the scaffold, including the reduced DOXY amount released at a later time and possibly also some biological activity loss over time. These results indicated that the encapsulation of DOXY in the nanospheres not only can control the DOXY release rate and prolong its release duration but also retain its antibacterial activity.

Discussion

The main objectives of this work were to fabricate the DOXY loaded NS with good encapsulation efficiency, to incorporate the NS onto a nano-fibrous scaffold, to release DOXY in a controlled manner, and to retain the antibacterial activity. In previous publications from our lab, novel nano-fibrous scaffolds capable of delivering growth factors were successfully developed [31] and [32]. While water-in-oil-in-water (w/o/w) double emulsion method can be readily used to entrap proteins into nanospheres, it is difficult to entrap very hydrophilic small molecules such as doxycycline into NS with an acceptable encapsulation efficiency (less than 5% showed in Table 3.3) since the high solubility of the drug in the external phase and its small size makes it easy for the majority of the drug to diffuse to the external phase during the emulsion and solvent evaporation process and results in very low encapsulation efficiency [41]. Some researchers made modifications to w/o/w method [22] or used other encapsulation method [20] to achieve a higher DOXY encapsulation efficiency. However, the EE increase was limited and the size of the spheres obtained became much larger, usually in the range of 100 μm [22]. The DOXY loaded spheres with this size may be used alone for antibacterial treatment, but they are too large to be incorporated into the nano-fibrous scaffolds [33]. To overcome these limitations, a modified w/o/o emulsion and solvent evaporation method was successfully adopted to encapsulate DOXY into spheres. By changing the external continuous phase from water to an organic solvent mixture, the diffusion of the drug was reduced due to the decreased solubility of the drug in the external phase, and the encapsulation efficiency was greatly improved. It was also discovered that the release profile of DOXY from the PLGA NS-scaffolds was mainly

determined by the release from NS which can be adjusted by tailoring the chemical composition and molecular weight of the PLGA copolymers. The PLGA85 NS-scaffolds with the highest molecular weight and highest LA/GA had the lowest initial burst release (25%) and longest release duration of DOXY (longer than 6 weeks). This trend is consistent with our lab's previous publications on the release profiles of growth factors from NS-scaffolds [31] and [32]. The difference in release profiles of PLGA NS-scaffold was possibly resulted from both the difference in the NS diameter and PLGA degradation rate. PLGA85-142K NS with the largest NS diameter had the smallest specific surface area and the longest average travel distance for the encapsulated DOXY to diffuse out of the spheres, resulting in the lowest burst release during the earlier release stage. It is also possible that the highest viscosity of PLGA85 polymer solution also reduced the diffusion of DOXY to the outer oil phase during the emulsion and solvent evaporation process so that the least amount of the drug was simply absorbed on or near the NS surface, resulting in a reduced initial burst release. PLGA85-142K NS also had the slowest degradation rate due to the highest molecular weight and LA/GA ratio, which contributed to the slower release rate of DOXY. It was also discovered that incorporating DOXY loaded PLGA NS into PLLA nano-fibrous scaffold effectively reduced burst release and slowed down the DOXY release rate. The reduced burst release of DOXY from nano-fibrous scaffold may have resulted from the adsorption and desorption of DOXY on the nanofibers before diffusing out of the scaffolds due to the very high surface area (100 m^2/g) of the nano-fibrous scaffolds.

The antimicrobial experiment demonstrated the biological function of the DOXY released from PLGA NS-scaffolds for a long duration (6 weeks), which is a great

improvement for the long-term treatment of dental, periodontal and bone infection or MMP-inhibition since the commercially available DOXY releasing gels typically release all DOXY within 2 weeks [42]. These novel DOXY NS-incorporated nano-fibrous scaffolds were intended for tissue engineering applications where microbial infection may be involved. While the macro-porous and nano-fibrous scaffolds may promote the tissue regeneration, the DOXY NS in the scaffolds may also protect the tissue from microbial invasion. Since DOXY is also an inhibitor of multiple MMPs such as MMP-8, -9 and -13, DOXY NS-scaffold may also be able to protect engineered bone from MMP destruction in situations with chronic inflammation in diseases such as periodontitis and rheumatoid arthristis [43].

The 3-D NS-scaffolds developed in this work have shown the capability of controlled delivery of DOXY and inhibition of bacterial growth for a prolonged period. This success has demonstrated the scaffolds to be capable of controlled delivering small hydrophilic drug molecules as well as large proteins. With the versatile delivery capability and macro-porous and nano-fibrous structure, the scaffolds may allow for the implementation of more comprehensive strategies in tissue engineering.

Conclusion

Results of *in vitro* release and antibacterial experiments suggest that the developed drug-containing nano-fibrous scaffolds are capable of effectively delivering doxycycline in a controlled fashion with prolonged duration. These biodegradable PLLA scaffolds have well interconnected macro-porous and nano-fibrous structure and can inhibit common bacterial growth for more than 6 weeks with the incorporation of DOXY

containing PLGA NS. Release kinetics from the scaffolds was found to be determined by PLGA formulation. The incorporation of the NS into scaffolds reduced the burst release. PLGA85-142K NS-scaffold has the lowest initial burst release and the longest release period compared to other formulations investigated. Taken together with earlier studies, the NS-scaffold system can be used as a delivery system for both large proteins and small drug molecules for various complex tissue engineering applications.

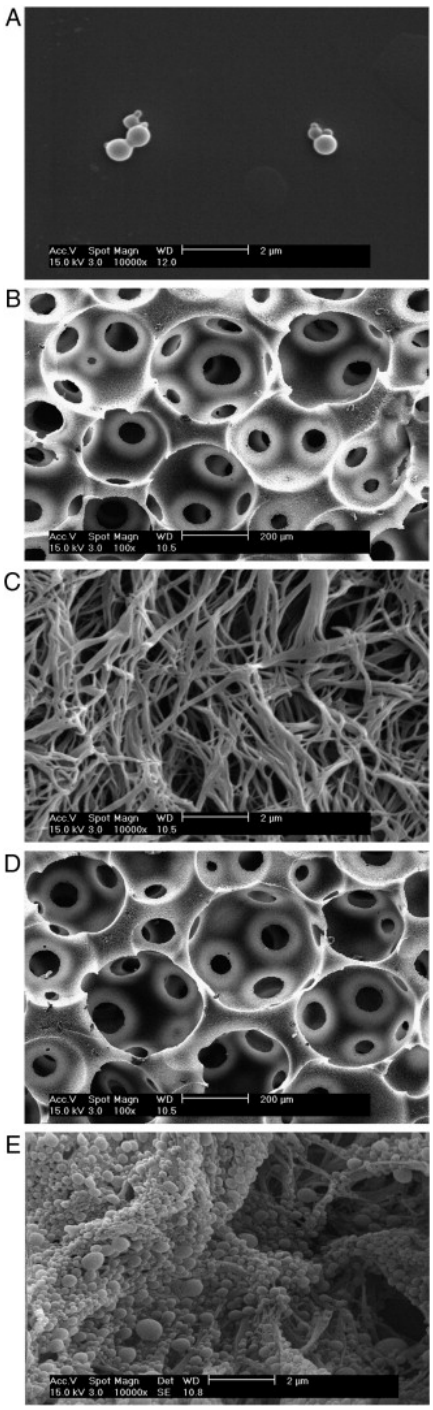

Fig. 3.1 Characterization of PLGA85-142 K nanospheres (NS) and PLLA nano-fibrous scaffold (NS-scaffold) before and after nanospheres incorporation. (A) SEM view of DOXY containing PLGA85-142 K NS; (B, C) SEM views of the PLLA scaffold before NS incorporation at 100× and 10,000× magnifications respectively; and (D, E) SEM views of PLLA scaffold after NS incorporation at 100× and 10,000× magnifications respectively.

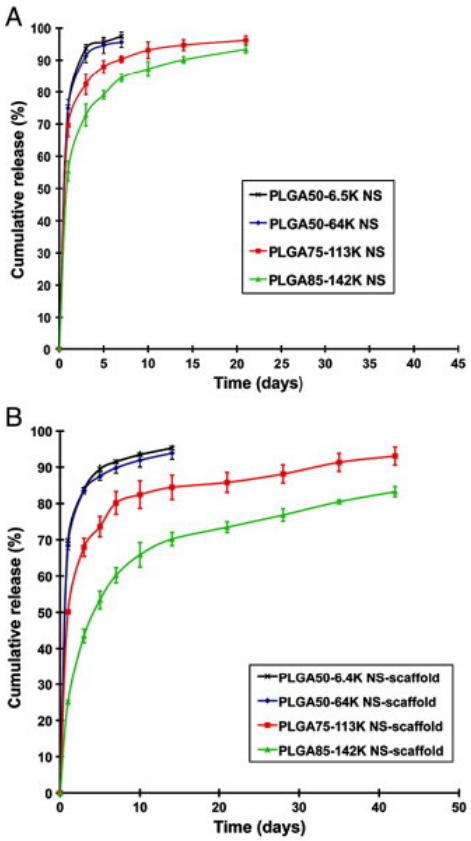

Fig. 3.2 *In vitro* release kinetics of DOXY from NS (A) and from NS-incorporated nanofibrous PLLA scaffolds (B): in 10 mM PBS with DOXY loading of 100 μg/scaffold. Each data point represents a mean ± standard deviation (n = 3).

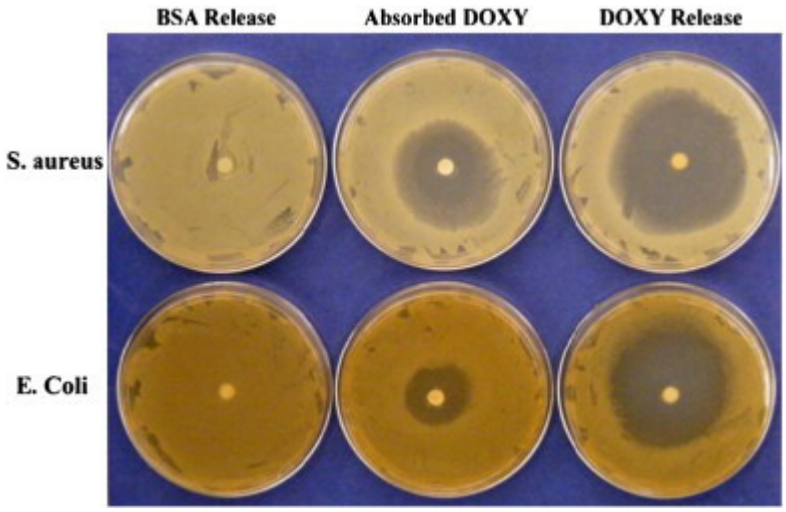

Fig. 3.3 Agar petri dish cultivated with *S. aureus* (upper) and *E. coli* (lower) with scaffold samples in the center after 5 days of incubation. Scaffolds on the left side were seeded with BSA containing NS. Scaffolds in the center absorbed 100 μg DOXY. Scaffolds on the right side were seeded with NS containing 100 μg DOXY.

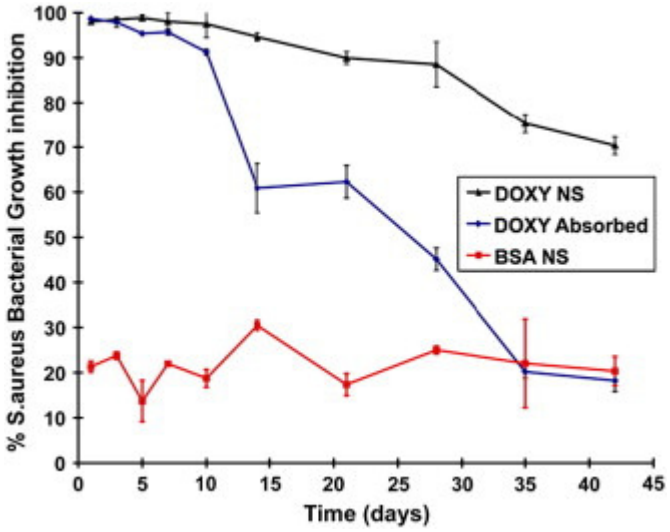

Fig. 3.4 Long-term *S. aureus* growth inhibition test for release solution from three groups of scaffolds. Each data point represents a mean ± standard deviation (n = 3).

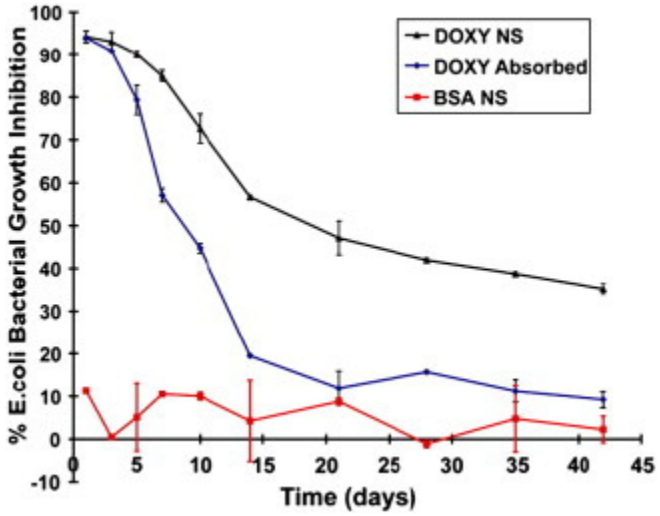

Fig. 3.5 Long-term *E. coli* growth inhibition test for release solution from three groups of scaffolds. Each data point represents a mean ± standard deviation (n = 3).

Table 3.1 Effects of various processing parameter on encapsulation efficiency of DOXY in PLGA85-142K nanospheres. Each EE data point represents a mean ± standard deviation (n = 3). Note: w: water phase; o_1: inner oil phase (PLGA solution); and o_2: outer oil phase (mineral oil solution).

PLGA85-142K concentration	w/o_1	PAA concentration	EE (%)
3%	1:10	0	13.3±5.2%
5%	1:10	0	15.3±4.1%
8%	1:10	0	25.3±3.0%
10%	1:10	0	25.9±3.9%
8%	1:4	0	8.6±2.1%
8%	1:5	0	10.8+3.2%
8%	1:20	0	26.4+3.5%
8%	1:10	2%	24.4±3.3%
8%	1:10	4%	23.5±4.5%
8%	1:10	8%	23.1±5.6%
8%	1:10	16%	25.7±3.1%

Table 3.2 Effects of PLGA composition on sphere diameter with the same other processing parameters (8% polymer concentration, 4% PR-15, 1:10 w/o_1, and 1:30 o_1/o_2). Each data point represents a mean ± standard deviation. Sphere diameters were measured using SEM.

Polymer	LA/GA ratio	Mw (kDa)	EE (%)	Sphere diameter (nm)
PLGA50-6.5K	50/50	6.5	26.1±4.8	300±110
PLGA50-64K	50/50	64	24.4±3.5	520±150
PLGA75-113K	75/25	113	23.1±4.4	570±130
PLGA85-142	85/15	142	25.3±3.0	730±160

Table 3.3 Encapsulation efficiencies (10% polymer concentration, 1% PVA, $w_1/o = 1:10$, $o/w_2 = 1:30$). Each data point represents a mean ± standard deviation. Note: w_1: aqueous drug solution, o: PLGA solution, and w_2: aqueous PVA solution.

Polymer	LA/GA ratio	Mw (kDa)	EE (%)	Sphere diameter (nm)
PLGA50-6.5K	50/50	6.5	3.2±1.8	280±70
PLGA50-64K	50/50	64	2.7±0.5	320±100
PLGA75-113K	75/25	113	3.1±1.4	370±90
PLGA85-142	85/15	142	2.3±1.0	410±120

References

1. JM A: Epidemiology and risk factors of periodontal diseases. *Dental Clinics of North America* 2005(49):517-532.

2. Bokor-Bratic M, Brkanic T: Clinical use of tetracyclines in the treatment of periodontal diseases. *Medicinski Pregled* 2000, 53(5-6):266-271.

3. C.W. Stratton VL: Mechanisms of action for antimicrobial agents: general principals and mechanisms for selected classes of antibiotics, Antibiotics in Laboratory Medicine, 4th ed. Baltimore: Williams & Wilkins; 1996.

4. Seymour RA, Heasman PA: Tetracyclines in the management of periodontal diseases. A review. *Journal of clinical periodontology* 1995, 22(1):22-35.

5. Amin AR, Attur MG, Thakker GD, Patel PD, Vyas PR, Patel RN, Patel IR, Abramson SB: A novel mechanism of action of tetracyclines: effects on nitric oxide synthases. *Proceedings of the National Academy of Sciences of the United States of America* 1996, 93(24):14014-14019.

6. Gapski R, Hasturk H, Van Dyke Thomas E, Oringer Richard J, Wang S, Braun Thomas M, Giannobile William V: Systemic MMP inhibition for periodontal wound repair: results of a multi-centre randomized-controlled clinical trial. *J Clin Periodontol* 2009, 36(2):149-156.

7. Giannobile WV: Host-response therapeutics for periodontal diseases. *J Periodontol* 2008, 79(8, Suppl.):1592-1600.

8. Greenwald RA, Moak SA, Ramamurthy NS, Golub LM: Tetracyclines suppress matrix metalloproteinase activity in adjuvant arthritis and in combination with flurbiprofen, ameliorate bone damage. *Journal of rheumatology* 1992, 19(6):927-938.

9. Shlopov BV, Stuart JM, Gumanovskaya ML, Hasty KA: Regulation of cartilage collagenase by doxycycline. *Journal of rheumatology* 2001, 28(4):835-842.

10. Joshi N, Miller DQ: Doxycycline revisited. *Archives of Internal Medicine* 1997, 157(13):1421-1428.

11. Slots J, Rams TE: Antibiotics in periodontal therapy: advantages and disadvantages. *Journal of clinical periodontology* 1990, 17(7 (Pt 2)):479-493.

12. Klein NC, Cunha BA: Tetracyclines. *Medical Clinics of North America* 1995, 79(4):789-801.

13. Attar SM: Tetracyclines: what a rheumatologist needs to know? *International Journal of Rheumatic Diseases* 2009, 12(2):84-89.

14. Loesche WJ: The antimicrobial treatment of periodontal disease: Changing the treatment paradigm. *Critical Reviews in Oral Biology & Medicine* 1999, 10(3):245-275.

15. McIlwraith CW: Treatment of infectious arthritis. *Veterinary clinics of North America-Large animal practice* 1983, 5(2):363-379.

16. Mombelli A, Samaranayake LP: Topical and systemic antibiotics in the management of periodontal diseases. *International Dental Journal* 2004, 54(1):3-14.

17. van der Ouderaa FJ: Anti-plaque agents. Rationale and prospects for prevention of gingivitis and periodontal disease. *Journal of clinical periodontology* 1991, 18(6):447-454.

18. Esposito E, Cortesi R, Cervellati F, Menegatti E, Nastruzzi C: Biodegradable microparticles for sustained delivery of tetracycline to the periodontal pocket: formulatory and drug release studies. *Journal of microencapsulation* 1997, 14(2):175-187.

19. Goodson JM, Holborow D, Dunn RL, Hogan P, Dunham S: Monolithic tetracycline-containing fibers for controlled delivery to periodontal pockets. *Journal of periodontology* 1983, 54(10):575-579.

20. Haerdi-Landerer MC, Suter MM, Steiner A, Wittenbrink MM, Pickl A, Gander BA: In vitro cell compatibility and antibacterial activity of microencapsulated doxycycline designed for improved localized therapy of septic arthritis. *Journal of Antimicrobial Chemotherapy* 2008, 61(2):332-340.

21. Kenawy E-R, Bowlin GL, Mansfield K, Layman J, Simpson DG, Sanders EH, Wnek GE: Release of tetracycline hydrochloride from electrospun poly(ethylene-co-vinylacetate), poly(lactic acid), and a blend. *Journal of Controlled Release* 2002, 81(1-2):57-64.

22. Mundargi RC, Srirangarajan S, Agnihotri SA, Patil SA, Ravindra S, Setty SB, Aminabhavi TM: Development and evaluation of novel biodegradable microspheres based on poly(D,L-lactide-co-glycolide) and poly(e-caprolactone) for controlled delivery of doxycycline in the treatment of human periodontal pocket: In vitro and in vivo studies. *Journal of Controlled Release* 2007, 119(1):59-68.

23. Schwach-Abdellaoui K, Vivien-Castioni N, Gurny R: Local delivery of antimicrobial agents for the treatment of periodontal diseases. *European journal of pharmaceutics and biopharmaceutics* 2000, 50(1):83-99.

24. Tamimi F, Torres J, Bettini R, Ruggera F, Rueda C, Lopez-Ponce M, Lopez-Cabarcos E: Doxycycline sustained release from brushite cements for the treatment of periodontal diseases. *Journal of Biomedical Materials Research, Part A* 2008, 85A(3):707-714.

25. Bae SE, Son JS, Park K, Han DK: Fabrication of covered porous PLGA microspheres using hydrogen peroxide for controlled drug delivery and regenerative medicine. *Journal of Controlled Release* 2009, 133(1):37-43.

26. Goraltchouk A, Scanga V, Morshead CM, Shoichet MS: Incorporation of protein-eluting microspheres into biodegradable nerve guidance channels for controlled release. *Journal of Controlled Release* 2006, 110(2):400-407.

27. Kakizawa Y, Nishio R, Hirano T, Koshi Y, Nukiwa M, Koiwa M, Michizoe J, Ida N: Controlled release of protein drugs from newly developed amphiphilic polymer-based microparticles composed of nanopcarticles. *Journal of Controlled Release* 2010, 142(1):8-13.

28. Kim HK, Chung HJ, Park TG: Biodegradable polymeric microspheres with "open/closed" pores for sustained release of human growth hormone. *Journal of Controlled Release* 2006, 112(2):167-174.

29. Mundargi RC, Babu VR, Rangaswamy V, Patel P, Aminabhavi TM: Nano/micro technologies for delivering macromolecular therapeutics using poly(D,L-lactide-co-glycolide) and its derivatives. *Journal of Controlled Release* 2008, 125(3):193-209.

30. Wang XQ, Wenk E, Zhang XH, Meinel L, Vunjak-Novakovic G, Kaplan DL: Growth factor gradients via microsphere delivery in biopolymer scaffolds for osteochondral tissue engineering. *Journal of Controlled Release* 2009, 134(2):81-90.

31. Wei G, Jin Q, Giannobile WV, Ma PX: Nano-fibrous scaffold for controlled delivery of recombinant human PDGF-BB. *Journal of Controlled Release* 2006, 112(1):103-110.

32. Wei G, Jin Q, Giannobile WV, Ma PX: The enhancement of osteogenesis by nano-fibrous scaffolds incorporating rhBMP-7 nanospheres. *Biomaterials* 2007, 28(12):2087-2096.

33. Wei G, Ma PX: Macroporous and nanofibrous polymer scaffolds and polymer/bone-like apatite composite scaffolds generated by sugar spheres. *Journal of Biomedical Materials Research, Part A* 2006, 78A(2):306-315.

34. Woo KM, Chen VJ, Ma PX: Nano-fibrous scaffolding architecture selectively enhances protein adsorption contributing to cell attachment. *Journal of Biomedical Materials Research, Part A* 2003, 67A(2):531-537.

35. Woo KM, Jun J-H, Chen VJ, Seo J, Baek J-H, Ryoo H-M, Kim G-S, Somerman MJ, Ma PX: Nano-fibrous scaffolding promotes osteoblast differentiation and biomineralization. *Biomaterials* 2006, 28(2):335-343.

36. Li Y, Jiang HL, Zhu KJ, Liu JH, Hao YL: Preparation, characterization and nasal delivery of alpha -cobrotoxin-loaded poly(lactide-co-glycolide)/polyanhydride microspheres. *Journal of Controlled Release* 2005, 108(1):10-20.

37. Schwendeman SP, Tobio M, Joworowicz M, Alonso MJ, Langer R: New strategies for the microencapsulation of tetanus vaccine. *Journal of Microencapsulation* 1998, 15(3):299-318.

38. Kim K, Luu YK, Chang C, Fang D, Hsiao BS, Chu B, Hadjiargyrou M: Incorporation and controlled release of a hydrophilic antibiotic using poly(lactide-co-glycolide)-based electrospun nanofibrous scaffolds. *Journal of Controlled Release* 2004, 98(1):47-56.

39. Wei GB, Pettway GJ, McCauley LK, Ma PX: The release profiles and bioactivity of parathyroid hormone from poly(lactic-co-glycolic acid) microspheres. *Biomaterials* 2004, 25(2):345-352.

40. Kawashima Y, Yamamoto H, Takeuchi H, Hino T, Niwa T: Properties of a peptide containing DL-lactide/glycolide copolymer nanospheres prepared by novel emulsion solvent diffusion methods. *European Journal of Pharmaceutics and Biopharmaceutics* 1998, 45(1):41-48.

41. Yin J, Noda Y, Yotsuyanagi T: Properties of poly(lactic-co-glycolic acid) nanospheres containing protease inhibitors: Camostat mesilate and nafamostat mesilate. *International Journal of Pharmaceutics* 2006, 314(1):46-55.

42. Stoller NH, Johnson LR, Trapnell S, Harrold CQ, Garrett S: The pharmacokinetic profile of a biodegradable controlled-release delivery system containing doxycycline compared to systemically delivered doxycycline in gingival crevicular fluid, saliva, and serum. *J Periodontol* 1998, 69(10):1085-1091.

43. Smith GN, Jr., Mickler EA, Hasty KA, Brandt KD: Specificity of inhibition of matrix metalloproteinase activity by doxycycline. relationship to structure of the enzyme. *Arthritis & Rheumatism* 1999, 42(6):1140-1146.

Chapter 4

Nano-fibrous scaffold for controlled release of Recombinant human basic fibroblast growth factor

Introduction

To address the conflict between the increasing need for tissue and organ transplantation and the donor tissue shortage, tissue engineering has been rapidly developing. One of the most common approaches in tissue engineering is to seed functional cells of interest into three dimensional (3-D) polymeric scaffolds and then either culture the tissue constructs in vitro or implant them [1, 2]. One major factor of determining the success of many implanted tissue constructs is whether they can vascularize rapidly. A lack of blood flow within a tissue may cause ischemia or delayed wound healing. [3-5] Inadequate vascularization hinders the regeneration of a variety of tissues and decreases the long term survival rate of these tissue implants, because sufficient supply of oxygen and nutrients is vital for cells' growth and function. However, native angiogenic process triggered by foreign body response to implantation is too slow or limited to support mass transport for cells in most thick tissue or cell/scaffold constructs. [6-8] Therefore, it is advantageous to incorporate angiogenic strategy in a tissue engeineering approach to stimulate rapid blood vessel formation of high local

density.

Basic fibroblast growth factor (bFGF), a 18-KDa heparin-binding protein, is capable of enhancing the proliferation of fibroblasts, smooth muscle cells, hepatocytes and endothelial cells.[9-12] bFGF is one of the angiogenic growth factors that have been used to stimulate angiogenesis for tissue regeneration in animal studies and clinical trials. [13-16] However, injected bFGF in a solution form loses its biological function rapidly due to its diffusion away from the application site and degradation in vivo, [17] high or repeated doses are usually needed to maintain sufficient therapeutic concentration. To avoid such growth factor waste and inconvenient administration mode, a localized delivery system to release bFGF in a controlled fashion is highly desired. While simple adsorption of growth factors onto a scaffold may help local delivery to certain degree, the loading efficiency is low and the release is not in a controlled way. [18] Several other attempts have been made to specifically incorporate bFGF into scaffolds such as gelatin hydrogels, alginate beads, collagen sponges, [19-22] but they suffered the drawback of short release duration (less than a week). We take a new approach to immobilize bFGF-encapsulated poly(lactide-co-glycolide) (PLGA) nanospheres onto the pore walls of scaffolds to achieve controlled release. By varying the protein loading amount, LA/GA ratio of PLGA copolymer, and the PLGA molecular weight, the release rate and initial burst release of the growth factors can be modulated primarily by the PLGA nanospheres. [23, 24] Several growth factors' bioactivity has been well preserved by incorporating them in biodegradable microspheres when appropriate formulations are used. [25-27]

Previously, our laboratory successfully fabricated macro-porous nano-fibrous PLLA scaffolds with good mechanical properties, [28, 29] which successfully enhanced cell attachment, proliferation, and differentiation due to its nano-fibrous structure similar to that of collagen[30-33]. We have also successfully encapsulated a few growth factors into microspheres or nanospheres and incorporated these spheres into scaffolds to achieve controlled release. [27, 34, 35] However, investigation on the effects of growth factor release profile and dosage on its in vivo function has not been performed before. In this work, basic fibroblast growth factor (bFGF) containing PLGA nanospheres were immobilized onto a PLLA nano-fibrous scaffold. The morphology of the scaffolds and bFGF-containing PLGA nanospheres was observed. The release profiles of the nanospheres, nanosphere incorporated scaffolds, bioactivity of released bFGF, in vivo angiogenesis were examined. The effects of bFGF release rate and bFGF incorporation dosage on in vivo cell penetration and vascularization were also investigated.

Materials and methods

Materials

bFGF was kindly provided by Shenandoah Biotechnology Inc (Warwick, PA) and Akron Biotechnology, LLC (Boca Raton, FL). Radio labeled bFGF (125I-bFGF) was purchased from PerkinElmer Life And Analytical Sciences, Inc (Waltham, MA). Bovine serum albumin (BSA, Fraction V), sodium heparin (Mw 12,000 KDa) D-fructose, mineral oil, and sorbitanmonooleate (span 80) were purchased from Sigma-Aldrich

Chemical Company (St. Louis, MO). PLGA copolymers with LA/GA ratio of 50:50 (Lakeshore BiomaterialsTM, PLGA 50-6.5K, Mw=6.5kDa; PLGA 50-64K, Mw=64KDa) and 75:25 (Lakeshore BiomaterialsTM, PLGA 75-113K, Mw=113 kDa) were purchased from SurModics Pharmaceuticals Inc. (Birmingham, AL). Poly (L-lactic acid) (PLLA) with inherent viscosity of 1.6 dl/g was purchased from Boehringer Ingelheim (Ingelheim, Germany). Poly (vinyl alcohol) (PVA) (88 mol% hydrolyzed, Mw= 25,000 KDa) was obtained from Polysciences Inc. (Warrington, PA). Dichloromethane (DCM), cyclohexane, hexane and tetrahydrofuran (THF) were purchased from Fisher Scientific (Pittsburgh, PA).

Preparation of PLGA NS and NS incorporated nano-fibrous scaffold (NS-scaffold)

bFGF powder was dissolved in 10 mM PBS with the same amount of heparin as bFGF and 50 folds of BSA to form a clear aqueous solution. PLGA nanospheres were fabricated to incorporate bFGF (50μg/100mg polymer) using an established double emulsion technique as described previously. [27, 34, 35] Three PLGA formulations: PLGA50-6.5K, PLGA50-64K and PLGA75-113K were used for *in vitro* release study and radio-labeled ^{125}I-bFGF was added as a tracer (^{125}I-bFGF: unlabeled bFGF= 1:100). bFGF (200μg/100mg polymer) were incorporated into PLGA50-64K NS for *in vivo* study. Blank NS containing only heparin and BSA were prepared as the control. Macro-porous nano-fibrous PLLA scaffolds were prepared by a combination of phase separation and

sugar leaching techniques as described previously. [29] These disc-shaped scaffolds were 7.2 mm in diameter and 2 mm in thickness.

PLGA50-64K NS was incorporated onto PLLA scaffolds using a post seeding method. Briefly, PLGA NS was dispersed in hexane and seeded onto NS-scaffolds drop wise. Then the scaffolds were subjected to a vapor of a mixed solvent of hexane/THF (volume ratio 9:1). The scaffolds were vacuum-dried for 3 days to remove the solvent. The morphology of the nanospheres and the scaffolds before and after nanospheres incorporation was examined using scanning electron microscopy (Philips XL30 FEG SEM).

In vitro release study

In vitro bFGF release profiles from both PLGA NS and PLGA NS incorporated PLLA scaffolds were determined by radioactivity detection as follows: One NS-scaffold or 10 mg nanospheres were suspended in 1.0 ml phosphate buffered saline (PBS, 10 mM, pH=7.4, with 0.1% BSA) at 37 ℃ with orbital shaking at 60 rpm. At the designated time points: 1, 3, 5, 7, 10, 14, 21, 28, 35, 42, 49, 56 and 63 days, supernatant was collected and replaced with an equal amount of fresh medium. The radioactivity of collected supernatant was analyzed by a gamma counter (Gamma 5500, Beckman) and the released bFGF amount was calculated. BSA/heparin containing NS and NS-scaffolds were used as controls.

Subcutaneous implantation

For implantation, male C57BL/6 mice with an age range of 6-8 weeks (Charles River Laboratories) were used in the study. The animal procedures were performed according to the protocol approved by the University of Michigan Committee of Use and Care of Laboratory Animals. Surgery was performed under general inhalation anesthesia with isofluorane as previously described [27]. The back of the animals was shaved, washed and disinfected with povidoneiodine. Two midsagittal incisions were made on the dorsa and two subcutaneous pockets were created using blunt dissection. One scaffold was implanted subcutaneously into each pocket. After placement of the scaffolds, the incisions were closed with staples. The scaffolds were randomly implanted into mice and three scaffolds were implanted for each experiment group (n=3 animals/group). In order to investigate the bioactivity of the released bFGF, three groups of scaffolds were implanted: controlled empty nanofibrous scaffold group, nanofibrous scaffold group with simple absorption of 3μg bFGF/scaffold and nanofibrous scaffold group with PLGA50-64K nanospheres containing 3μg bFGF/scaffold. At the end of each implantation period (4, 7 and 14 days), the mice were sacrificed and the scaffolds were harvested. In order to investigate the effects of bFGF release rate and dosage on bFGF biological functions in vivo, seven groups of scaffolds were implanted into mice (n=3 animals/group). They are: controlled group, group with PLGA50-6.5K nanospheres (3μg bFGF/scaffold), group with PLGA50-64K nanospheres (3μg bFG/scaffold), nanofibrous scaffold group with PLGA75-113K nanospheres (3μg bFGF/scaffold), group

with PLGA50-6.5K nanospheres (0.3µg bFGF/scaffold), nanofibrous scaffold group with PLGA50-6.4K nanospheres (1.5µg bFGF/scaffold) and group with PLGA50-6.5K nanospheres (6µg bFGF/scaffold). The mice were sacrificed and the scaffolds were harvested after 7 days.

Histological examination

The harvested grafts were fixed in 10% neutral buffered formalin, embedded in paraffin, and longitudinally cut into **5** mm thick cross sections. Selected sections were stained with hematoxylin and eosin to evaluate the nature of tissue neogenesis. Images of these specimens were captured using a Nikon Eclipse 50i Microscope (Nikon, Inc., Melville, NY) fitted with a Nikon Digital Sight DS U1 Camera (Nikon, Inc, Melville, NY) for analysis using Image Pro PlusTM Software (Media Cybernetics, Silver Spring, MD). The entire area of the specimen and the area with tissue penetration were measured. The remaining slides were used to perform Factor VIII-related antigen/von Willebrand factor immunohistochemical staining with an anti-human Factor VIII-related antigen/von Willebrand factor rabbit polyclonal antibody (NeoMarkers, Fremont, CA) or a rabbit anti-mouse polyclonal antibody (1:50 dilution) (Abcam, Cambridge, MA). The number of positive-stained blood vessels within the scaffolds was measured.

Results

Characterization of bFGF nanospheres and NS scaffolds

bFGF was incorporated into PLGA nanospheres using a double emulsion technique and three different PLGA formulations (PLGA50-6.5K, PLGA50-64K, PLGA75-113K) were used. All nanospheres made from different PLGA formulations were in a spherical shapes as shown in Figure 4.1(A). The nanospheres of all PLGA formulations have a high encapsulation efficiency of bFGF (68-73%), which was determined by radioactivity detection. Based on SEM observation, the average diameter of the NS was approximately 500 nm.

3-D macro-porous and nano-fibrous PLLA scaffolds were prepared with a high porosity of 98%. SEM observation showed (Figure 4.1(b-c)) that the scaffold possessed multi-level porous architecture. It had spherical macro-pores of 250-425 μm in diameter, inter-pore opening of ~ 100 μm, and nano-fibers of 50-500 nm in diameter within the pore wall of the scaffolds. These nano-fibers were similar to type I collagen fibers in size. The well interconnected porous structure and the nano-fibrous structure were not only important for the cellular activity and tissue penetration, but also efficient for the incorporation of the growth factor containing NS.

Figure 4.1(d-e) shows the morphology of scaffolds after PLGA50-64K nanosphere incorporation. Both the spherical macro-pore and inter-pore opening structures of the scaffolds were well preserved after NS incorporation. The nanospheres were attached to nano-fibers on the pore walls and distributed throughout the scaffolds.

In vitro bFGF release kinetics

Cumulative release of bFGF from PLGA NS and PLGA NS incorporated PLLA scaffolds was shown in Figure. 4.2 (A) and (B). The release of bFGF from PLGA NS and PLGA NS incorporated scaffolds showed similar pattern, while NS-scaffold had a lower initial burst release. This observation was in accordance with our lab's earlier finding on BMP-7 release. [27] It was also discovered that release patterns of different PLGA formulations were different. bFGF was released from PLGA 50-6.5K NS and PLGA50-64K NS scaffold with a 66% and 56% initial burst release respectively. After two weeks, 87% and 78% of bFGF were released from these two scaffolds. bFGF release from PLGA50-64K NS and PLGA50-64k NS scaffolds showed a multi-phasic pattern. The NS and NS scaffolds first rapidly release 46% and 43% during the first two weeks with the burst release of 35% and 26% respectively. From week 4, there was a second rapid release of near 30% bFGF, which was in accordance with the significant mass loss and disintegration of PLGA NS at that time. [27] The bFGF release from both PLGA75-113K NS and NS scaffolds were slow with low burst release and sustained throughout the whole time period. The initial burst release was decreased significantly with an increase in the molecular weight of PLGA and/or LA/GA ratio in the PLGA copolymer. This result shows that by adjusting the chemical and degradation property of the PLGA nanosphere, bFGF release pattern can be controlled.

Controlled release of bFGF stimulated tissue neogenesis and neovascularization

Four days after implantation, tissue in-growth into the scaffolds was minimal in the BSA and bFGF adsorbed groups, while there was more tissue in-growth into the superficial layers of the scaffolds(1-2 layers) in the bFGF NS scaffold release group (Fig. 4.3A). At Day 7, penetrating tissue occupied half the scaffold space in bFGF NS scaffold group, while the tissue penetration was seen only in the superficial regions of the scaffolds in the other two groups (Fig. 4.3B). In addition, there was more vascularization in the bFGF NS scaffold group than the other two groups. At 14 days, penetrating tissue occupied the entire scaffolds in bFGF NS scaffold group. There were still some regions without tissue in the bFGF-Adsorbed only scaffold and BSA NS scaffold (Fig. 4.3C). Parallel to the histological observations, the histomorphometry measurements of 7 and 14 days specimens (Fig. 4.4) showed that the tissue penetration percentage (penetration tissue area versus the whole area), was significantly higher in the bFGF NS release group than in the other two groups. Then, the vascularization within scaffolds was investigated for the *in vivo* effect of released bFGF on blood vessel formation. Factor VIII-related antigen/von Willebrand factor immunohistochemical staining was used. Fig. 4.5 indicated that at 7 days, vascularization inside the scaffolds was greatest in the bFGF NS release group, which is in accordance with the results of measurement of the blood vessel number (Fig.4. 6). However, at 3, and 14 days, the blood vessel numbers in the scaffolds were not significant different among all groups.

Release profile and dosage of bFGF influenced tissue neogenesis and neovascularization

Seven days after implantation, penetrating tissue occupied almost the entire scaffolds in PLGA50-6.5K NS scaffold group (3.0μg bFGF/scaffold), while only approximately half of the scaffolds were penetrated by tissue in-growth in PLGA50-64K NS scaffold group (3.0μg bFGF/scaffold) and PLGA75-113K NS scaffold group (3.0μg bFGF/scaffold). The tissue penetration was seen only in the superficial regions of the scaffold in control group without bFGF. (Fig. 4.5A) The histomorphometry measurements (Fig. 4.5B) showed that the tissue penetration percentage was significantly higher in PLGA50-6.5K NS scaffold group than in the PLGA50-64k NS group and PLGA75-113K NS group (Fig. 4.5B). These three scaffolds all have significant higher cell penetration than control group. In addition, Fig. 4.6A indicated that at 7 days, vascularization inside the scaffolds was greatest in PLGA50-6.5K NS scaffold groups which is in accordance with the results of measurement of the blood vessel number(Fig. 4.6B). According to Fig 4.7. and Fig. 4.8, the tissue penetration and vascularization inside scaffolds increased with the increase of bFGF dosage and peaked at 3μg /scaffold dosage, while the same PLGA1A NS were used to incorporate bFGF.

Discussion

The present study reports for the first time that a 3-D nanofibrous PLLA scaffolds with incorporated PLGA NS provides a desired controlled bFGF delivery in vivo and

enhances tissue neogenesis and angiogenesis. The biologic function of bFGF depends on its release profile from scaffold. With the increase of bFGF release rate, the biologic function of bFGF is enhanced. It was also discovered that the biologic function of bFGF also depends on bFGF incorporation dosage. It increases with the increase of bFGF dosage until an optimal dosage is reached and then it decreases.

One of the great challenges in tissue engineering is to provide adequate oxygen and nutrients transport to the implants to improve cell penetration and vascular invasion to support tissue neogenesis and function. Potent angiogenic agents delivered from the tissue engineered scaffolds can enhance this vascularization process. Basic fibroblast growth factor, one of the angiogenic agents, has good angiogenic and mitogenic properties so that it has been used to stimulate the regeneration of blood vessel [13]and other organs. [36, 37] A sustained and controlled drug delivery system is often necessary to deliver bioactive bFGF over a prolonged period at the target site to increase the therapeutic efficacy of bFGF since bFGF has a short half-life (12 hours in vitro and less than three minutes in vivo). [38, 39] Various natural [19, 40-42]and synthetic [43-45] polymer delivery systems have been developed for bFGF. The ideal delivery system should be able to not only deliver bioactive bFGF in a controlled way but also provide a suitable physical and chemical environment for cellular activity and tissue formation.

Compared to other delivery systems, this new delivery system offers several advantages: First, it provides an excellent environment for cell penetration and neogenesis. In the scaffold, PLLA and PLGA are both FDA approved biodegradable and

biocompatible synthetic. The scaffolds offer good mechanical properties, high porosity (98%), well interconnected macro-pores and inter-pore openings, and a nano-fibrous structure. These structures promotes cell attachment, proliferation, differentiation. [30, 32, 46] Second, bFGF containing PLGA nanospheres were successfully incorporated onto nanofibrous scaffolds using a post seeding technique so that the macro and microstructures of the scaffolds were well preserved. Third, bFGF released from NS immobilized scaffolds were mainly determined by the release pattern of PLGA nanospheres and the NS release pattern was controlled by PLGA copolymer's degradation properties. So, it is appropriate to tailor the release kinetics of growth factors from NS incorporated scaffold by simply choosing or synthesizing the suitable PLGA copolymer for a specific tissue engineering research.

Due to the interconnected macro-pores and inter-pore micro openings and the nano-fibous structures, after 14 days of implantation, cells and tissues penetrated into all scaffold (control, bFGF Absorbed, bFGF NS incorporated) groups (Fig 4.3C). Only bFGF NS incorporated scaffolds showed tissue penetration into the entire scaffolds. The same trend was observed for tissue in-growth at 7 days after subcutaneous implantation (Fig 4.3B). At day 4, only bFGF NS incorporated scaffolds showed significant tissue in-growth into the superficial layer. Immunohistochemical staining after 7 days and blood vessel number measurement (Fig. 4.4B) also confirmed the advantage of NS incorporated NS scaffold over the other two groups in terms of its ability to stimulate blood vessel formation throughout the scaffolds. Results from the 4^{th} and 14^{th} day

showed no significant difference between groups. It is possible that it was too early for the released bFGF to be effective in stimulating blood vessel at Day 4, while at Day 14, native angiogenesis process completes, so no significant difference could be observed. From these results, it was confirmed that bFGF containing NS scaffolds not only protect the bioactivity of the protein against denaturation or degradation, but also release the bioactive growth factors in a prolonged and controlled way, while bFGF Absorbed scaffolds failed to do so.

We also explored the effects of release profile and dosage of bFGF from scaffolds on its in vivo biological functions. It was found at 7 days, PLGA50-6.5K NS scaffold group showed much higher cell penetration percentage (Fig.4.5) and blood vessel formation (Fig. 4.6) than PLGA50-64K and PLGA75-113K NS scaffold groups, while the bFGF dosage of all three scaffolds were kept the same at 3μg/scaffold. PLGA50-6.5K NS scaffold with the lowest molecular weight and lowest LA/GA ratio releases bFGF fastest with a 65% of bFGF released within one week compared to 35% and 25% of bFGF released from PLGA50-64K and PLGA75-113K NS scaffold during the same time period (Fig 4.2B). The higher amount bFGF released from PLGA50-6.5K NS scaffolds stimulated more cell migration into the scaffolds, more cell proliferation and caused more blood vessel formation. It was also found at 7 days, bFGF biological function was enhanced with the increase of bFGF dosage from 0.3 to 3.0μg/scaffold, while all scaffold groups used PLGA50-6.5K NS to incorporate bFGF. (Fig4.7. and Fig 4.8.) This effect is also caused by the increased concentration of bFGF present inside the

scaffolds and surrounding the scaffolds. However, when the dosage of bFGF was increased from 3.0 to 6.0μg/scaffold, a decrease in both cell penetration and blood vessel formation was observed. The possible explanation for this phenomena is that with the excess released bFGF diffused out of the scaffold stimulated cell growth and formed much thick connective tissue capsules surrounding scaffolds compared to other groups (showed with arrows in Fig. 4.7A). This thick tissue capsules layer prevented both more bFGF diffusion out of the scaffolds to recruit cells and cell migration into scaffolds and resulted in a decrease in cell penetration percentage and less blood vessel formation in 7 day time period.

Thus, in order to achieve the goal to improve cell penetration and vascular invasion into the tissue engineering implants to support neogenesis and function, not only angiogenic factors like bFGF needs to be provided with protected bioactivity in a prolonged time period, but also they need be provided with a suitable rate and dosage to achieve optimal effect. If the dosage is too low, not enough cells will be recruited and migrated into scaffold which will result in less tissue penetration and less neo-blood vessel formation. On the other hand, if the dosage is applied too high, tissue encapsulation will be formed around scaffold to block cell migration which will also result in decreased cell penetration and less blood vessel formation. The PLGA NS incorporated nano-fibrous PLLA scaffold descried in this study with its cell attachment, proliferation, differentiation beneficial macro-porous and nanofibrous 3D structure and its easily adjustable controlled release capability of growth factors offers an excellent

tool for tissue engineering scientists to achieve this goal.

Conclusion

We have developed bFGF containing NS incorporated nano-fibrous scaffold, which is capable of releasing bioactive bFGF in a localized and temporally controlled fashion with prolonged duration. This NS-scaffold system functioned well to improve tissue penetration and blood vessel formation due to both its highly interconnected porous structure and its sustained release of bioactive bFGF. The released bFGF functions in vivo in a release rate dependent and dosage dependent fashion. This novel PLGA NS nano-fibrous scaffold with its 3D refined complex structure and controlled bioactive bFGF release capability provides significant potential for multiple tissue engineering applications.

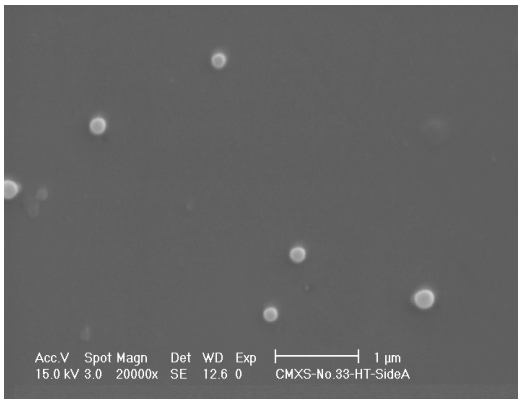

Fig 1A

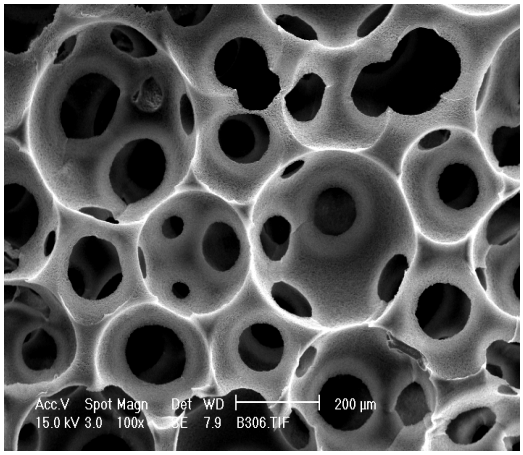

Fig1B

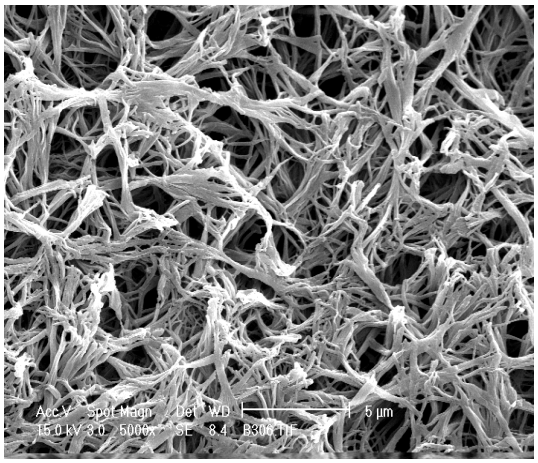

Fig 1C

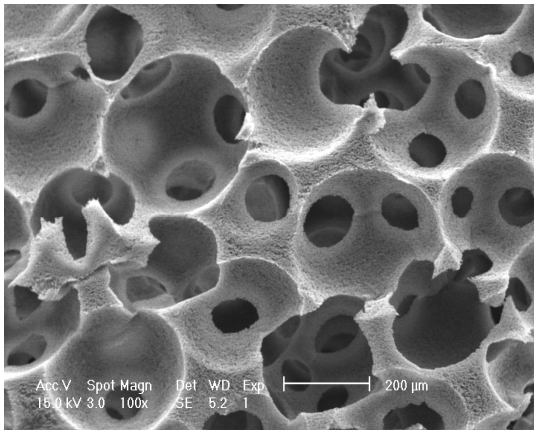

Fig1D

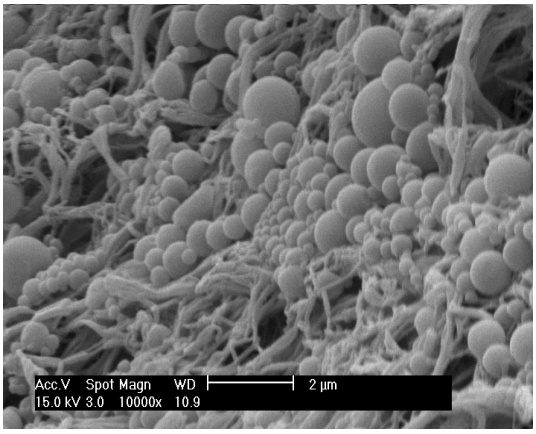

Fig 1E

Fig.4.1. Characterization of PLGA50-64K Nanospheres (NS) and PLLA nano-fibrous scaffold (NS scaffold) before and after NS loading. (A) SEM view of bFGF containing PLGA 50-64K NS; (B, C) SEM view of the PLLA scaffold before NS loading at 100 x (B) and 10,000 x (C); (D, E) SEM view of PLLA scaffold after NS loading at 100 x (D) and 10,000 x (E).

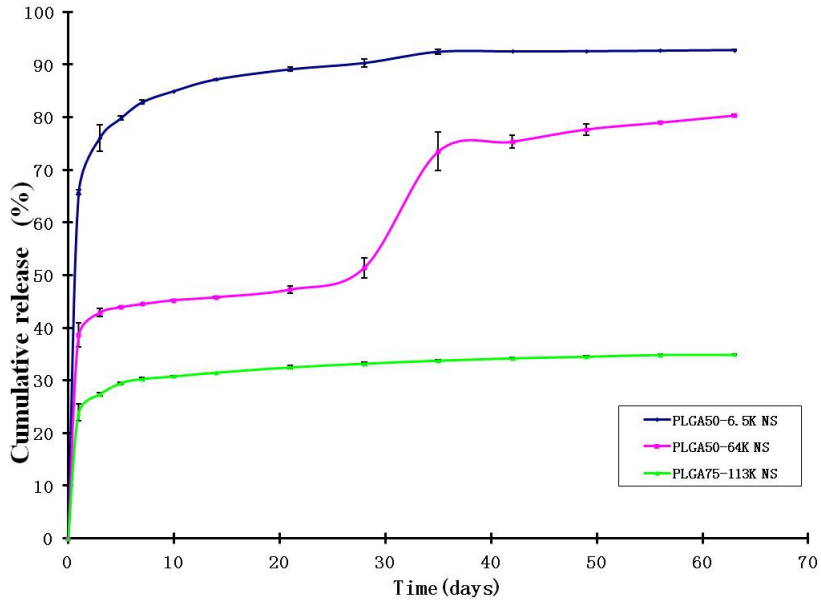

Fig 2 (A)

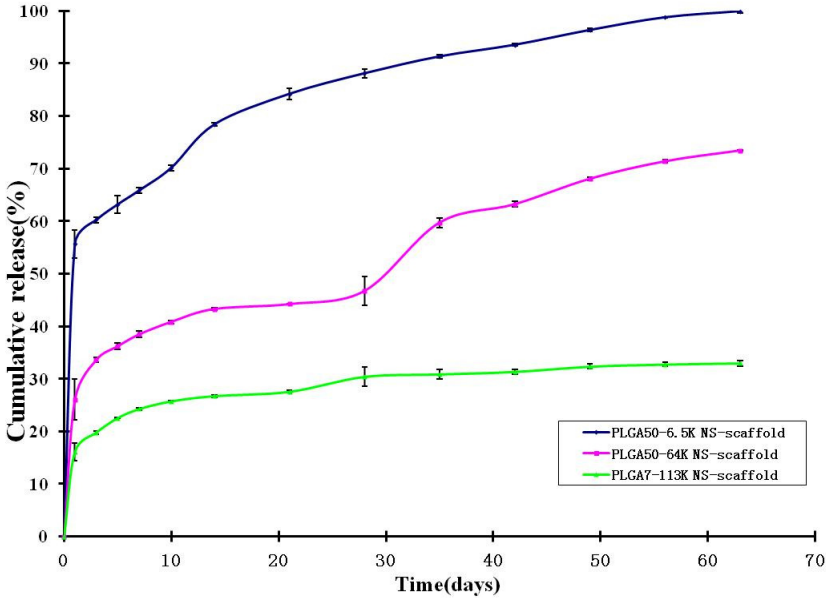

Fig 2(B)

Fig.4.2 *In vitro* release kinetics of bFGF from PLGA NS (200 µg bFGF/100 mg polymer) (A) and PLGA NS loaded nano-fibrous scaffolds (3 µg bFGF/scaffold) (B) in 10 mM PBS. Each data point represents a mean ± standard deviation (n=3).

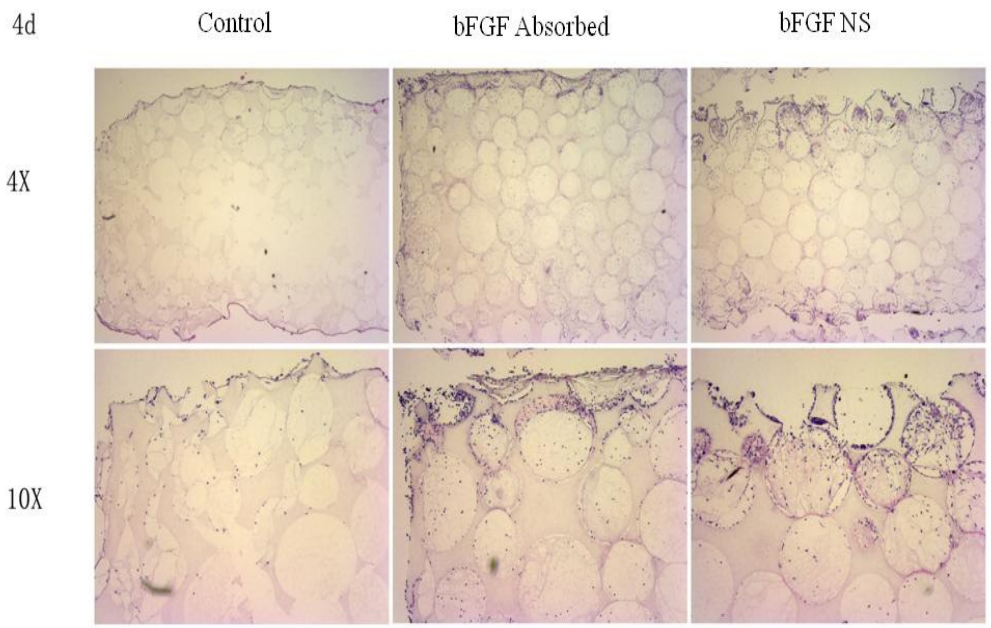
4d
Control
bFGF Absorbed
bFGF NS
4X
10X

Fig 3(A)

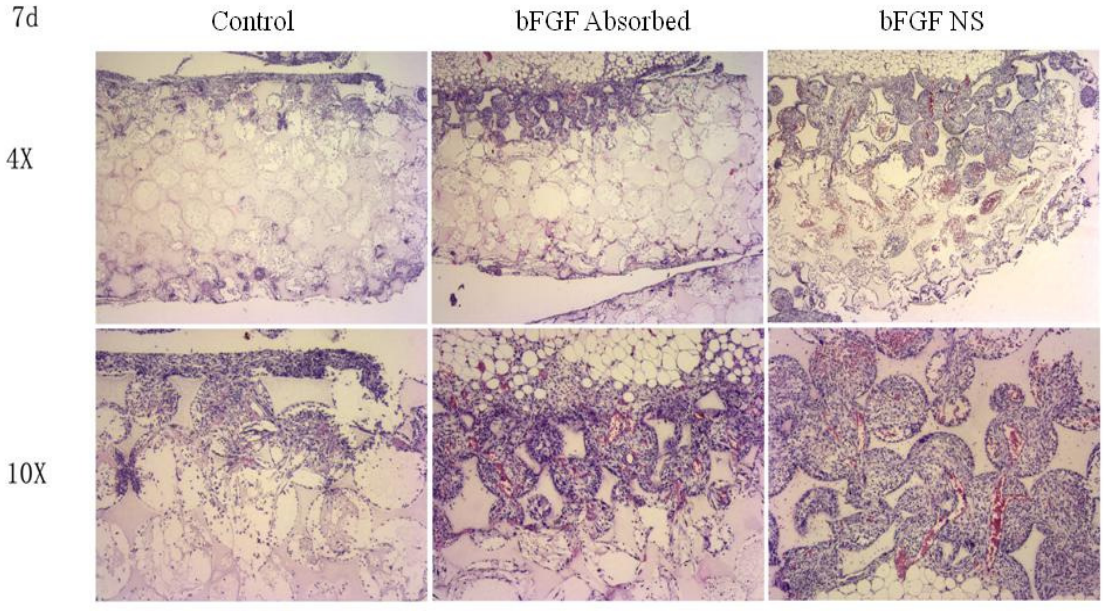
7d
Control
bFGF Absorbed
bFGF NS
4X
10X

Fig 3 (B)

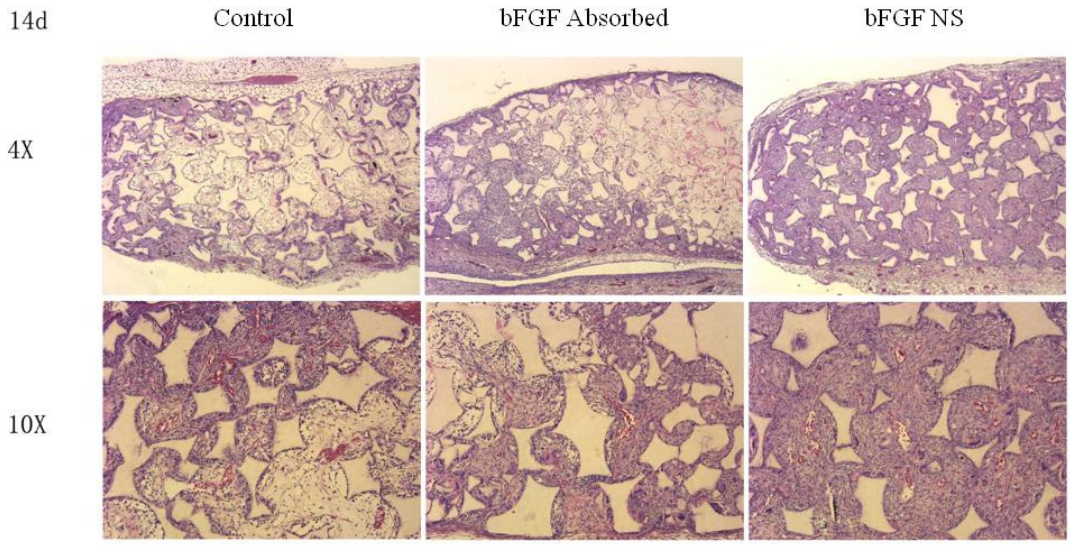

Fig 3(C)

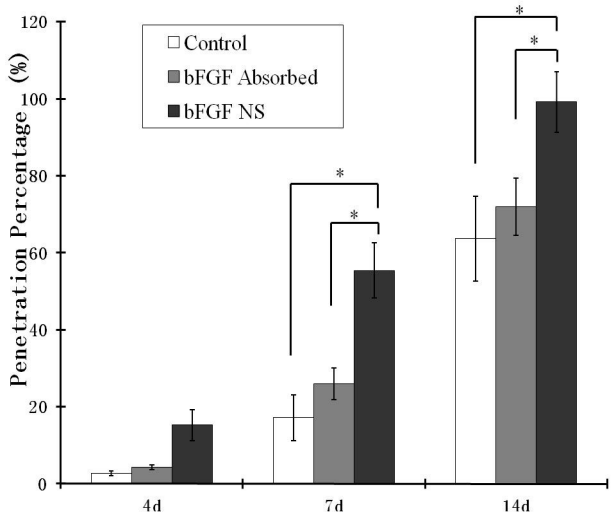

Fig 3(D)

Fig.4.3. Microscopic observation of the H & E stained tissue sections harvested of three scaffolds groups (4 days (A); 7 days (B); 14 days (C) after implantation (Control: no bFGF, bFGF Absorbed: 3µg bFGF simple absorption, bFGF NS: 3µg bFGF loaded in NS); 4 x for full cross sections, and 10 x for high magnification views. Tissue Penetration percentage calculated from sectioned scaffold groups 4 days, 7days, 14days after implantation (D). Each data point represents a mean ± standard deviation (n=3). *P<0.05.

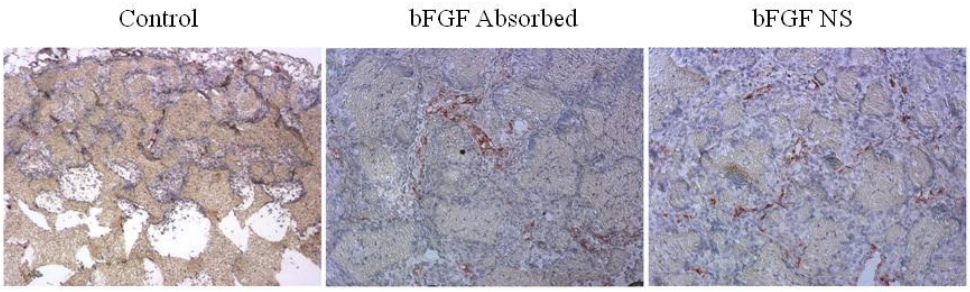

Fig 4(A).

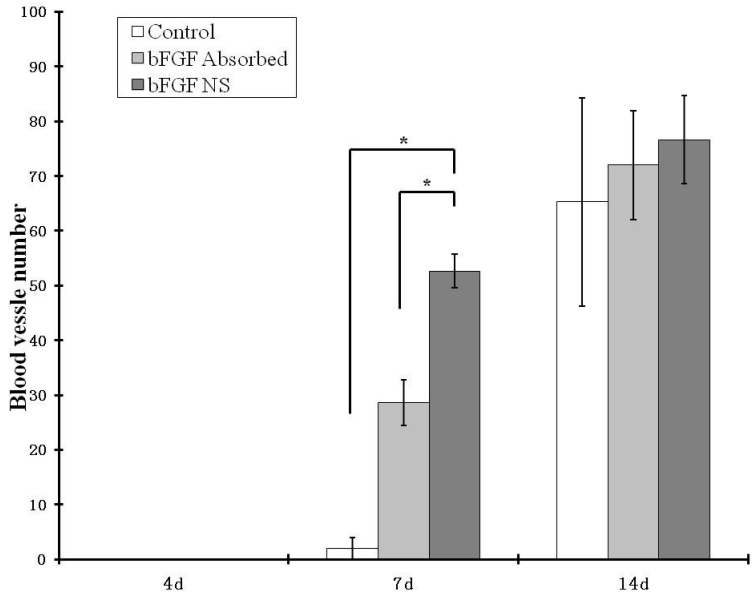

Fig 4(B).

Fig.4.4 (A) Microscopic observation of the Factor VIII-related antigen/von Willebrand factor stained tissue sections harvested of three scaffolds groups 7 days after implantation (Control: no bFGF, bFGF Absorbed: 3µg bFGF simple absorption, bFGF NS: 3µg bFGF loaded in NS), 10 x for high magnification views. (4days and 14days microscopic data not shown) (B) Blood vessel number calculated from sectioned scaffold groups 4 days, 7days, 14days after implantation. Each data point represents a mean $\pm$ standard deviation (n=3). *P<0.05.

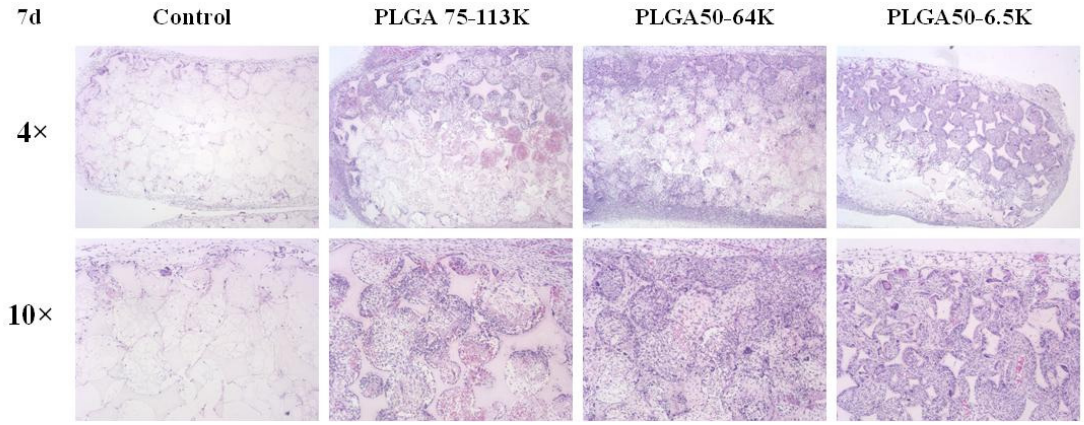

Fig 5 (A)

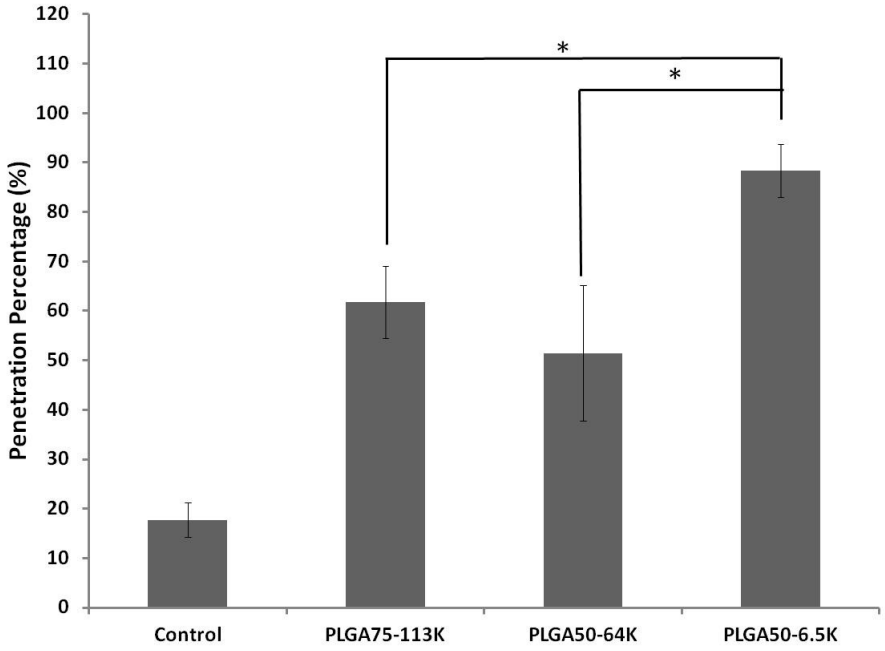

Fig 5(B)

Fig.4.5. (A) Microscopic observation of the H & E stained tissue sections harvested of three scaffolds groups 7 days after implantation (3µg bFGF/scaffold); 4 x for full cross sections, and 10 x for high magnification views. **(B)** Tissue Penetration percentage calculated from sectioned scaffold implant groups 7days after implantation, Each data point represents a mean ± standard deviation (n=3). *P<0.05. Control group was significantly lower than the other three groups, P<0.05.

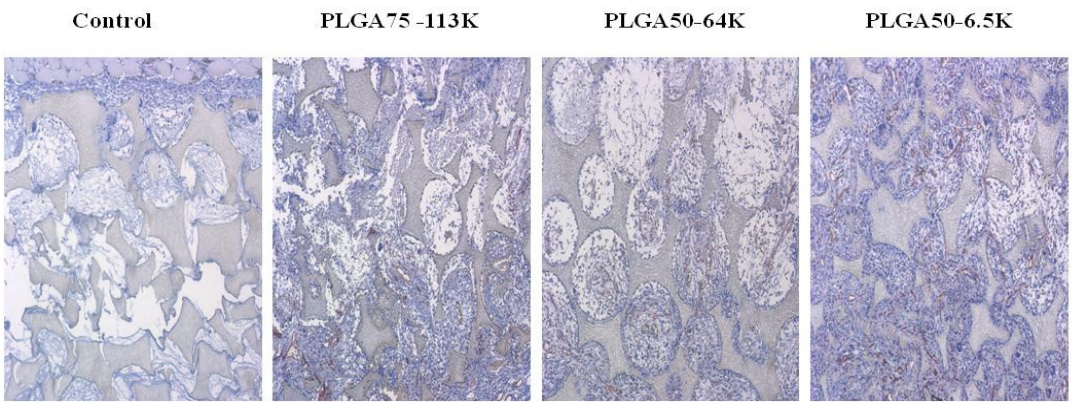

Fig 6 (A)

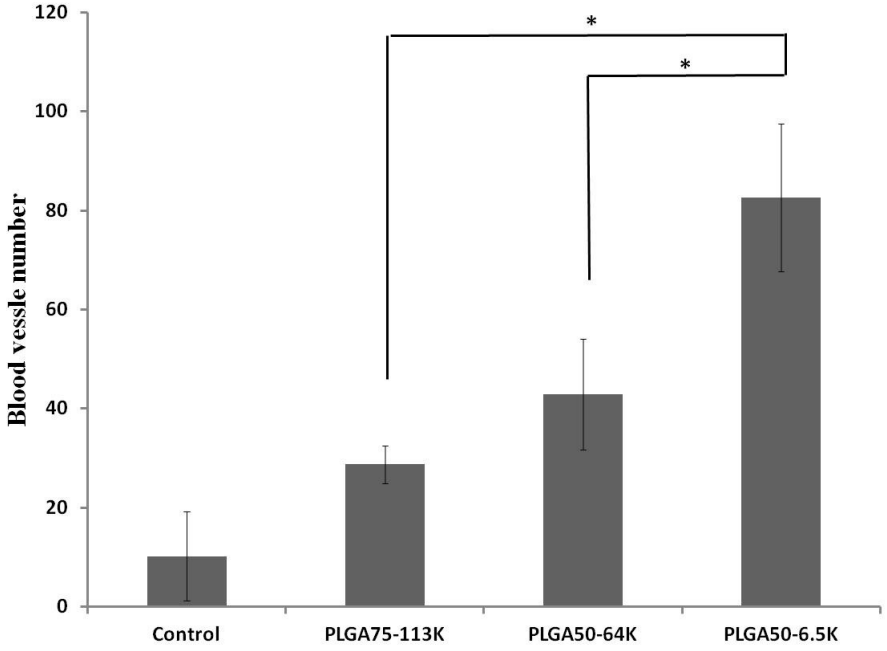

Fig 6 (B)

Fig.4.6. (A) Microscopic observation of the H & E stained tissue sections harvested of three scaffolds groups 7 days after implantation; 4 x for full cross sections, and 10 x for high magnification views. **(B)** Tissue Penetration percentage calculated from sectioned scaffold groups 7days after implantation. Each data point represents a mean ± standard deviation (n=3). *P<0.05, Control group was significantly lower than PLGA50-6.5K-1.5µg, PLGA50-1A-3µg and PLGA50-6.5K-6µg groups, P<0.05. There is no significant difference between control group and PLGA50-6.5K-0.3 µg group.

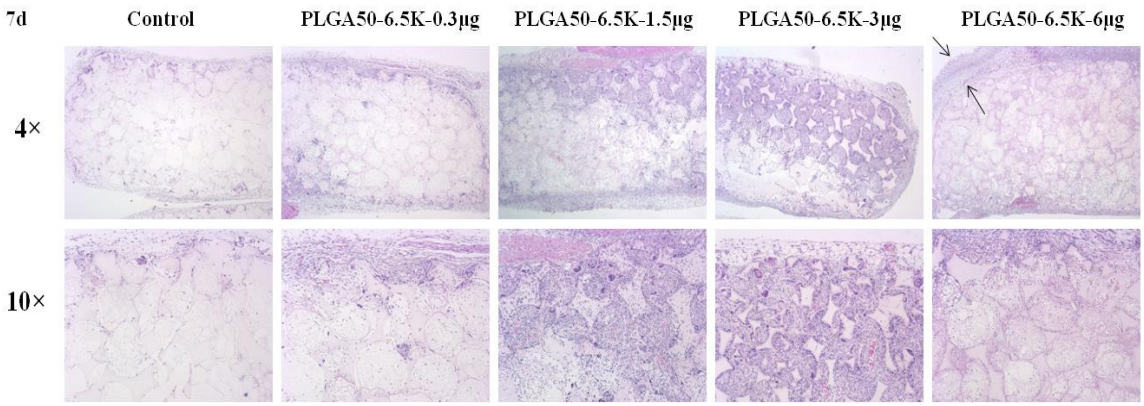

Fig 7(A)

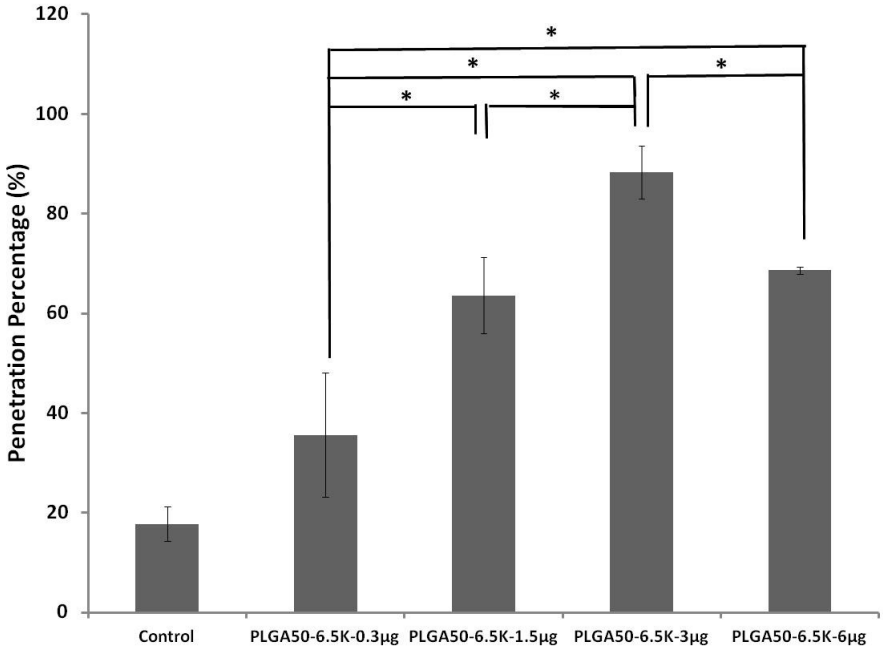

Fig 7 (B)

Fig.4.7. (A) Microscopic observation of CD31 stained tissue sections harvested of three scaffolds groups 7 days after implantation (3µg bFGF/scaffold), 10 x for high magnification views. **(B)** Blood vessel number calculated from sectioned scaffold groups 7days after implantation. Each data point represents a mean ± standard deviation (n=3). *P<0.05. Control group was significantly lower than the PLGA50-64K and PLGA50-6.5K groups, P<0.05, there is no significant difference between control and PLGA75-113K group.

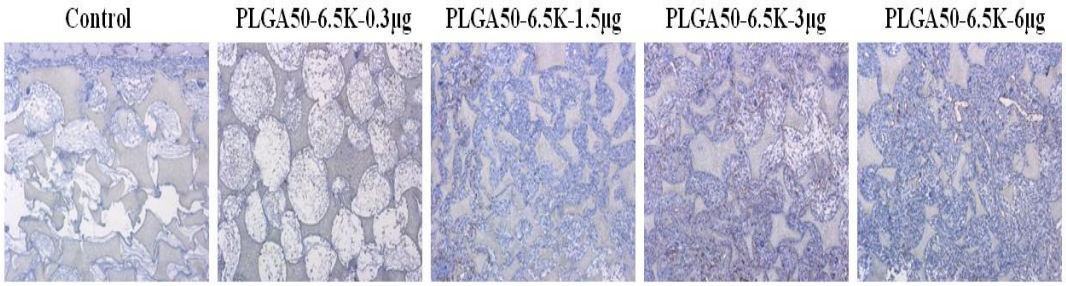

Fig 8(A)

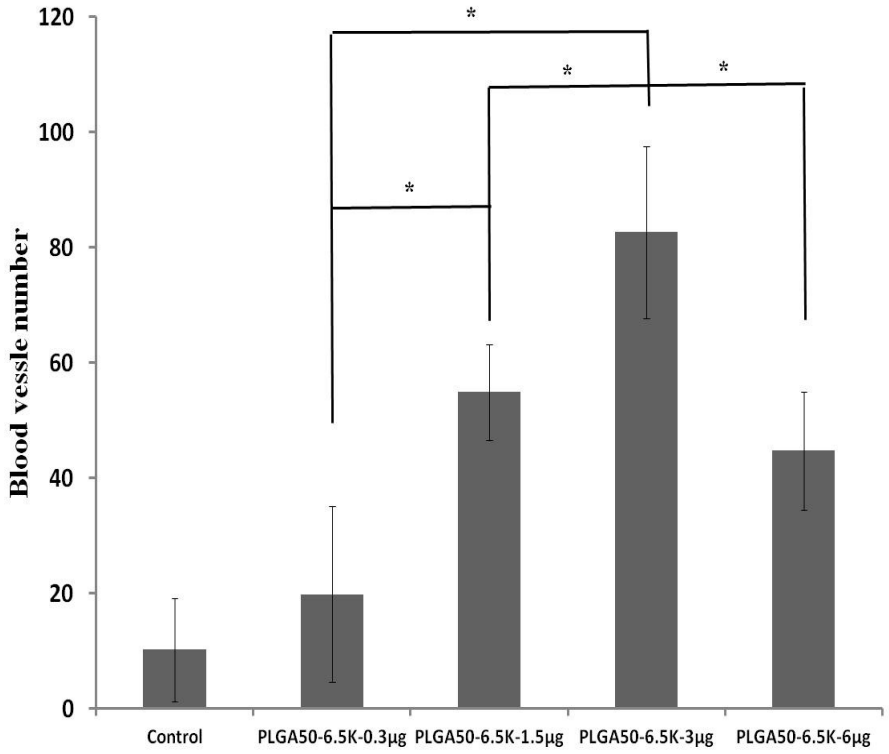

Fig 8(B)

Fig.4.8. (A) Microscopic observation of CD31 stained tissue sections harvested of three scaffolds groups 7 days after implantation, 10 x for high magnification views. **(B)** Blood vessel number calculated from sectioned scaffold groups 7days after implantation. Each data point represents a mean $\pm$ standard deviation (n=3). *P<0.05. Control group was significantly lower than PLGA50-6.5K-1.5µg, PLGA50-6.5K-3µg and PLGA50-6.5K-6µg, P<0.05. There is no significant difference between control group and PLGA50-6.5K-0.3 µg group.

References

1. Langer R, Vacanti JP: Tissue engineering. *Science* 1993, 260(5110):920-926.

2. Vacanti JP, Langer R: Tissue engineering: the design and fabrication of living replacement devices for surgical reconstruction and transplantation. *Lancet* 1999, 354 Suppl 1:SI32-34.

3. Carmeliet P: Angiogenesis in health and disease. *Nat Med* 2003, 9(6):653-660.

4. Li J, Zhang Y-P, Kirsner RS: Angiogenesis in wound repair: angiogenic growth factors and the extracellular matrix. *Microsc Res Tech* 2003, 60(1):107-114.

5. Carmeliet P: Mechanisms of angiogenesis and arteriogenesis. *Nat Med* 2000, 6(4):389-395.

6. Mikos AG, Sarakinos G, Lyman MD, Ingber DE, Vacanti JP, Langer R: Prevascularization of porous biodegradable polymers. *Biotechnol Bioeng* 1993, 42:716-723.

7. Perets A, Baruch Y, Weisbuch F, Shoshany G, Neufeld G, Cohen S: Enhancing the vascularization of three-dimensional porous alginate scaffolds by incorporating controlled release basic fibroblast growth factor microspheres. *J Biomed Mater Res A* 2003, 65A(4):489-497.

8. Radisic M, Euloth M, Yang L, Langer R, Freed LE, Vunjak-Novakovic G: High-density seeding of myocyte cells for cardiac tissue engineering. *Biotechnol Bioeng* 2003, 82(4):403-414.

9. Neufeld G, Gospodarowicz D: Identification of the fibroblast growth factor receptor in human vascular endothelial cells. *J Cell Physiol* 1988, 136(3):537-542.

10. Burgess WH, Maciag T: The heparin-binding (fibroblast) growth factor family of proteins. *Annu Rev Biochem* 1989, 58:575-606.

11. Baruch Y, Shoshany G, Neufeld G, Enat R: Basic fibroblast growth factor is hepatotropic for rat liver in regeneration. *J Hepatol* 1995, 23(3):328-332.

12. Baird A, Walicke PA: Fibroblast growth factors. *Br Med Bull* 1989, 45(2):438-452.

13. Asahara T, Bauters C, Zheng LP, Takeshita S, Bunting S, Ferrara N, Symes JF, Isner JM: Synergistic effect of vascular endothelial growth factor and basic fibroblast growth factor on angiogenesis in vivo. *Circulation* 1995, 92(9):365-371.

14. Gibran NS, Isik FF, Heimbach DM, Gordon D: Basic fibroblast growth factor in the early human burn wound. *J Surg Res* 1994, 56(3):226-234.

15. Laham RJ, Sellke FW, Edelman ER, Pearlman JD, Ware JA, Brown DL, Gold JP, Simons M: Local perivascular delivery of basic fibroblast growth factor in patients undergoing coronary bypass surgery: results of a phase I randomized, double-blind, placebo-controlled trial. *Circulation* 1999, 100(18):1865-1871.

16. Radomsky ML, Thompson AY, Spiro RC, Poser JW: Potential role of fibroblast growth factor in enhancement of fracture healing. *Clin Orthop Relat Res* 1998(355 Suppl):S283-293.

17. Nimni ME: Polypeptide growth factors: targeted delivery systems. *Biomaterials* 1997, 18(18):1201-1225.

18. Ziegler J, Mayr-Wohlfart U, Kessler S, Breitig D, Gunther KP: Adsorption and release properties of growth factors from biodegradable implants. *J Biomed Mater Res A* 2002, 59(3):422-428.

19. DeBlois C, Cote MF, Doillon CJ: Heparin-fibroblast growth factor-fibrin complex: in vitro and in vivo applications to collagen-based materials. *Biomaterials* 1994, 15(9):665-672.

20. Edelman ER, Mathiowitz E, Langer R, Klagsbrun M: Controlled and modulated release of basic fibroblast growth factor. *Biomaterials* 1991, 12(7):619-626.

21. Tabata Y, Yamada K, Miyamoto S, Nagata I, Kikuchi H, Aoyama I, Tamura M, Ikada Y: Bone regeneration by basic fibroblast growth factor complexed with biodegradable hydrogels. *Biomaterials* 1998, 19(7-9):807-815.

22. Yamada K, Tabata Y, Yamamoto K, Miyamoto S, Nagata I, Kikuchi H, Ikada Y: Potential efficacy of basic fibroblast growth factor incorporated in biodegradable hydrogels for skull bone regeneration. *J Neurosurg* 1997, 86(5):871-875.

23. Yang YY, Chung TS, Ping Ng N: Morphology, drug distribution, and in vitro release profiles of biodegradable polymeric microspheres containing protein

fabricated by double-emulsion solvent extraction/evaporation method. *Biomaterials* 2000, 22(3):231-241.

24. Yeo Y, Park K: A new microencapsulation method using an ultrasonic atomizer based on interfacial solvent exchange. *J Controlled Release* 2004, 100(3):379-388.

25. Gospodarowicz D, Ferrara N, Schweigerer L, Neufeld G: Structural characterization and biological functions of fibroblast growth factor. *Endocr Rev* 1987, 8(2):95-114.

26. Jansen JA, Vehof JWM, Ruhe PQ, Kroeze-Deutman H, Kuboki Y, Takita H, Hedberg EL, Mikos AG: Growth factor-loaded scaffolds for bone engineering. *J Controlled Release* 2005, 101(1-3):127-136.

27. Wei G, Jin Q, Giannobile WV, Ma PX: The enhancement of osteogenesis by nano-fibrous scaffolds incorporating rhBMP-7 nanospheres. *Biomaterials* 2007, 28(12):2087-2096.

28. Chen VJ, Ma PX: Nano-fibrous poly(l-lactic acid) scaffolds with interconnected spherical macropores. *Biomaterials* 2004, 25(11):2065-2073.

29. Wei G, Ma PX: Macroporous and nanofibrous polymer scaffolds and polymer/bone-like apatite composite scaffolds generated by sugar spheres. *J Biomed Mater Res A* 2006, 78A(2):306-315.

30. Woo KM, Chen VJ, Ma PX: Nano-fibrous scaffolding architecture selectively enhances protein adsorption contributing to cell attachment. *J Biomed Mater Res A* 2003, 67A(2):531-537.

31. Smith LA, Liu X, Hu J, Ma PX: The influence of three-dimensional nanofibrous scaffolds on the osteogenic differentiation of embryonic stem cells. *Biomaterials* 2009, 30(13):2516-2522.

32. Woo KM, Jun J-H, Chen VJ, Seo J, Baek J-H, Ryoo H-M, Kim G-S, Somerman MJ, Ma PX: Nano-fibrous scaffolding promotes osteoblast differentiation and biomineralization. *Biomaterials* 2006, 28(2):335-343.

33. Jing W, Xiaohua L, Xiaobing J, Haiyun M, Jiang H, Longxing N, Peter XM: The odontogenic differentiation of human dental pulp stem cells on nanofibrous poly(l-lactic acid) scaffolds in vitro and in vivo. *Acta Biomater*.

34. Wei G, Jin Q, Giannobile WV, Ma PX: Nano-fibrous scaffold for controlled delivery of recombinant human PDGF-BB. *J Controlled Release* 2006, 112(1):103-110.
35. Wei G, Pettway GJ, McCauley LK, Ma PX: The release profiles and bioactivity of parathyroid hormone from poly(lactic-co-glycolic acid) microspheres. *Biomaterials* 2003, 25(2):345-352.

36. Ono I, Gunji H, Zhang JZ, Maruyama K, Kaneko F: A study of cytokines in burn blister fluid related to wound healing. *Burns* 1995, 21(5):352-355.

37. Chen WY, Rogers AA, Lydon MJ: Characterization of biologic properties of wound fluid collected during early stages of wound healing. *J Invest Dermatol* 1992, 99(5):559-564.

38. Edelman ER, Nugent MA, Karnovsky MJ: Perivascular and Intravenous Administration of Basic Fibroblast Growth-Factor - Vascular and Solid Organ Deposition. *Proc Natl Acad Sci U S A* 1993, 90(4):1513-1517.

39. Westall FC, Rubin R, Gospodarowicz D: Brain-derived fibroblast growth factor: a study of its inactivation. *Life Sci* 1983, 33(24):2425-2429.

40. Cote M-F, Laroche G, Gagnon E, Chevallier P, Doillon CJ: Denatured collagen as support for a FGF-2 delivery system: physicochemical characterizations and in vitro release kinetics and bioactivity. *Biomaterials* 2004, 25(17):3761-3772.

41. Kawai K, Suzuki S, Tabata Y, Ikada Y, Nishimura Y: Accelerated tissue regeneration through incorporation of basic fibroblast growth factor-impregnated gelatin microspheres into artificial dermis. *Biomaterials* 2000, 21(5):489-499.

42. Tanihara M, Suzuki Y, Yamamoto E, Noguchi A, Mizushima Y: Sustained release of basic fibroblast growth factor and angiogenesis in a novel covalently crosslinked gel of heparin and alginate. *J Biomed Mater Res A* 2001, 56(2):216-221.

43. Desire L, Mysiakine E, Bonnafous D, Couvreur P, Sagodira S, Breton P, Fattal E: Sustained delivery of growth factors from methylidene malonate 2.1.2-based polymers. *Biomaterials* 2006, 27(12):2609-2620.

44. Maquet V, Martin D, Scholtes F, Franzen R, Schoenen J, Moonen G, Jerome R: Poly(d,l-lactide) foams modified by poly(ethylene oxide)-block-poly(d,l-lactide)

copolymers and a-FGF: in vitro and in vivo evaluation for spinal cord regeneration. *Biomaterials* 2001, 22(10):1137-1146.

45. Hile DD, Amirpour ML, Akgerman A, Pishko MV: Active growth factor delivery from poly(dl-lactide-co-glycolide) foams prepared in supercritical CO2. *J Controlled Release* 2000, 66(2-3):177-185.

46. Chen VJ, Smith LA, Ma PX: Bone regeneration on computer-designed nano-fibrous scaffolds. *Biomaterials* 2006, 27(21):3973-3979.

Chapter 5

Dual release of bone morphogenetic protein-7(BMP-7) and platelet derived growth factor (PDGF) from nano-fibrous PLLA scaffolds for periodontal tissue regeneration

Introduction

Today, there are more than 50 million adults suffer from severe periodontitis in US. [1] Periodontitis, being the leading cause of tooth loss, is a common oral inflammatory infectious disease that can lead to the destruction of tooth supporting tissues such as alveolar bone, periodontal ligament and cementum.[2] Clinical periodontal therapies which mainly deal with eliminating inflammation sources and halting disease progression are not sufficient in complete regeneration of these multi-tissue tooth supporting structures and restoration of their full biological functions. [3] Therefore, it will be a great clinical impact to be able to restore these soft/hard multi tissue structures with dental tissue engineering approach. One important strategy in dental tissue engineering is to deliver signaling cues (e.g, growth factors) [4, 5] Bone morphogenetic proteins (BMPs) and Platelet derived growth factor (PDGF) are two important growth factors for dental tissue development.

Bone morphogenetic proteins (BMPs) are important growth factors in bone development and regeneration. [6, 7] BMP-2, BMP-4 and BMP-7 are the most effective ones in inducing bone formation at both orthotopic and ectopic sites among members of BMP family.[8-13] BMP-7 has been used in periodontal regeneration to promote

osteogensis, cementogenesis and periodontal ligament reconstruction. [14-16] However, despite BMPs' success in bone regeneration in animal and preclinical studies, their clinical success are limited due to their very high dosage requirement and the high cost and complications associated with it. [17, 18] First possible solution to this problem could be the development of an appropriate BMP delivery system which enables a prolonged BMP release duration and protects BMP from proteolysis, denaturation and bioactivity loss to stimulate bone regeneration. [19-21] Second possible solution to this problem could be delivery of other growth factors alone with BMP to introduce synergetic effect and lower BMP dosage needed. [22] Platelet derived growth factor (PDGF) belongs to a multifunctional growth factor family. PDGF is composed of A, B, C and D polypeptide chains to form homo- or heterodimeric molecules. [23] PDGF can bind to two structurally related, intrinsic tyrosine kinase receptors (PDGF-Rα and PDGF-Rβ) [24]to modulate cell migration and proliferation, prevent cell apoptosis and promote extracellular matrix synthesis and vascularization.[24-27] PDGF plays an important role in both organ development [26]and tissue repair. [28-30] Recombinant PDGF has been widely studied as a potential therapeutic agent to enhance periodontal wound repair [29] and regeneration preclinically [31-33]and clinically. [34, 35] PDGF has been approved by FDA for enhancing bone repair of periodontal osseous defects. [29, 36]

Our previous researches developed novel PLGA nanospheres immobilized PLLA nanofibrous scaffold that could locally release single growth factor in a controlled fashion. [37, 38] Sustained release of BMP-7 from this PLLA scaffold induced significant ectopic bone formation [38]while sustained release of PDGF promoted neogenesis and angiogenesis successfully[39]. One advantage of this scaffold release

system is its ability to deliver multiple growth factors in distinct dosages and release rates. Therefore, we hypothesize that localized dual release of BMP-7 and PDGF from PLLA nanofibrous scaffold in a controlled fashion can significantly improve bone formation. In the present study, we investigate the synergetic effect of controlled dual release of BMP-7 and PDGF from the novel PLLA nano-fibrous scaffolds in both mouse ectopic bone formation model and rat periodontal fenestration defect repair model.

Materials and Methods

Materials

RhBMP-7 and rhPDGF were kindly provided by Stryker Biotech (Hopkinton, MA) and Biomimetic Therapeutics (Franklin, TN) respectively. PLGA copolymers with LA/GA ratio of 50:50 (Lakeshore Biomaterials™, PLGA50-6.5K, Mw = 6.5 kDa; PLGA50-64K, Mw = 64KDa) were purchased from SurModics Pharmaceuticals Inc. (Birmingham, AL). Poly(L-lactic acid) (PLLA) with inherent viscosity of 1.6 dl/g was purchased from Boehringer Ingelheim (Ingelheim, Germany). Poly(vinyl alcohol) (PVA) (88 mol% hydrolyzed, M_W = 25,000) were obtained from Polysciences Inc. Trifluoroacetic acid (TFA), Bovine serum albumin (BSA, Fraction V) and gelatin (type B from bovine skin) were obtained from Sigma Aldrich (St Louis MO). Dichloromethane (DCM), cyclohexane, hexane, tetrahydrofuran (THF) were purchased from Fisher Scientific (Pittsburgh, PA).

Preparation of nanosphere-immobilized nano-fibrous scaffolds (NS-NFS)

Nanofibrous PLLA scaffolds were fabricated as previously described. The scaffolds have high porosity of 98%. They have macropores 250-425 μm in diameter and an

average interpore opening size of 116 μm. [40] For mouse subcutaneous implantation, highly porous scaffold were cut into circular disks with dimensions of 3.6 mm in diameter and 2 mm in thickness. For rat periodontal fenestration defect implantation, scaffolds were cut into rectangular cylinder with dimensions of 3mm(L)×3mm(W)×2mm(H).

rhBMP-7 was incorporated into PLGA50-6.5K NS and rhPDGF was encapsulated into PLGA50-64K NS respectively using a double emulation techniques as previously described. [37, 38] PLGA NS were incorporated nanofibrous PLLA scaffolds using a post-seeding method. [37, 38] The growth factor amount in a scaffold was determined by the concentration of growth factor encapsulated in the PLGA NS and the amount of NS immobilized onto scaffold. NS containing gelatin/BSA was also incorporated into scaffolds and used as a control. After the post-seeding, the NS were further immobilized onto the scaffold wall by exposing the scaffold to a mixed vapor of hexane/THF (volume ratio 9/1) followed by vacuum drying for 3 days. The morphology of the scaffolds before and after the dual growth factors immobilization was observed using scanning electron microscopy (SEM, Philips SL30 FEG).

Preparation of implants

For the mouse subcutaneous implantation study, 18 groups of scaffold implants (total 216 scaffold implants) were prepared as listed in table 5.1. Three BMP-7 dosages chosen for subcutaneous study were 0, 0.5 and 1.5 μg/scaffold, while the PDGF dosages were varied from 5 times to one fifth of each corresponding BMP-7 dosage. For rat periodontal fenestration defect implantation, four groups of scaffold implants (total 26

scaffold implants) were prepared as listed in table 5.2. The BMP-7 dosage was 1.5 μg/scaffold, and the PDGF was kept at 3 μg/scaffold, BMP/PDGF ratio was kept at 1:2.

Mouse subcutaneous implantation

All animal procedures were approved by the University of Michigan Committee on Use and Care of Animals. For surgical procedures, general anesthesia was administered to six-week old, male C57/BL6 mice (Harlan Laboratories, Indianapolis, IN) by isoflurane inhalation. The backs of the animals were shaved and disinfected with a 10% povidone-iodine solution. Two midsagittal incisions (approx. 1 cm) were made on the dorsa of each mouse and two subcutaneous pockets were created using blunt forceps on each side of the incision, allowing four scaffolds to be implanted in each mouse. The NF-scaffolds were carefully implanted into each pocket and the incisions were closed with surgical staples. At the end of each implantation period (3 or 6 weeks), the mice were euthanized by carbon dioxide overdose and the scaffolds were harvested for analysis.

Rat periodontal fenestration defect implantation

General anesthesia was performed on rat with ketamine (90 mg/kg) and xylazine (10 mg/kg). Ophthalmic ointment was applied to prevent irritation and reduce eye dryness during surgery. After reflecting the skin and the muscle by incision, full thickness mucoperiosteal flaps were elevated around the mandibular 1st molar. One periodontal fenestration defect was created on the buccal side of the mandible in each rat. The standard fenestration defect (3×2 mm^2 dimension) exposed the distal root surface of the 1st molar tooth. The cementum layer on the exposed root surface was removed and the

dentin surface was exposed. Each scaffold was implanted into the fenestration defect. The muscle and skin incisions were sutured and closed with surgical staples, respectively. Caprofen (5 mg/kg) was administrated subcutaneously as analgesic approximately 1 hour post-surgery. To maintain energy and prevent infection, animals were given a 5% dextrose solution in water containing 268 g/L ampicillin for one week post-surgery. 5 weeks later, animals were euthanized with CO_2 and biopsies were collected and fixed with 10% phosphate-buffered neutral formalin. All animal surgeries were performed under a protocol approved by the University Committee on Use and Care of Animals at the University of Michigan.

Micro-computed tomography volumetric measurements

Both mouse subcutaneous implantation and rat periodontal fenestration defect implantation scaffold samples were subject to micro-computed tomography (micro-CT) Volumetric Measurements. Non-decalcified subcutaneous implant and mandible specimens were scanned at a resolution of 18x18x18 μm^3 voxels using a µCT 100 cabinet cone-beam micro-CT system (Scanco USA, Inc, Wayne, PA). GEHC MicroView Analysis+ 2.1.2® software (GE Healthcare, Little Chanlfont, UK) was used to create three-dimensional (3D) reconstructions of harvested specimens as previously described [41]. Specimen scans were then oriented into standardized position. For subcutaneous implant specimens, the region of interest (ROI) for analysis of mineralized tissue formation encompassed the entire specimen. The ROI for analysis of mineralized tissue formation in mandible specimens was created using the horizontal length of entire defect and vertical length of the recessed surface along the exposed distal root of the first molar

[42]. To distinguish between mineralized and non-mineralized voxels, the threshold gray-scale value for each subcutaneous implant specimen was determined by one masked and calibrated examiner, while the other masked and calibrated examiner determined the threshold value for each of the mandible specimens. The average threshold gray-scale value was calculated and used as the representative value to derive the following parameters: tissue mineral content (TMC, mg), and tissue mineral density (TMD, mg/cm^3) for implant and mandible specimens. Bone volume fraction represents the ratio between the bone volume and total ROI volume. TMC represents the amount of calcified tissue present, while TMD is a measure of bone quality – represented by the formula TMC/BV.

Calcium content measurement

Mouse subcutaneous implantation samples were subject to calcium content measurement. After MicroCT scanning of non-decalcified subcutaneous implant, the implants were rinsed with MilliQ water, lyophilized, dissolved with 10 ml HClO. One microlitter of the resulting solution was added to 5 ml mix solution of calcium buffer reagent and calcium color reagent in the calcium measure kit (Pointe Scientific, Inc. Canton, MI). The solution was incubated at room temperature for 5 minutes, and read at 650 nm in UV spectrophotometer. Five mg/ml of calcium chloride solution was used as a standard.

Histological examination

Both mosue subcutaneous implantation and Rat periodontal fenestration defect implantation scaffold samples were subject to histological examination. For mice

subcutaneous study, after 3 and 6 weeks, scaffolds implants were harvested. They were fixed in neutral buffered 10% formalin and then embedded in paraffin. Five-micrometer sections were cut and stained with hematoxylin and eosin (H&E) for light microscopic observation. [15, 43]

For rat periodontal fenestration defect implantation study, regenerated tissue on scaffolds was harvest 2 and 5 weeks after surgery and were then placed into Bouin's fixative, decalcified with 10% vol/vol acetic acid, 4% vol/vol formaldehyde, 0.85% NaCl for 2 to 3 weeks and then embedded in paraffin. The specimens were cut into 4 to 5 μm coronal sections and stained with hematoxylin and eosin (H & E) or toluidine blue for visualization by light microscopy.

Periodontal tissue repair and regeneration was determined using computer-assisted image analysis. Images of specimens were captured at 2, 4, 10, and 20x magnification using a Nikon Eclipse 50i microscope (Nikon Inc., Melville, NY) fitted with a Nikon Digital Sight DS U1 camera (Nikon Inc., Melville, NY). Histomorphometric analysis was performed using NIS Elements Basic Research Imaging software (Nikon Inc., Melville, NY). A single masked, calibrated examiner examined all of the slides. The parameters of periodontal regeneration measured included: 1) length of new cementum on the distal root of the first molar in mm (measured at 5-week time point only); 2) length of new bridging bone measured from the borders of the original osseous defect (mesially-distally) in mm (2 and 5 week time points); 3) area of new bone associated with the osseous defect and nanofibrous scaffold in mm^2 (2 and 5 week time points). Mean values were generated for each of the groups and significant differences were determined using an analysis of variance.

Results

Characterization of dual BMP-7/PDGF nanosphere-immobilized scaffold

Fig 5.1 shows that the 3D multi-level porous architecture of PLLA scaffold after BMP and PDGF containing nanosphere incorporation. Regular spherical macropores (250-425 μm in diameter) and interpore openings (approximately 100 μm in diameter) remained open and unaltered. After NS incorporation, the nanofibers (50-500 nm in diameter) on the scaffold wall were adhered with PLGA MS/NS. PLGA MS/NS were uniformly distributed throughout the scaffolds. In vitro release studies of single BMP-7 [38] or PDGF [37] from PLLA nanofibrous scaffold were performed and the results were published in previous papers. Briefly, the release profiles of single protein from nanospheres in scaffold was determined by PLGA formulation. 48% of BMP-7 was released from PLGA50-6.5K NS scaffold in initial first day burst release and 78% of BMP-7 released within the first two weeks. [38] PLGA50-64K NS scaffold released PDGF in a multi-phasic pattern. 23% of PDGF were released in initial first day burst release and 40% released within two weeks, followed by a 3 weeks slow release (0.3% per day). From week 5 to 8, there is another fast release of 20% which corresponds to PLGA NS degradation. [37, 38]

Mouse subcutaneous implantation results

Three weeks after subcutaneous implantation, Fig 5.2 A and B showed that the highest calcium content and highest Micro-CT tissue mineral content were found in the BMP-7 (1.5 μg/scaffold) +PDGF (3 μg/scaffold), BMP-7/PDGF 1:2 group (group 17). It was noted that both the calcium content and tissue mineral content were much lower in

BMP-7 (1.5 µg/scaffold) single release group (group 3), even though group 17 and group 3 had the same BMP dosage. It was also observed that these two values were lower in group 14, 15, 16, 18, even though they shared the same dosage of BMP-7 with group 17 but with different BMP/PDGF ratio. In consistence with calcium content and micro-CT measurement, Fig 5.3 of microscopic observations of the H&E stained tissue sections of scaffolds harvested 3 weeks after subcutaneous implantation showed robust neo bone formation (stained pink) in scaffold group 17. Although tissues have penetrated all the scaffold groups (1-18), no bone formation was found in control groups (group 1) and PDGF single release groups (4, 5, 6, 7, 8) While any groups with BMP-7 release showed some neo-bone formation, group 17 with BMP-7 (1.5 µg/scaffold) +PDGF (3 µg/scaffold), BMP-7/PDGF 1:2 ratio showed highest amount neo-bone formation. After six weeks of subcutaneous implantation, Fig 5.4 of microscopic observations showed there is still no bone formation found in control group (1) or low dosage PDGF single release group (4-7). Cells presented in those scaffolds are mainly fibroblasts and macrophages. High dosage PDGF single release group (8) showed some neo-bone formation but the amount is smaller compared to any BMP-7/PDGF dual release group. Group 17 showed significant neo-bone formation and was one of the best groups in terms of calcium content and micro-CT tissue mineral content. (Fig 5.2 A and B) These results suggest that release of BMP-7 from PLLA nanofibrous scaffolds with proper controlled delivery system induces ectopic bone formation. The release of PDGF from the scaffold significantly enhances BMP induced ectopic bone formation. The best synergetic ectopic bone forming effect of the dual release of these two growth factors occurred in scaffold group 17 with BMP-7 (1.5 µg/scaffold) +PDGF (3 µg/scaffold), BMP-7/PDGF 1:2. This

dosage combination was used as the optimal dosage combination for rat periodontal fenestration defect repair study.

Rat periodontal fenestration defect repair results

Histology examination

Fig 5.5 of microscopic observations of the H&E stained tissue sections of scaffolds harvested 2 weeks implantation showed minimal bridging and no neo cementum formation in all scaffolds groups, which was normal for such an early time point. However, bone formation lateral to the defect (indicated by open arrow) was observed in BMP single release groups (e) as small and scattering distributed bone tissues that were stained pink. BMP-7/PDGF dual-release groups (g) showed much more larger and complete pink bone tissue structures, which indicated most extensively neo bone formation. Fig 5.6 showed a close look at these scaffolds at defect regions and lateral defect border at higher magnifications. It was also observed that the dual release group induced higher bone formation (with largest integrated pink bone areas) and more blood vessel formation (with larger number of red vessel structure). Consistent to histological observation, histomorphometric analysis at 2 weeks (Fig 5.7) confirmed that BMP-7/PDGF dual release scaffold groups resulted in significant increase in new bone area above control and PDGF single-release groups, and larger bone area than BMP-7 single release group, although the difference was not significant at this time point.

Fig 5.8 of microscopic observations of the H&E stained tissue sections of scaffolds harvested 5 weeks implantation showed that bridging and bone formation was observed in all scaffold groups, with pink bone tissue areas observed in all experiment groups.

However, the dual release group (g) formed integrated neo-bone structure to occupy the whole defect region and the bone bridging in this group is continuous while the bone bridging in all the other groups was disrupted and the bone structures are incomplete. New cementum formation was also observed in all groups at this time point. Fig 5.6 showed a close look at these scaffolds at defect regions and lateral defect border at higher magnifications. It was confirmed that dual release group forms complete large bone to cover the whole defect area, while neo-formed bone tissues were discontinuous and scattered inside the defect in other groups. Dual release group also showed most obvious blood vessel formations. In accordance to histology micrograph observation, Histomorphometric analysis at 5 weeks (Fig 5.10) confirmed that BMP-7/PDGF dual release scaffold groups resulted in significant improvements in new bone area above all the other groups at this time point.

Quantitative and qualitative micro-CT analysis

In sectional views of micro-CT images, (Fig. 5.11), sagittal views of the representative three-dimensional (3-D) micro-CT isosurface images demonstrated the differences in mineralized tissue healing and bone regeneration between the experimental groups. While distal root was still exposed in control scaffold only group, PDGF and BMP single release groups, it was not exposed anymore and covered by regenerated bone in BMP-7/PDGF dual release group after 5 weeks defect repair. The dual BMP-7/PDGF release group presented larger amounts of tooth supporting mineralized tissue inside of the marked ROIs in both transverse and coronal sections compared to the control group and BMP-7, PDGF single release group. Although periodontal osseous defects with

standardized dimensions were created, mineralized tissue formation was not limited to the defect site and was sometimes present along the native bone (denoted by white dashed lines) on the buccal side of the mandible. It was obvious that dual release group had most bone formation extended beyond the bony envelope.

In accordance to the micro-CT sectional view images, qualitative analysis (Fig 5.12 A) confirmed that dual release scaffold groups induced significant higher amount of mineralized tissue formation in the total defect area of all the experiment groups. These tissue mineral content includes both tooth supporting tissue and non-tooth supporting tissues. Overall, none of the experimental groups demonstrated statistically significant differences in tissue mineral density at 5 weeks.

Discussion

The major goal of periodontal tissue engineering is to reconstruct tooth supporting multi-tissue structures destroyed by either injury or severe chronic periodontitis. One important strategy is to deliver growth factor to periodontal lesions to achieve periodontal tissue repair. Although success has been achieved by deliver of single growth factor to periodontal lesions to stimulate partial periodontal tissue regeneration, [14, 32, 44] their clinical utility was limited. One major reason is that periodontal tissue regeneration, for example periodontal bone regeneration is a multi-step process that requires the stimulation from multiple biological factors including (inflammatory, angiogenetic and osteogenetic) in a dynamic and coordinated manner. So, the periodontal bone regeneration relied on single delivery of BMP-7 is not sufficient for clinical applications. Thus, in order to significantly to improve bone formation, multiple growth factors

delivery in distinct dosage and rate to mimic natural regeneration process is absolutely needed. PDGF was found to stimulate periodontal wound repair [29] and enhance bone regeneration of periodontal osseous defects. [29, 36] In addition, our previous research demonstrated that controlled delivery of PDGF stimulates neogenesis and angiogenesis, [37, 39] which usually couples with bone regeneration. [45] Therefore, angiogenesis factor such as PDGF could be applied along with BMP in periodontal tissue regeneration to improve BMP induced bone repair. Early angiogenesis can be improved by the release of PDGF, thus, more nutrients, growth factors and oxygen are transported to the defect site by larger number of newly-formed blood vessels, which favors neo bone formation. Invasion of blood vessel is also desirable in cartilage to bone transformation during endochondral ossification process since they transport both stem cells and osteo-progenitors. [46] These cells deposit bone on cartilage matrix at the later stage of endochondral ossification which favors more bone formation as a final outcome.

However, this promising strategy has not achieved significant clinical success yet mostly due to the lack of localized controlled delivery system which can release multiple growth factors with distinct dosages and rates, since the synergistic effect of angiogenetic factor with BMP to promote bone regeneration can only be achieved when a defined suitable release dosage and kinetics are applied. [47-50]

Previously, a nanofibrous tissue engineering scaffold has been developed in our lab which can serve as both a growth factor delivery vehicle and a 3-dimensional cellular construct for multiple tissue regeneration. [37, 38, 40, 51] Both BMP-7 and PDGF have successfully been delivered from this nanofibrous scaffold with controllable release dosage and kinetics and these released growth factors have successfully exerted their

biological functions in vivo. [38, 39] The capability to deliver multiple growth factors with distinct release dosages and kinetics is one of the advantage of this type of scaffold. Our data has shown that ectopic bone formation was increased by the dual release of PDGF along with BMP-7 from this scaffold system and the improvement depended on the ratio of the two growth factors. The most improvement came with the combination of BMP-7 (1.5 μg/scaffold), PDGF (3.0 μg/scaffold), BMP-7/PDGF ratio 1:2. (Fig 5.2-5.4). Our data also showed that using this dual release scaffold with BMP-7/PDGF 1:2 ratio in rat periodontal fenestration defect repair model, improved periodontal repair was observed with this dual release group compared to the control and single BMP-7 and PDGF release groups. In dual release group, more mineralized tissues were regenerated to fill more spaces in the total defect region (Fig 5.7 and Fig. 5.10) and the distal root was no longer exposed, while in other groups, part of root was still exposed. (Fig 5.11). The bridging along the defect in dual release group was much more continuous than in other groups. (Fig 5.8).

Our data suggested that early angiogenesis was improved by the release of PDGF in dual release group, with more new blood vessels formed. (Fig 5.6). These new formed blood vessels transported more growth factors, nutrients and oxygen to the defect site to promote neogenesis. It was also observed more blood vessels were presented close to newly formed bone areas in dual release scaffold groups, (Fig. 5.10) which proved that the invasion of blood vessels also promoted bone marrow cells invasion and deposition of bone matrix on cartilage matrix during later stage of endochondral ossification. All these effects were combined together and resulted in stronger bone formation in dual release group.

Besides, It was also noted that when the dual release scaffold system was applied in periodontal defect repair, mineralized tissue formation was not limited to the defect site which demonstrated the potential of this scaffold to be used in much larger sized osseous defect repair applications.

Conclusion

We have developed a novel PLLA nanofibrous scaffold which can fulfill localized dual release of BMP-7 and PDGF in a controlled fashion with distinct dosage and release kinetics. Both ectopic bone formation and periodontal fenestration defect regeneration was significantly improved with this dual release scaffold system. The improvement was dependent on the dosage and the release kinetics of the two growth factors. This nanofibrous scaffold with its controlled multiple growth factor delivery capacity can be applied in various tissue regeneration and large sized defect repair.

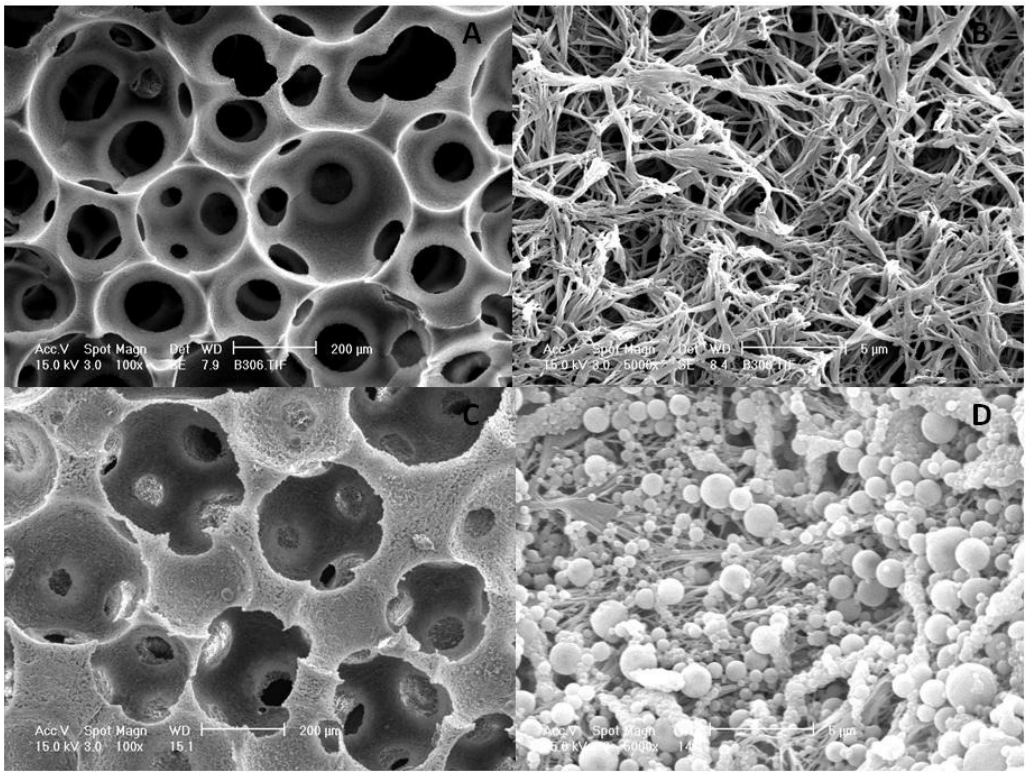

Fig5.1. SEM micrograph of PLLA nanofibrous scaffold before and after PLGA50-6.5K NS containing BMP-7 and PLGA50-64K NS containing PDGF incorporation (BMP-7: 1.5 µg/scaffold and PDGF: 3 µg/scaffold). PLLA nanofibrous scaffold before NS incorporation at 100× (A) and 5000× (B) PLLA nanofibrous scaffold after dual growth factors NS incorporation at 100× (C) and 5000× (D)

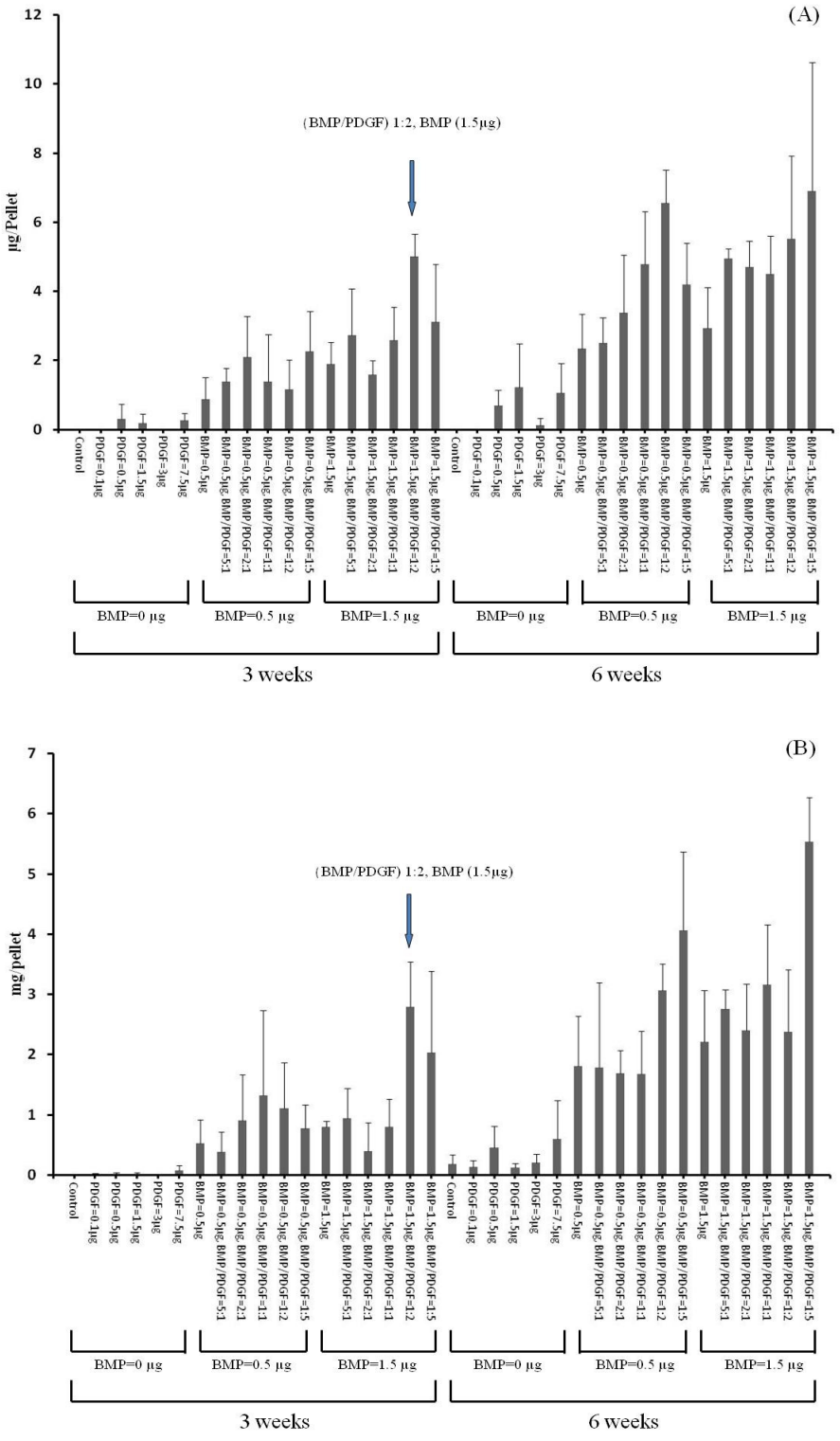

Fig 5.2. (A) Results of calcium content measurement (B) Results of Micro-CT mineral content measurement of scaffolds harvested after 3 and 6 weeks subcutaneous implantation.

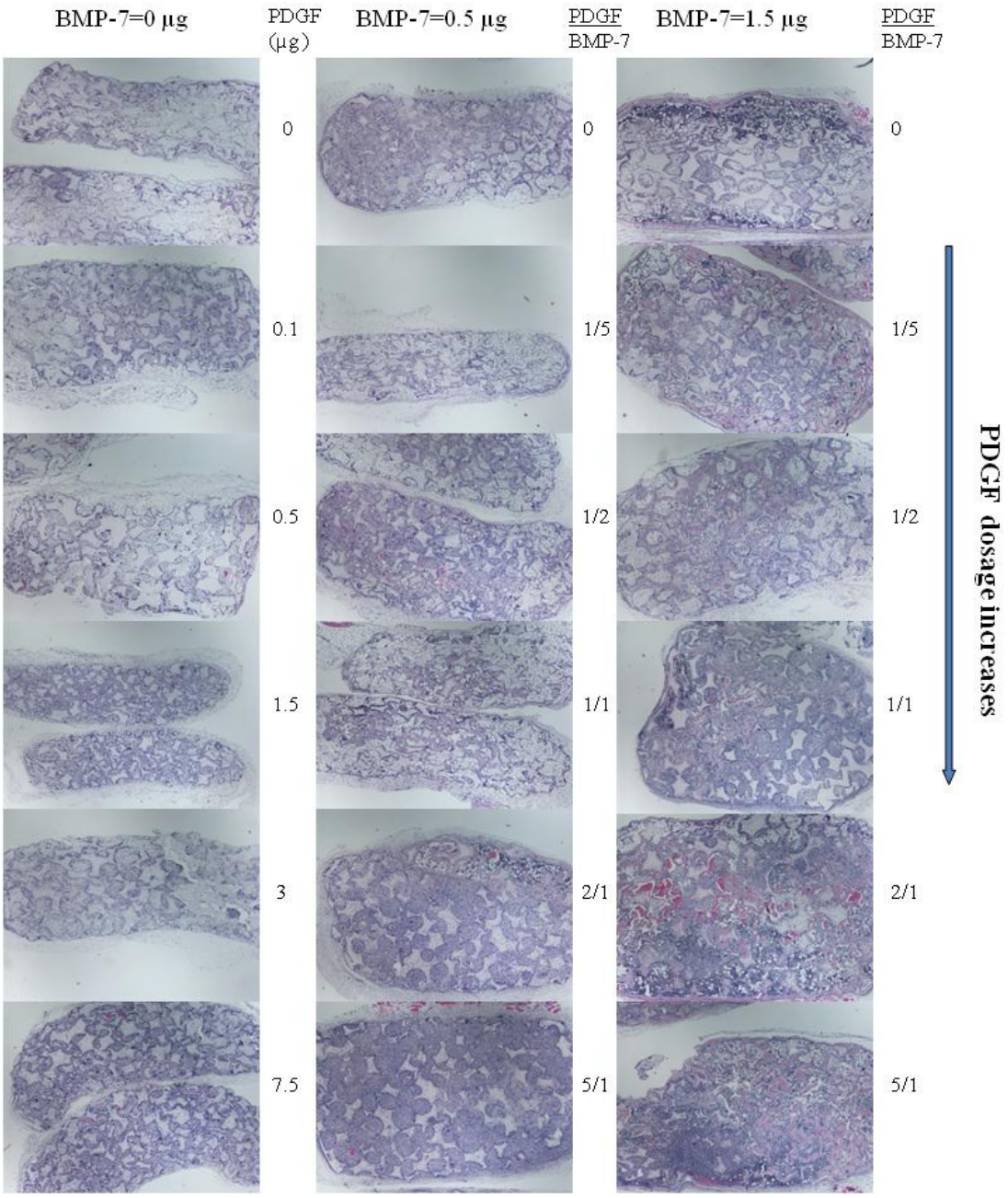

Fig5.3. Microscopic observations of the H&E stained tissue sections of scaffolds harvested 3 weeks after subcutaneous implantation at magnification 40× full cross sections.

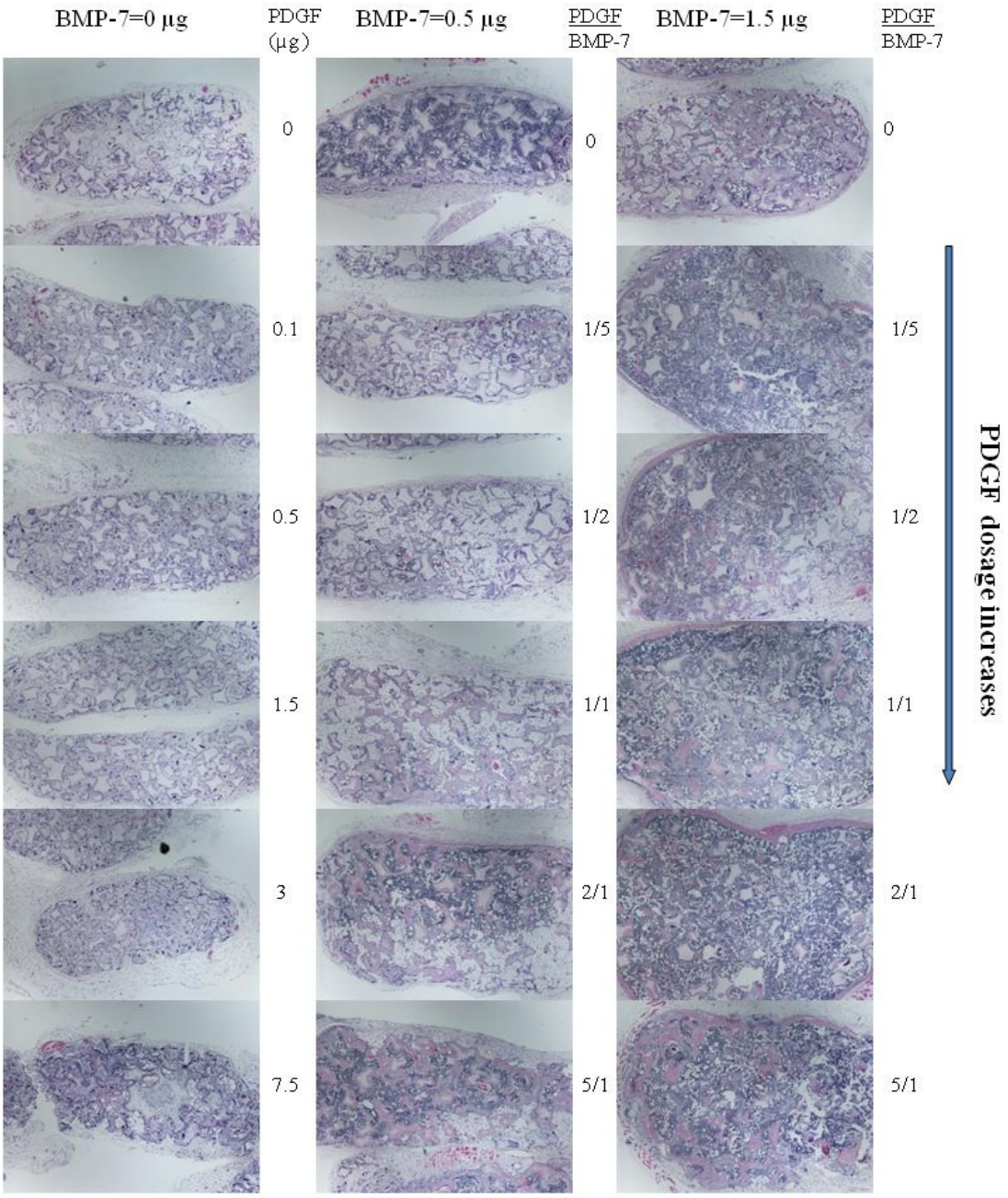

Fig 5.4. Microscopic observations of the H&E stained tissue sections of scaffolds harvested 6 weeks after subcutaneous implantation at magnification 40× full cross sections.

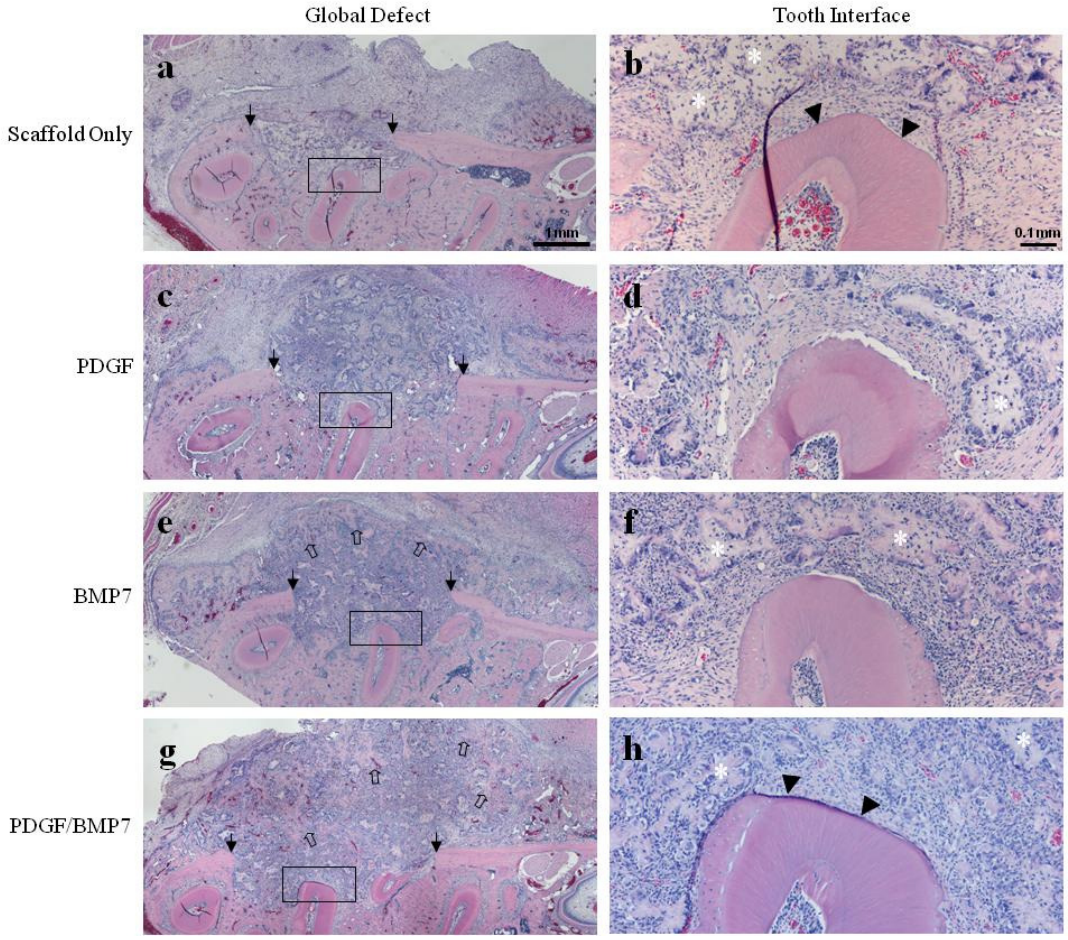

Fig. 5.5. Dual release of PDGF/BMP-7 from scaffolds stimulations periodontal defect repair and bone formation after 2 weeks. Panels a, c, e, g show 4x magnification of the global defect region at 2 weeks following surgery. The black arrows indicate the edges of the original osseous lesion. Open arrows show areas of bone formation. Panels b, d, f, h show a 10x view of the denuded tooth root surface at 2 weeks. In these panels, white asterisks indicate scaffold and closed arrow heads indicate areas of close approximation to tooth surface.

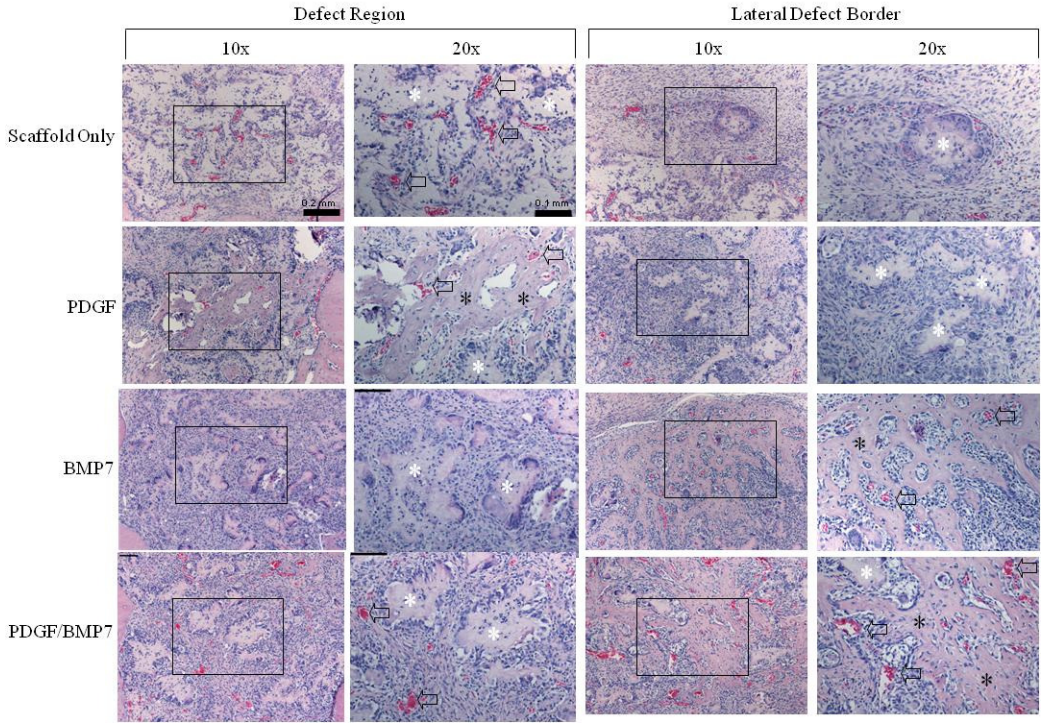

Fig 5.6. Descriptive histology within the defect region and lateral to the defect at 10x and 20x magnification. (2 weeks) White asterisks indicate nanofibrous scaffold material. Black asterisks indicate new bone formation. Open arrows point to blood vessels.

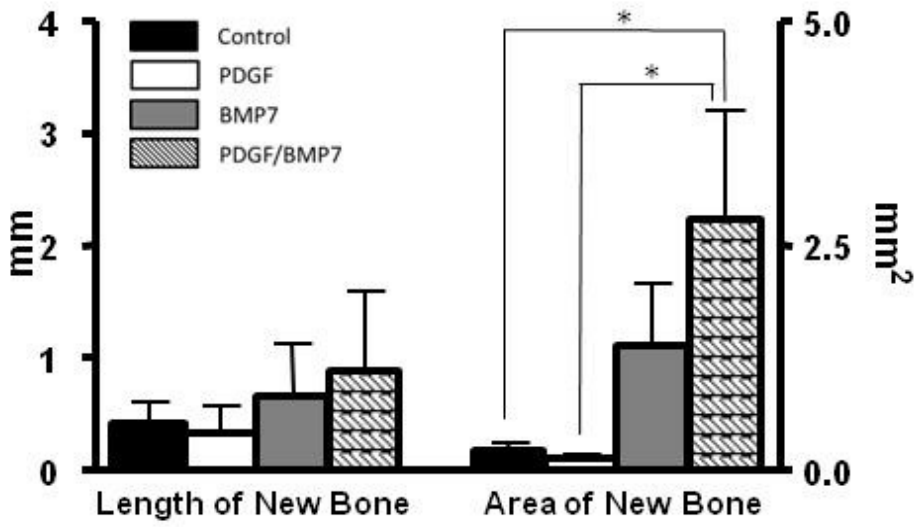

Fig.5.7. PDGF/BMP-7 dual-release from nanofibrous scaffolds stimulates osteogenesis at 2weeks. At 2 weeks, PDGF/BMP7 dual-release resulted in statistically significant improvements in new bone area above control and either BMP-7 or PDGF release alone (*P<0.05).

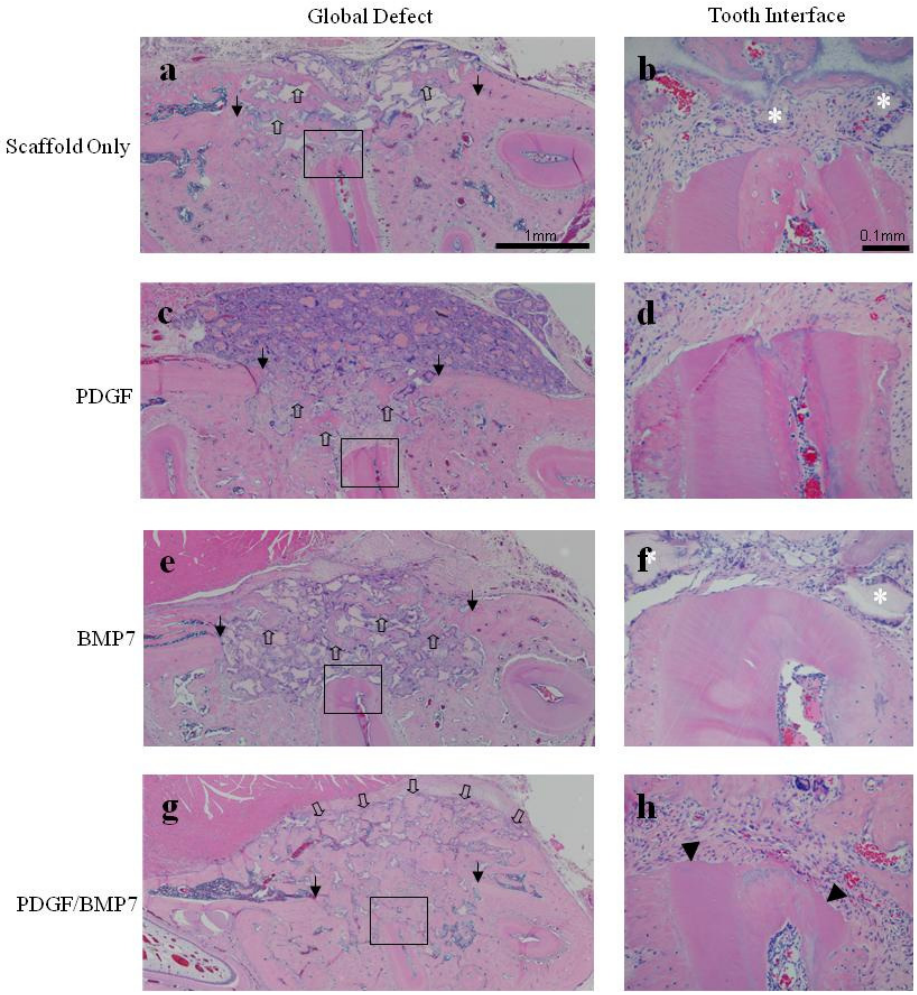

Fig.5.8. Dual release of PDGF/BMP-7 from scaffolds stimulations periodontal defect repair and bone formation after 5 weeks. Panels a, c, e, g show 4x magnification of the global defect region at 14 days following surgery. The black arrows indicate the edges of the original osseous lesion. Open arrows show areas of bone formation. Panels b, d, f, h show a 10x view of the denuded tooth root surface at 5 weeks. Cementum formation was observed at 5weeks time point. In these panels, white asterisks indicate scaffold and closed arrows indicate areas of close approximation to tooth surface.

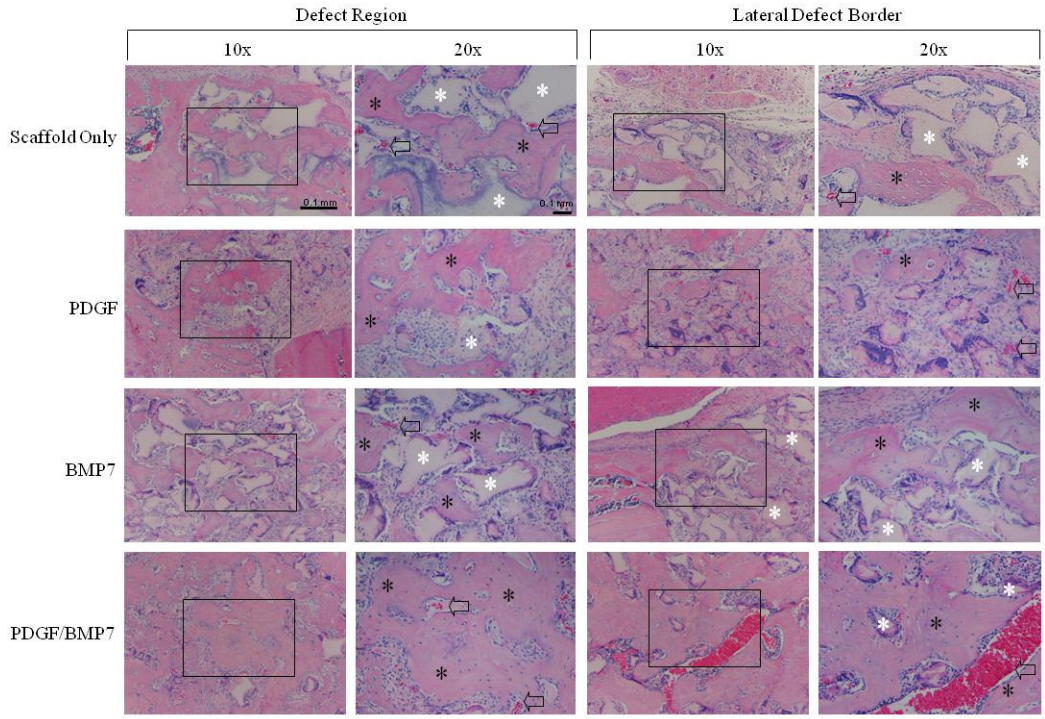

Fig.5.9. Descriptive histology within the defect region and lateral to the defect at 10x and 20x magnification. (5 weeks) White asterisks indicate nanofibrous scaffold. Black asterisks indicate new bone formation. Open arrows demonstrate blood vessels.

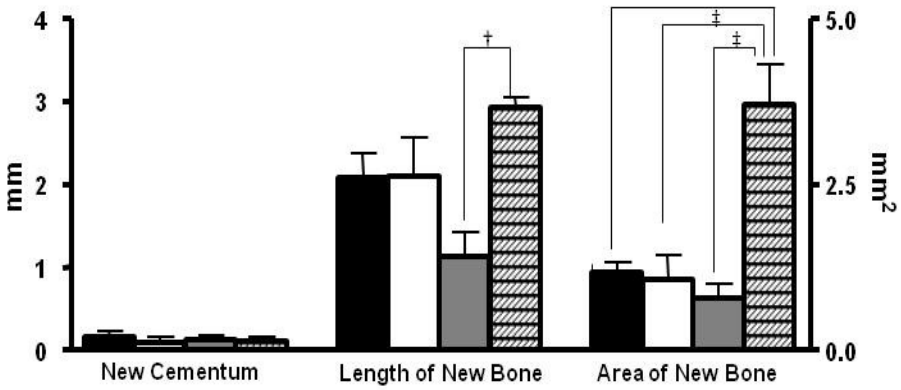

Fig.5.10. PDGF/BMP-7 dual-release from nanofibrous scaffolds stimulates osteogenesis at 5 weeks. At 5 weeks, dual release resulted in statistically significant improvement in new bone area above all groups (‡ P<0.001). The 5-weeks dual-release samples also exhibited statistically significant increase in new bridging bone compared with BMP-7 single-release († p<.01).

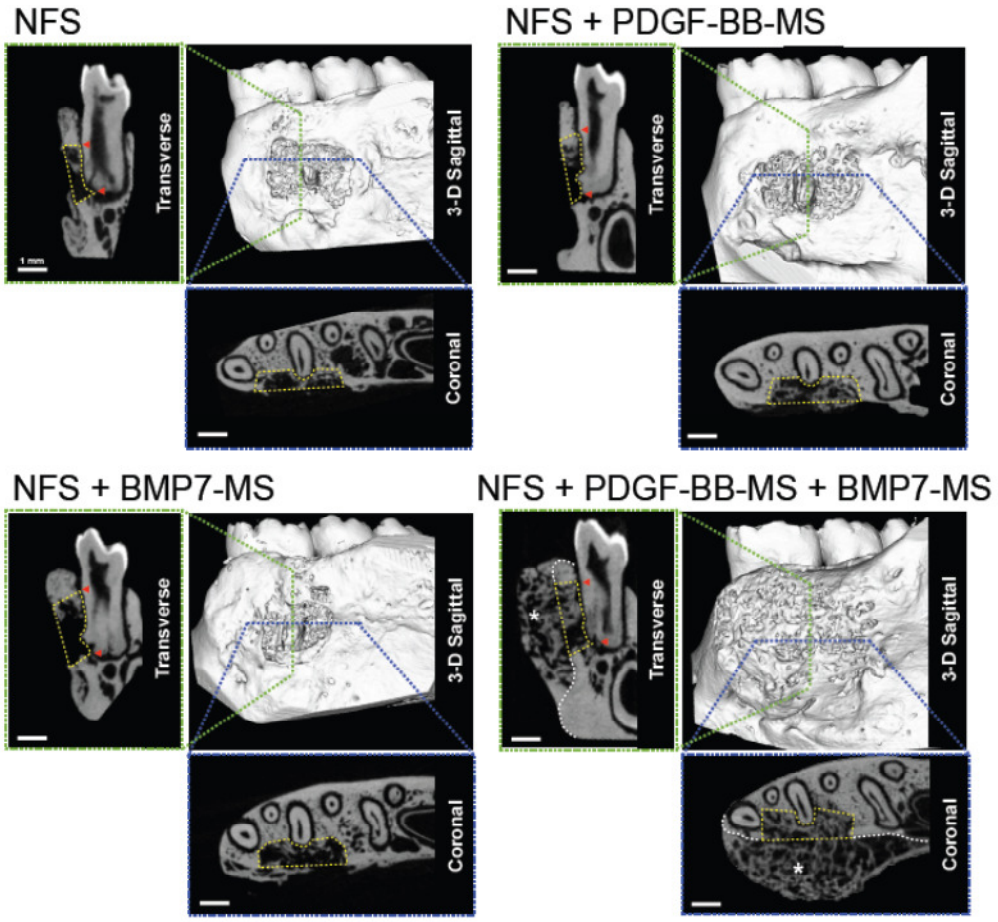

Fig.5.11. Micro-CT analysis for evaluation of mineralized tissue formation in standardized surgically created mandibular-alveolar bone defects. In the transverse sections (green dashed line), yellow dashed lines mark the borders of the ROI, while red triangles demarcate the recessed tooth-root surface region that resulted from removal of cementum layer. Coronal slices (blue dashed line) also provide an alternative view of the ROI borders identified by the yellow dashed lines. In both transverse and coronal sections, varying amounts of tooth-supporting mineralized tissue is evident inside of the marked ROIs. Bone formation extending beyond the bony envelope is denoted by white asterisks.

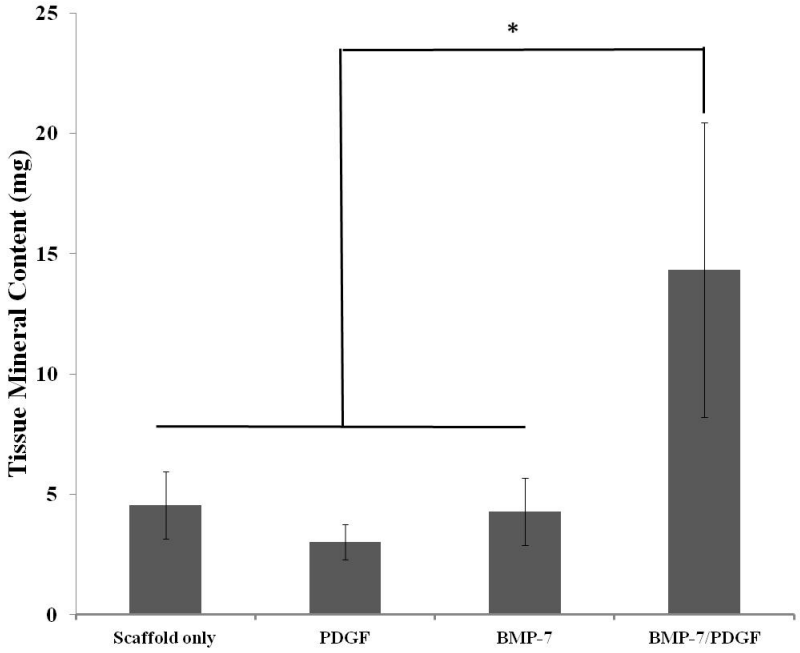

(A)

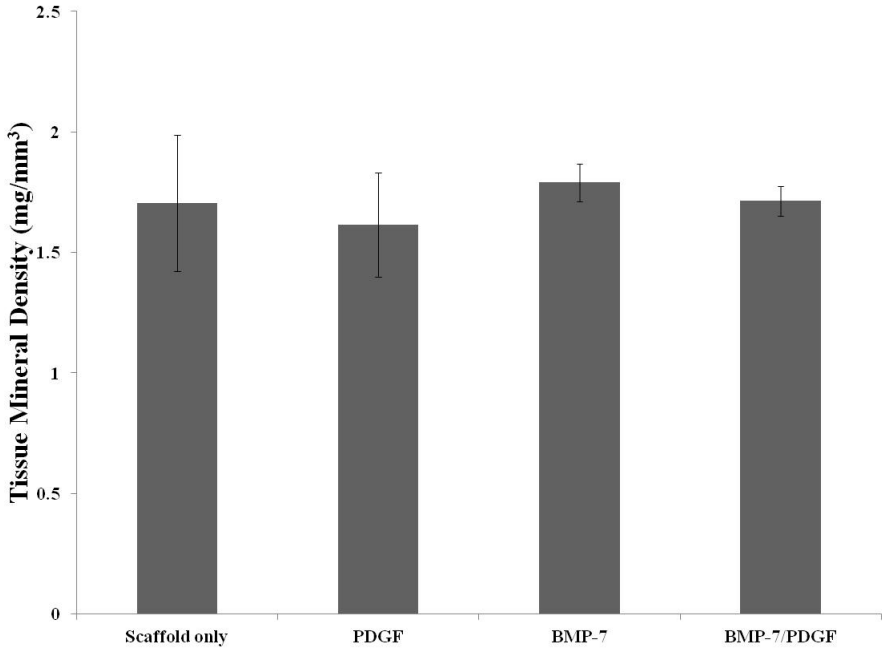

(B)

Fig 5.12. (A) Micro-CT tissue mineral content (TMC) results of all scaffolds groups in total defect region after 5 weeks periodontal defect repair. (B) Micro-CT tissue mineral density of all scaffolds groups in total defect region after 5 weeks periodontal defect repair. (* $P<0.05$)

Table 5.1 Experiment design of BMP-7/PDGF dual releasing PLLA scaffold for subcutaneous implantation.

	Group	BMP-7 (fast) μg/scaffold	PDGF-BB (slow) μg/scaffold	BMP/PDGF
BMP-7 (0 μg)	1	0	0	
	2	0	0.1	
	3	0	0.5	
	4	0	1.5	
	5	0	3	
	6	0	7.5	
BMP-7 (0.5 μg)	7	0.5	0	
	8	0.5	0.1	5:1
	9	0.5	0.25	2:1
	10	0.5	0.5	1:1
	11	0.5	1	1:2
	12	0.5	2.5	1:5
BMP-7 (1.5 μg)	13	1.5	0	
	14	1.5	0.3	5:1
	15	1.5	0.75	2:1
	16	1.5	1.5	1:1
	17	1.5	3	1:2
	18	1.5	7.5	1:5

1. PDGF-BB and BMP-7 were encapsulated in PLGA microspheres which are incorporated into PLLA nano-fibrous scaffold.
2. Scaffold size: 3.6 mm in diameter, 2 mm in thickness, time points: 3 weeks, 6 weeks
3. 6 scaffolds/time point/group (18), total 216 scaffolds, 60 mice (6 extra), 3 scaffolds/time point/group for Micro-CT and histology (108 scaffolds), 3 scaffolds/time point/ group for Ca content (108 scaffolds).

Table 5.2 Experiment design of BMP-7/PDGF dual releasing PLLA scaffold for 2 weeks rat periodontal fenestration defect implantation.

	Group	BMP-7 fast (ug/scaffold)	PDGF-bb slow (ug/scaffold)	BMP/PDGF
control	1	0	0	
	2	1.5	0	
	3	0	3.0	
	4	1.5	3.0	1:2

1. PDGF-BB and BMP-7 were encapsulated in PLGA microspheres which are incorporated into PLLA nano-fibrous scaffold.
2. Scaffold size: 3 mm(L)*3mm(w)*2mm(H), time point: 2 week
3. 6 scaffolds/time point/group (4), total 48 scaffolds, 26 rats (2 extra), 6 scaffold/time point/group for histology (24 scaffolds)

Table 5.3 Experiment design of BMP-7/PDGF dual releasing PLLA scaffold for 5 weeks rat periodontal fenestration defect implantation.

	Group	BMP-7 (ug/scaffold)	PDGF-bb (ug/scaffold)	BMP-PDGF
control	1	0	0	
	2	0	3.0 (S)	
	3	1.5(F)	0	
	4	1.5(F)	3.0(S)	1:2

1. PDGF-BB and BMP-7 were encapsulated in PLGA microspheres which are incorporated into PLLA nano-fibrous scaffold
2. Scaffold size: 3*3*2 (18 mm^3), rat periodontal defect model, time point: 5 week
3. 6 scaffolds/time point/group (4), total 24 scaffolds, 28 rats (4 extra), 6 scaffold/time point/group for Micro-CT and histology (24 scaffolds)

Reference

1. Pihlstrom BL, Michalowicz BS, Johnson NW: Periodontal diseases. *Lancet* 2005, 366(9499):1809-1820.

2. Williams RC: Periodontal-Disease. *N Engl J Med* 1990, 322(6):373-382.

3. Hughes FJ, Ghuman M, Talal A: Periodontal regeneration: a challenge for the tissue engineer? *Proc Inst Mech Eng Part H-J Eng Med* 2010, 224(H12):1345-1358.

4. Baum BJ, Mooney DJ: The impact of tissue engineering on dentistry. *J Am Dent Assoc* 2000, 131(3):309-318.

5. Nakashima M, Reddi AH: The application of bone morphogenetic proteins to dental tissue engineering. *Nat Biotechnol* 2003, 21(9):1025-1032.

6. Groeneveld EHJ, Burger EH: Bone morphogenetic proteins in human bone regeneration. *Eur J Endocrinol* 2000, 142(1):9-21.

7. Urist MR: Bone - Formation by Autoinduction. *Science* 1965, 150(3698):893-&.

8. Cook SD: Preclinical and clinical evaluation of osteogenic protein-1 (BMP-7) in bony sites. *Orthopedics* 1999, 22(7):669-671.

9. Ripamonti U, VandenHeever B, Sampath TK, Tucker MM, Rueger DC, Reddi AH: Complete regeneration of bone in the baboon by recombinant human osteogenic protein-1 (hOP-1, bone morphogenetic protein-7). *Growth Factors* 1996, 13(3-4):273-&.

10. Saito N, Murakami N, Takahashi J, Horiuchi H, Ota H, Kato H, Okada T, Nozaki K, Takaoka K: Synthetic biodegradable polymers as drug delivery systems for bone morphogenetic proteins. *Adv Drug Deliv Rev* 2005, 57(7):1037-1048.

11. Welch RD, Jones AL, Bucholz RW, Reinert CM, Tjia JS, Pierce WA, Wozney JM, Li XJ: Effect of recombinant human bone morphogenetic protein-2 on fracture healing in a goal tibial fracture model. *J Bone Miner Res* 1998, 13(9):1483-1490.

12. Wozney JM, Rosen V: Bone morphogenetic protein and bone morphogenetic protein gene family in bone formation and repair. *Clin Orthop Rel Res* 1998(346):26-37.

13. Zegzula HD, Buck DC, Brekke J, Wozney JM, Hollinger JO: Bone formation with use of rhBMP-2 - (Recombinant human bone morphogenetic protein-2). *J Bone Joint Surg-Am Vol* 1997, 79A(12):1778-1790.

14. Giannobile WV, Ryan S, Shih MS, Su DL, Kaplan PL, Chan TCK: Recombinant human osteogenic protein-1 (OP-1) stimulates periodontal wound healing in class III furcation defects. *J Periodont* 1998, 69(2):129-137.

15. Jin QM, Anusaksathien O, Webb SA, Rutherford RB, Giannobile WV: Gene therapy of bone morphogenetic protein for periodontal tissue engineering. *J Periodont* 2003, 74(2):202-213.

16. Ripamonti U, Parak R, Petit JC: Induction of cementogenesis and periodontal ligament regeneration by recombinant human transforming growth factor-beta 3 in Matrigel with rectus abdominis responding cells. *J Periodont Res* 2009, 44(1):81-87.

17. Cahill KS, Chi JH, Day A, Claus EB: Prevalence, Complications, and Hospital Charges Associated With Use of Bone-Morphogenetic Proteins in Spinal Fusion Procedures. *JAMA-J Am Med Assoc* 2009, 302(1):58-66.

18. Gautschi OP, Frey SP, Zellweger R: Bone morphogenetic proteins in clinical applications. *ANZ J Surg* 2007, 77(8):626-631.

19. Seeherman H, Wozney J, Li R: Bone morphogenetic protein delivery systems. *Spine* 2002, 27(16):S16-S23.

20. Luginbuehl V, Meinel L, Merkle HP, Gander B: Localized delivery of growth factors for bone repair. *Eur J Pharm Biopharm* 2004, 58(2):197-208.

21. Rose F, Hou QP, Oreffo ROC: Delivery systems for bone growth factors - the new players in skeletal regeneration. *J Pharm Pharmacol* 2004, 56(4):415-427.

22. Einhorn TA: Clinical applications of recombinant human BMPs: Early experience and future development. *J Bone Joint Surg-Am Vol* 2003, 85A:82-88.

23. Ostman A, Heldin CH: Involvement of platelet-derived growth factor in disease: Development of specific antagonists. *AdvCancer Res* 2001, 80:1-38.

24. Heldin CH, Westermark B: Mechanism of action and in vivo role of platelet-derived growth factor. *Physiol Rev* 1999, 79(4):1283-1316.

25. Heldin CH, Ostman A, Ronnstrand L: Signal transduction via platelet-derived growth factor receptors. *Biochim Biophys Acta-Rev Cancer* 1998, 1378(1):F79-F113.

26. Kaminski WE, Lindahl P, Lin NL, Broudy VC, Crosby JR, Hellstrom M, Swolin B, Bowen-Pope DF, Martin PJ, Ross R *et al*: Basis of hematopoietic defects in

platelet-derived growth factor (PDGF)-B and PDGF beta-receptor null mice. *Blood* 2001, 97(7):1990-1998.

27. Kaplan DR, Chao FC, Stiles CD, Antoniades HN, Scher CD: Platelet Alpha-Granules Contain a Growth-Factor for Fibroblasts. *Blood* 1979, 53(6):1043-1052.

28. Alvarez RH, Kantarjian HM, Cortes JE: Biology of platelet-derived growth factor and its involvement in disease. *Mayo Clin Proc* 2006, 81(9):1241-1257.

29. Cooke JW, Sarment DP, Whitesman LA, Miller SE, Jin QM, Lynch SE, Giannobile WV: Effect of rhPDGF-BB delivery on mediators of periodontal wound repair. *Tissue Eng* 2006, 12(6):1441-1450.

30. Taba M Jr JQ, Sugai JV, Giannobile WV: Current concepts in periodontal bioengineering. *Orthodontics and Craniofacial Research* 2005, 8(292–302).

31. Giannobile WV, Finkelman RD, Lynch SE: Comparison of Canine and Nonhuman Primate Animal-Models for Periodontal Regenerative Therapy - Results Following a Single Administration of Pdgf Igf-I. *J Periodont* 1994, 65(12):1158-1168.

32. Giannobile WV, Hernandez RA, Finkelman RD, Ryan S, Kiritsy CP, Dandrea M, Lynch SE: Comparative effects of platelet-derived growth factor-BB and insulin-like growth factor-I, individually and in combination, on periodontal regeneration in Macaca fascicularis. *J Periodont Res* 1996, 31(5):301-312.

33. Park YJ, Lee YM, Park SN, Sheen SY, Chung CP, Lee SJ: Platelet derived growth factor releasing chitosan sponge for periodontal bone regeneration. *Biomaterials* 2000, 21(2):153-159.

34. Hollinger JO, Hart CE, Hirsch SN, Lynch S, Friedlaender GE: Recombinant human platelet-derived growth factor: Biology and clinical applications. *J Bone Joint Surg-Am Vol* 2008, 90A:48-54.

35. Nevins M, Giannobile WV, McGuire MK, Kao RT, Mellonig JT, Hinrichs JE, McAllister BS, Murphy KS, McClain PK, Nevins ML *et al*: Platelet-derived growth factor stimulates bone fill and rate of attachment level gain: Results of a large multicenter randomized controlled trial. *J Periodont* 2005, 76(12):2205-2215.

36. Sarment DP, Cooke JW, Miller SE, Jin QM, McGuire MK, Kao RT, McClain PK, McAllister BS, Lynch SE, Giannobile WV: Effect of rhPDGF-BB on bone turnover during periodontal repair. *J Clin Periodontol* 2006, 33(2):135-140.

37. Wei GB, Jin QM, Giannobile WV, Ma PX: Nano-fibrous scaffold for controlled delivery of recombinant human PDGF-BB. *J Control Release* 2006, 112(1):103-110.

38. Wei GB, Jin QM, Giannobile WV, Ma PX: The enhancement of osteogenesis by nano-fibrous scaffolds incorporating rhBMP-7 nanospheres. *Biomaterials* 2007, 28(12):2087-2096.

39. Jin QM, Wei GB, Lin Z, Sugai JV, Lynch SE, Ma PX, Giannobile WV: Nanofibrous Scaffolds Incorporating PDGF-BB Microspheres Induce Chemokine Expression and Tissue Neogenesis In Vivo. *PLoS One* 2008, 3(3).

40. Wei GB, Ma PX: Macroporous and nanofibrous polymer scaffolds and polymer/bone-like apatite composite scaffolds generated by sugar spheres. *J Biomed Mater Res Part A* 2006, 78A(2):306-315.

41. Park CH, Abramson ZR, Taba M, Jin Q, Chang J, Kreider JM, Goldstein SA, Giannobile WV: Three-dimensional micro-computed tomographic imaging of alveolar bone in experimental bone loss or repair. *J Periodont* 2007, 78(2):273-281.

42. Park CH, Rios HF, Jin Q, Sugai JV, Padial-Molina M, Taut AD, Flanagan CL, Hollister SJ, Giannobile WV: Tissue engineering bone-ligament complexes using fiber-guiding scaffolds. *Biomaterials* 2011, 33(1):137-145.

43. Ma PX, Zhang RY, Xiao GZ, Franceschi R: Engineering new bone tissue in vitro on highly porous poly(alpha-hydroxyl acids)/hydroxyapatite composite scaffolds. *J Biomed Mater Res* 2001, 54(2):284-293.

44. Murakami S, Takayama S, Kitamura M, Shimabukuro Y, Yanagi K, Ikezawa K, Saho T, Nozaki T, Okada H: Recombinant human basic fibroblast growth factor (bFGF) stimulates periodontal regeneration in class II furcation defects created in beagle dogs. *J Periodont Res* 2003, 38(1):97-103.

45. Wan C, Gilbert SR, Wang Y, Cao X, Shen X, Ramaswamy G, Jacobsen KA, Alaql ZS, Eberhardt AW, Gerstenfeld LC *et al*: Activation of the hypoxia-inducible factor-1 alpha pathway accelerates bone regeneration. *Proc Natl Acad Sci U S A* 2008, 105(2):686-691.

46. Mackie EJ, Ahmed YA, Tatarczuch L, Chen KS, Mirams M: Endochondral ossification: How cartilage is converted into bone in the developing skeleton. *Int J Biochem Cell Biol* 2008, 40(1):46-62.

47. Huang YC, Kaigler D, Rice KG, Krebsbach PH, Mooney DJ: Combined angiogenic and osteogenic factor delivery enhances bone marrow stromal cell-driven bone regeneration. *J Bone Miner Res* 2005, 20(5):848-857.

48. Kempen DHR, Lu LC, Heijink A, Hefferan TE, Creemers LB, Maran A, Yaszemski MJ, Dhert WJA: Effect of local sequential VEGF and BMP-2 delivery on ectopic and orthotopic bone regeneration. *Biomaterials* 2009, 30(14):2816-2825.

49. Li GH, Corsi-Payne K, Zheng B, Usas A, Peng HR, Huard J: The Dose of Growth Factors Influences the Synergistic Effect of Vascular Endothelial Growth Factor on Bone Morphogenetic Protein 4-Induced Ectopic Bone Formation. *Tissue Eng Part A* 2009, 15(8):2123-2133.

50. Peng HR, Usas A, Olshanski A, Ho AM, Gearhart B, Cooper GM, Huard J: VEGF improves, whereas sFlt1 inhibits, BMP2-induced bone formation and bone healing through modulation of angiogenesis. *J Bone Miner Res* 2005, 20(11):2017-2027.

51. Hu J, Feng K, Liu XH, Ma PX: Chondrogenic and osteogenic differentiations of human bone marrow-derived mesenchymal stem cells on a nanofibrous scaffold with designed pore network. *Biomaterials* 2009, 30(28):5061-5067.

Chapter 6

Fabrication of an anisotropic bilayered composite scaffold to induce zonal development of cartilage tissue

Introduction

Cartilage is a connective tissue consisting of chondrocytes embedded in a complicated extra-cellular matrix (ECM) composed of collagen, glycosaminoglycans, fibronectin, elastin, laminin and water [1]. Articular cartilage, being the most abundant cartilage type, can be divided into four zones, namely the superficial, middle, deep and calcified zones. Each zone has its distinctive matrix organization, chondrocyte morphology and biochemical compositions [2], which plays important roles in its corresponding biomechanical function. Accordingly, the functional recovery of articular cartilage defect requires the reconstruction of the damaged zonal structure. Unfortunately, cartilage tissue shows little tendency of self-repair and regeneration, owing to its lack of internal vascular network and low mitotic activity of chondrocytes [3, 4]. Consequently, articular cartilage injuries caused by osteoarthritis or trauma often persist for years and result in scar formation, which is structurally and functionally inferior to normal cartilage and eventually lead to further cartilage degeneration (i.e., Secondary osteoarthritis) [5]. Several strategies have been applied to treat these cartilage related diseases including

resection, cartilage shaving or other surgical intervention, bone marrow stimulation and tissue grafts. Despite some encouraging clinical results, these methods are usually associated with drawbacks like pain reoccurrence and donor site morbidity [2, 6]. Over the past decades, cartilage tissue engineering has emerged as a promising approach in treatment of these diseases, which involves the expansion of isolated chondrocytes followed by delivery to the cartilage defects to promote in situ tissue regeneration [7, 8]. Efforts have been made to develop appropriate cell delivery scaffolds to create an advantageous artificial ECM microenvironment for chondrocytes to adhere and maintain their differentiated phenotype and function. Various naturally derived and synthetic polymers have been tested as scaffold materials [9-11] and two types of scaffolding have been widely applied: porous foams and hydrogels [12]. Hydrogels are highly hydrated polymeric networks due to chemical or physical crosslinking of individual polymer chains [13]. Hydrogels are used as cartilage engineering scaffold materials because they can mimic the in vivo chondrocyte growth environments and preserved their differentiated phenotypes due to the highly hydrated structure and maintenance of rounded cell shape [14]. However, their poor mechanical strength limits their applications in load-bearing areas such as articular cartilage defects [12]. Besides, it remains difficult to create a zonal articular cartilage structure with hydrogel materials, despite limited success to introduce three dimensional (3D) patterning structure to hydrogels to alter their normal isotropic structure [15]. Porous foams, in contrast, usually have better mechanical

properties and are easier to design architectural structure [12]. However, chondrocytes cultured on most of the porous foam scaffolds lost their rounded morphology quickly and therefore de-differentiated [16, 17]. In our previous study, macro-porous PLLA scaffolds with nano-fibrous (NF) matrix structure were shown to support chondrogenic differentiation of human bone marrow-derived mesenchymal stem cells (hMSCs). Cells showed a more rounded shape on the NF matrix and the porous NF scaffolds were able to support long-term 3D cartilaginous development [18], indicating the importance of bio-mimicking NF structures in cartilage engineering. Electrospinning is another commonly used method to create porous NF or micro-fibrous architecture [19, 20]. However, the pores are too small to allow deep cell penetration when the fibers are at the nano-scale. Therefore the electrospun NF mesh is more suitable for regeneration of the thinner surface layer of cartilage.

In this study, a two-layered composite scaffold was fabricated, which combined the two nano-fiber fabrication techniques, with a thin electrospun NF top layer mimicking the superficial zone and a phase-separated NF bottom layer mimicking the middle zone. And the effect of the anisotropic architecture of composite scaffolds on in vitro chondrogenesis of hMSCs was investigated.

Materials and methods

Materials

Poly (L-lactic acid) (PLLA) with inherent viscosity of 1.6 dl/g was purchased from Boehringer Ingelheim (Ingelheim, Germany). D-fructose (m.p. 119-122°C) is from Sigma (St. Louis, MO). Tetrahydrofuran, acetone, cyclohexane, hexane and dichloromethane were purchased from Fisher Scientific (Pittsburgh, PA).

Fabrication of NF PLLA composite scaffolds

The composite scaffold is composed of two layers: a top layer fabricated by electrospinning method and a bottom layer fabricated by temperature induced phase separation method combined with sugar sphere template and leaching technique. The schematic diagram of fabrication process is illustrated in Figure 1. Fabrication of bottom phase-separation layer has been described previously [21]. Briefly, 10 wt/v% PLLA/tetrahydrofuran (THF) solution was cast into an assembled sugar sphere template (sphere diameters were 125-250 μm, 250-425 μm and 425-600 μm respectively for small, medium and large pore scaffolds) under vacuum. The polymer-sugar construct was phase separated at -20°C overnight and then immersed into cyclohexane to exchange THF for 2 days. The construct was then freeze-dried and the sugar sphere templates were leached out in distilled water to obtain highly porous scaffolds. Scaffolds were cut into circular disks with dimensions of 3.6 mm in diameter and 1 mm in thickness. A top layer of PLLA NF or micro-fibrous mesh was then electrospun onto the bottom layer to fabricate composite scaffolds. Briefly, The PLLA was dissolved in chloform/acetone mixture (2:1 V/V) with a concentration of 6, 8 or 12 wt/v%. The prepared PLLA solution was then fed

into a plastic syringe with a needle (inner diameter of 0.18 mm). A syringe pump (Model # 78-01001, Fisher Scientific) was used to feed the solution to needle at a feed rate of 1.5 mL/hr. An external voltage of 18kV was applied to the needle using a high-voltage power supplier (Model # ES30P-5w, Gamma High voltage). The phase separated bottom layer was placed on a grounded collection plate of aluminum foil, located at a fixed distance of 12 mm from the needle tip. After the fabrication of top electrospun layer with desired thickness (50μm-250μm) by adjusting the total electrospinning time, the composite scaffold was subjected to a vapor of a mixture of hexane/THF (9:1 V/V) for 30 min to increase the bonding between the two layers. After that, the composite scaffolds were vacuum-dried for 3 days to remove the remaining solvent. Some of the scaffolds were sterilized with ethylene oxide for cell culture studies.

Characterization of scaffolds

The thickness of the top layer and bottom layer was measured with a micrometer. The morphology of the composite scaffold was examined using a scanning electron microscope (SEM, Philips XL30 FEG). The measurement of nano-fiber diameters was performed according to a previous report [22]. Fiber orientation was counted with a representative cross-section of composite scaffolds.

Cell seeding and culture

Human bone marrow-derived mesenchymal stem cells (hMSCs) were obtained from Lonza Walkersville, Inc. (Walkersville, MD). The cells were cultured according to the manual provided by the supplier. Scaffolds (3.6 mm in diameter and 1 mm in thickness) were soaked in 70% ethanol for 30 min, washed three times with PBS for 30 min each, and twice in complete medium for 2 hr each on an orbital shaker at 75 rpm. 2.5×105 cells were seeded into each scaffold from the side of phase-separated layer. To induce chondrogenesis, cell-seeded scaffolds were transferred to 15 ml polypropylene culture tubes and maintained in 0.5 ml chondrogenic medium supplemented with 10 ng/ml TGF-β1 (R&D Systems Inc., Minneapolis, MN). The medium was changed twice a week.

Histological observations

Constructs were washed in PBS, fixed with 3.7% formaldehyde in PBS overnight, dehydrated through a graded series of ethanol, embedded in paraffin, and sectioned at a thickness of 5 μm. For histological observations, sections were deparaffinized, rehydrated, and stained with hematoxylin-eosin or Alcian blue. For each layer, 2 areas were randomly selected and the cell numbers per area were counted. Cell orientation in the top electrospun layer was counted with a representative cross-section of constructs. For immunofluorescence staining of collage type II, rehydrated sections were pre-treated with

pepsin solution for 15 min, incubated with collage type II antibody at 1:100 dilutions for 1 hour, rinsed with PBS three times for 5 min each, then incubated with FITC-conjugated secondary antibody at 1:100 dilution for 1 hour. After rinsing three times with PBS, sections were mounted using mounting medium containing 4'-6-diamidino-2-phenylindole (DAPI) and observed under a fluorescence microscope.

Statistical analysis

For cell culture experiments, numerical values were reported as mean ±S.D. (n=3). To test the significance of observed differences between the study groups, the Student's *t*-test was applied. A value of $p < 0.05$ was considered to be statistically significant different.

Results

Morphological properties of composite scaffolds

A composite scaffold was designed with a top layer made using an electrospining technique and a bottom layer made using a temperature induced phase separation method combined with porogen (sugar sphere) templating and leaching, mimicking the architectural structures of articular cartilage superficial zone and middle zone. Fig.6.2A-C show the electrospun NF layers with different thickness (50 μm, 150 μm and 250 μm respectively) formed on a macro-porous phase separated bottom layer (pore size: 125-250 μm in diameter) under the conditions of 6wt/v% PLLA concentration and

various electrospinning times. With the increase of electrospinning time, the thickness of top electrospun NF layer increases. Fig.6.2D-E show a 50 μm thick electrospun NF layer formed on macro-porous phase-separated bottom layers with different pore sizes (250-425 μm and 425-600 μm in diameters respectively). The results demonstrated the formation of PLLA bilayered composite scaffolds with tunable macro-pore size of the bottom layer and thickness of the top layer. Fig.6.2F-G show the random shaped pore structure and NF morphology of electrospun top layer, and Fig.6.2H-I show the uniform macro-porous structure and NF morphology of the phase-separated bottom layer. The fiber diameters of this layer are in the range of 50-500nm.

Fig. 6.3 shows the NF layers electrospun from PLLA solutions with various polymer concentrations (Fig. 6.3A-3C, from 6wt/v% PLLA, Fig. 6.3D-3F, from 8wt/v% PLLA, Fig. 6.3G-3I, from 12wt/v% PLLA) formed on a macro-porous phase-separated bottom layer (pore size: 250-425μm in diameter). The average fiber diameters of electrospun NF layers increased with the increase of PLLA concentrations from 155nm (6wt/v% PLLA) to 1750nm (12wt/v% PLLA), listed in table 6.1. The average pore sizes in the electrospun NF layers also increased with the increase of PLLA concentration. The formation of beads was observed in the electrospun NF layers at 6wt/v% PLLA (Fig 3A-C), which is a common phenomenon that occurs when low polymer concentration solution is used to electrospin nanofiber mat due to its low viscosity [23]. Fig 6.3J showed that the majority of the electrospun fibers in top layer orientated parallel to the scaffold surface plane. The

top and bottom layers of the composite scaffolds have distinctive pore structures and fiber morphologies shown in both Fig.6.2. and Fig.6.3. The structural parameters of the two layers can be adjusted independently with their respective processing parameters.

Chondrogenesis of hBMSCs on composite scaffolds

The hBMSCs were seeded from the side of macro-porous phase-separated bottom layer. Then the scaffold was flipped over and the electrospun NF layer was positioned up during cell culture. The hBMSCs grew throughout the whole composite scaffolds after 2wk and 4wk of chondrogenic culture (Fig.4A-B) and an anisotropic distribution of cells and cell morphology developed. The cells in the electrospun top layer were more flattened compared to the more rounded shape of the cells in macro-porous phase-separated bottom layer. The top layer has higher cell density than bottom layer during the culture period (Fig.6.4C). Consistent with the more paralleled orientation of PLLA fibers in top layer, the cells were more aligned along the constructs surface plane (Fig.6.4D). Alcian blue staining (Fig.6.5A) and collagen type II immunofluorescence staining (Fig.6.5B) further showed the differentiated cells began to deposit cartilagous ECM into the scaffold more isotropically distributed in the bottom layer and an orientation more in parallel to the surface plane in the top layer.

Discussions

This study aims at reconstructing cartilage zonal structure by advanced scaffold design and subsequent modulation of the chondrogensis process of stem cells. Attempts to grow cartilage tissue with native zonal structure have been made by mimicking specific zonal cartilage separately on different specific hydrogel scaffolds [27], by creating spatial gradients of growth factor concentration [28], or scaffold chemical composition [29] inside scaffold, and by using different chondrocytes from different cartilage zones [30]. Chondrogenesis is a tightly controlled development event, involving multiple steps including condensation of mesenchymal stem cells, chondrogenic commitment, and differentiation into chondrocytes. Studies have showed that the phenotype of cells can be affected by the physical architecture of scaffolds [24-26]. However, few studies have applied this concept to establish the anisotropic zonal morphology of articular cartilage tissue in a single scaffold, due to the complexity of the structures.

In this study, we designed a NF composite scaffold to support chondogenic differentiation of hBMSCs and facilitated zonal development. The results were consistent with our earlier publication that NF matrix structures improved chondrogenic differentiation [18]. This novel bilayered composite scaffold system offers several advantages: the composite scaffolds were fabricated from one single biocompatible and biodegradable polymer PLLA, and the scaffolds were cultured with one single cell source, which simplified the fabrication and culture process. The scaffolds created a complex

zonal structural microenvironment for chondrogensis. The two layers of the scaffold were fabricated with different pore shape, pore size, fiber morphology, fiber diameter and fiber orientation to mimic the complex organization of cartilage ECM in superficial and middle zone respectively. Chondrocytes grew in the two scaffold layers showed different cell orientations. Chondrocytes in the electrospun top layer showed parallel orientation to the scaffold surface plane while chondrocytes in the bottom phase-separated layer showed random orientation. The chondrocytes in the two scaffold layers showed different cell morphology, with a more flattened cell morphology in the top layer and a more rounded morphology in the bottom layer. The cell densities in the two layers were also different, with a higher cell density observed in the top layer than in the bottom layer. Taken together, this anisotropic composite scaffold provides a new strategy in constructing complex zonal cartilage tissues. However, further implantation studies are needed to investigate the in vivo performance of the bilayered composite scaffolds.

Conclusion

We have developed anisotropic composite NF PLLA scaffolds with a electrospun NF top layer and a phase-separated macro-porous NF bottom layer. The top layer mimicked the cartilage superfacial zone with small pores and more parallel nano-fiber orientation. The bottom layer mimicked the cartilage middle zone with a macro-porous structure and more random nano-fiber orientation. In vitro chondrogenesis of human bone

marrow-derived mesenchymal stem cells study illustrated the promise of this anisotropic composite scaffold held in constructing complex zonal cartilage tissues.

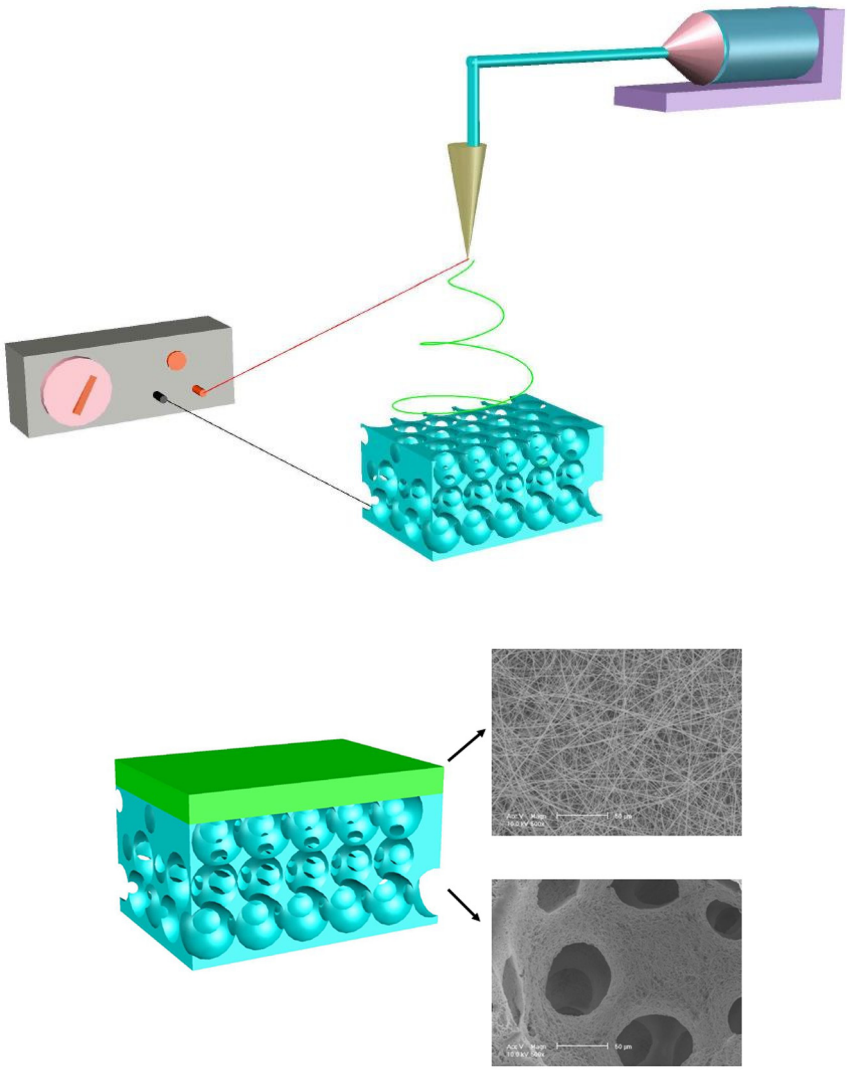

Fig.6.1. Schematic illustration of the design and fabrication of a nano-fibrous bilayer composite scaffold with a top electrospun layer and a bottom macro-porous phase separation layer that mimics the architecture of superfacial and middle zone layers of articular cartilage tissue.

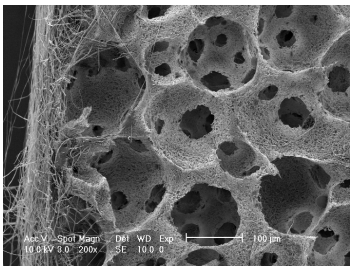

Fig. 2A

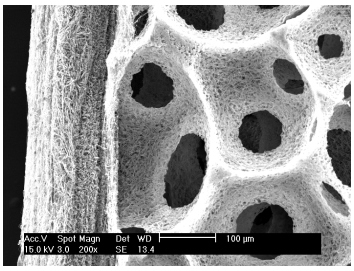

Fig. 2B

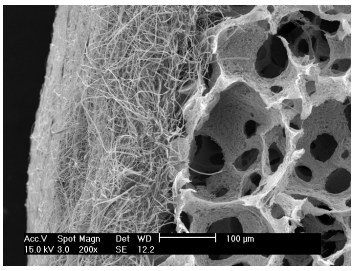

Fig. 2C

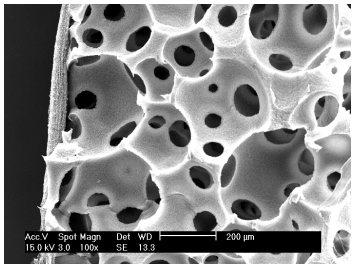

Fig. 2D

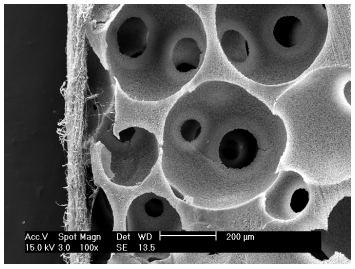

Fig. 2E

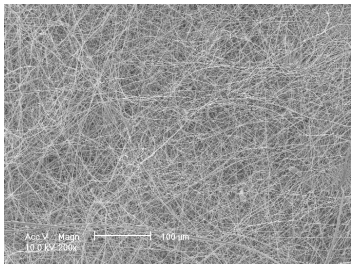

Fig. 2F

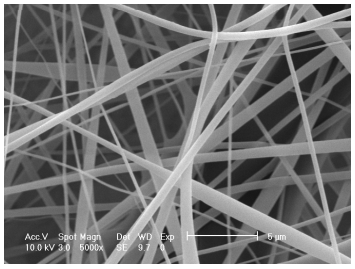

Fig. 2G

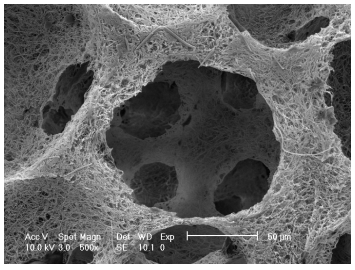

Fig. 2H

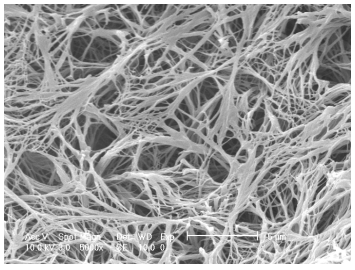

Fig. 2I

Fig.6.2. SEM micrographs of composite scaffolds with pre-designed bilayer features. (A-E) cross-section: phase-separated layer with small pore size (macro-pore size 125-250 μm) with a top electrospun layer of 50 μm (A), 150 μm (B) or 250 μm (C) thickness respectively; phase-separated layer with medium pore size (macro-pore size 250-425 μm) (D) or phase-separated layer with large-pore size (macro-pore size 425-600 μm) (E) with a top electrospun layer of 50 μm thickness. The nano-fibous matrix structure of electrospun layer (F, G) and phase-separated layer with small pore size (H, I) observed with different magnifications. The electrospun layers were fabricated from 8% PLLA solution.

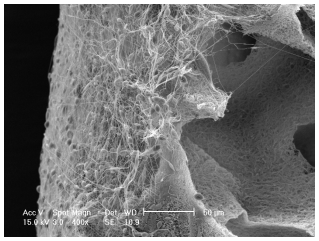

Fig. 3A

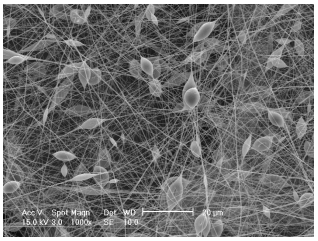

Fig. 3B

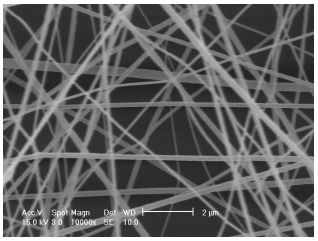

Fig. 3C

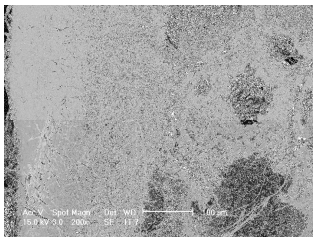

Fig. 3D

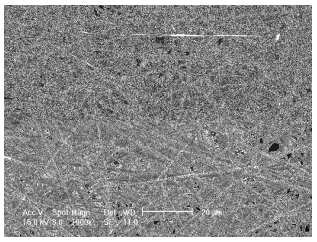

Fig. 3E

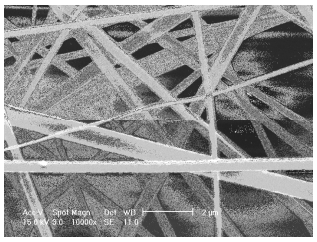

Fig. 3F

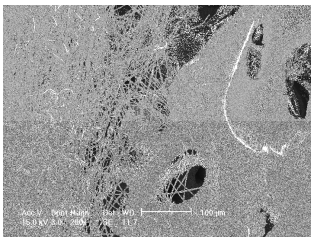

Fig. 3G

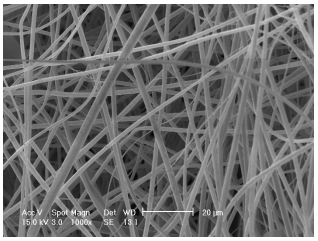

Fig. 3H

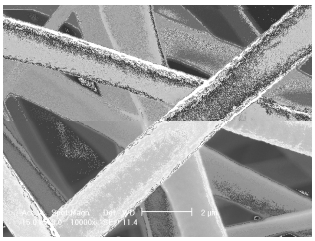

Fig. 3I

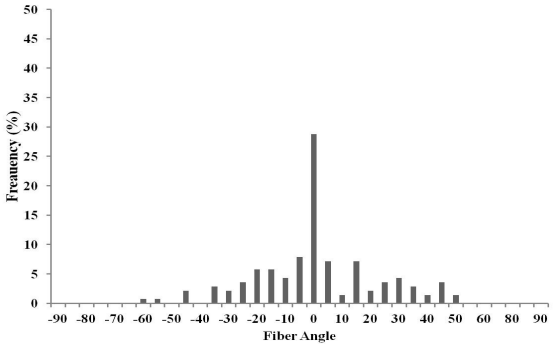

Fig 3J

Fig.6.3. SEM micrographs of cross-section of composite scaffolds with a top electrospun layer of different fiber diameters on a medium-pore phase separation layer (250-425 μm). (A-C) electrospun layer with small fiber diameter generated from 6% PLLA solution; Fig 3C was chosen from a bead-free area to show fiber diameter (D-F) electrospun layer with medium fiber diameter generated from 8% PLLA solution; (G-I) electrospun layer with large fiber diameter generated from 12% PLLA solution. (J) Fiber orientation distribution of medium fiber diameter electrospun layer (8%) to the composite scaffold surface plane. The fiber angle was defined as an angle between fiber and the scaffold surface plane. Fibers having zero degree fiber angle are oriented parallel to the scaffold surface plane. Fiber orientation distribution of medium fiber diameter electrospun layer to the composite scaffold surface plane.

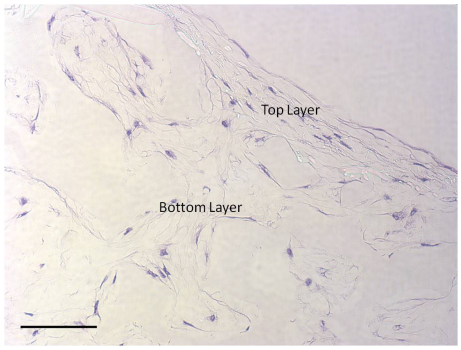

Fig. 4A

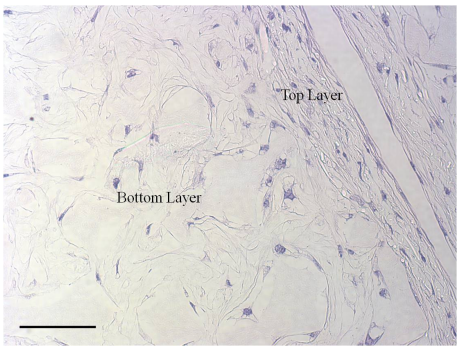

Fig. 4B

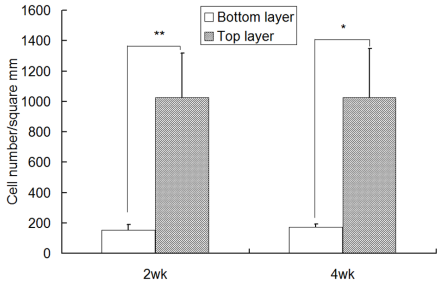

Fig. 4C

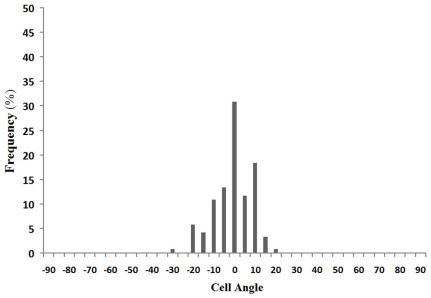

Fig. 4D

Fig.6.4. H-E staining of composite scaffolds after 2wk (A) and 4wk (B) of in vitro chondrogenic culture. (C) Quantification of cell numbers in top electrospun layer and bottom phase-separated layer of composite scaffolds. (D) Cell orientation distribution inside the top layer. The cell angle was defined as an angle between cell and scaffold surface plane. Cells having zero degree fiber angle are oriented parallel to the scaffold surface plane. Scale bar: 100 μm. *$p<0.05$, ** $p<0.01$.

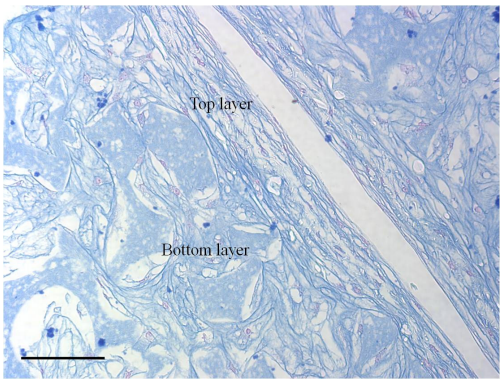

Fig. 5A

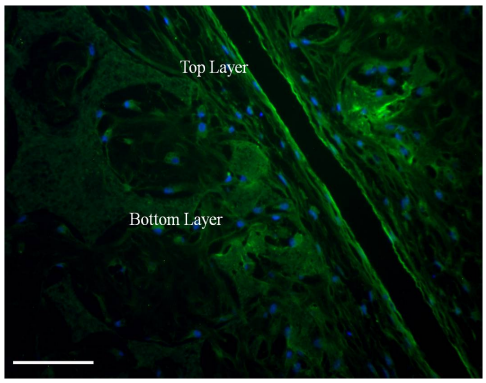

Fig. 5B

Fig.6.5. Alcian blue staining (A) and Collagen type II immunofluorescence staining (B) of cell-scaffold constructs after 4wk of in vitro chondrogenic culture. Green: Collagen type II; blue: nuclei. Scale bar: 100 μm

Table 6.1 Fiber diameters of electrospun layer generated with different PLLA concentrations

PLLA concentration	Fiber diameter(nm)
6%	155±65
8%	720±250
12%	1750±570

References

1. Moss ML, Moss-Salentijin, L: Vertebrate cartilages. In: *Cartilage Structure, Function and Biochemistry.* Edited by Hall BK. New York: Academic Press; 1983: 1-30.

2. Temenoff JS, Mikos AG: Review: tissue engineering for regeneration of articular cartilage. *Biomaterials* 2000, 21(5):431-440.

3. Hunziker EB: Articular cartilage repair: problems and perspectives. *Biorheology FIELD Full Journal Title:Biorheology* 2000, 37(1-2):163-164.

4. Silver FH, Glasgold AI: Cartilage wound healing. An overview. *Otolaryngol Clin North Am FIELD Full Journal Title:Otolaryngologic clinics of North America* 1995, 28(5):847-864.

5. O'Driscoll SW: The healing and regeneration of articular cartilage. *Journal of Bone and Joint Surgery-American Volume* 1998, 80A(12):1795-1812.

6. Peretti GM, Xu JW, Bonassar LJ, Kirchhoff CH, Yaremchuk MJ, Randolph MA: Review of injectable cartilage engineering using fibrin gel in mice and swine models. *Tissue Eng* 2006, 12(5):1151-1168.

7. Brittberg M, Lindahl A, Nilsson A, Ohlsson C, Isaksson O, Peterson L: Treatment of Deep Cartilage Defects in the Knee with Autologous Chondrocyte Transplantation. *New England Journal of Medicine* 1994, 331(14):889-895.

8. Langer R, Vacanti JP: Tissue Engineering. *Science* 1993, 260(5110):920-926.

9. Hutmacher DW: Scaffolds in tissue engineering bone and cartilage. *Biomaterials* 2000, 21(24):2529-2543.

10. Keeney M, Lai JH, Yang F: Recent progress in cartilage tissue engineering. *Curr Opin Biotechnol* 2011, 22(5):734-740.

11. Makris EA, Hadidi P, Athanasiou KA: The knee meniscus: Structure-function, pathophysiology, current repair techniques, and prospects for regeneration. *Biomaterials* 2011, 32(30):7411-7431.

12. Gong YH, He LJ, Li J, Zhou QL, Ma ZW, Gao CY, Shen JC: Hydrogel-filled polylactide porous scaffolds for cartilage tissue engineering. *Journal of*

Biomedical Materials Research Part B-Applied Biomaterials 2007, 82B(1):192-204.

13. Peppas NA, Hilt JZ, Khademhosseini A, Langer R: Hydrogels in biology and medicine: From molecular principles to bionanotechnology. *Advanced Materials* 2006, 18(11):1345-1360.

14. Drury JL, Mooney DJ: Hydrogels for tissue engineering: scaffold design variables and applications. *Biomaterials* 2003, 24(24):4337-4351.

15. DeForest CA, Polizzotti BD, Anseth KS: Sequential click reactions for synthesizing and patterning three-dimensional cell microenvironments. *Nature Materials* 2009, 8(8):659-664.

16. Deng Y, Zhao K, Zhang XF, Hu P, Chen GQ: Study on the three-dimensional proliferation of rabbit articular cartilage-derived chondrocytes on polyhydroxyalkanoate scaffolds. *Biomaterials* 2002, 23(20):4049-4056.

17. Li WJ, Tuli R, Okafor C, Derfoul A, Danielson KG, Hall DJ, Tuan RS: A three-dimensional nanofibrous scaffold for cartilage tissue engineering using human mesenchymal stem cells. *Biomaterials* 2005, 26(6):599-609.

18. Hu J, Feng K, Liu XH, Ma PX: Chondrogenic and osteogenic differentiations of human bone marrow-derived mesenchymal stem cells on a nanofibrous scaffold with designed pore network. *Biomaterials* 2009, 30(28):5061-5067.

19. Feng K, Ma P.X.: Nanostructured biomaterials for tissue engineering. In: *Translational Approaches in Tissue Engineering and Regenerative Medicine.* Edited by Mao J. Boston: Artech House; 2008: 311-324.

20. Lee J, Tae G, Kim YH, Park IS, Kim SH, Kim SH: The effect of gelatin incorporation into electrospun poly(L-lactide-co-epsilon-caprolactone) fibers on mechanical properties and cytocompatibility. *Biomaterials* 2008, 29(12):1872-1879.

21. Wei GB, Ma PX: Macroporous and nanofibrous polymer scaffolds and polymer/bone-like apatite composite scaffolds generated by sugar spheres. *J Biomed Mater Res Part A* 2006, 78A(2):306-315.

22. Ma PX, Zhang RY: Synthetic nano-scale fibrous extracellular matrix. *J Biomed Mater Res* 1999, 46(1):60-72.

23. Fong H, Reneker DH: Elastomeric nanofibers of styrene-butadiene-styrene triblock copolymer. *J Polym Sci Pt B-Polym Phys* 1999, 37(24):3488-3493.

24. Nguyen LH, Kudva AK, Guckert NL, Linse KD, Roy K: Unique biomaterial compositions direct bone marrow stem cells into specific chondrocytic phenotypes corresponding to the various zones of articular cartilage. *Biomaterials* 2011, 32(5):1327-1338.

25. Grayson WL, Bhumiratana S, Chao PHG, Hung CT, Vunjak-Novakovic G: Spatial regulation of human mesenchymal stem cell differentiation in engineered osteochondral constructs: effects of pre-differentiation, soluble factors and medium perfusion. *Osteoarthritis Cartilage* 2010, 18(5):714-723.

26. Erisken C, Kalyon DM, Wang HJ: Functionally graded electrospun polycaprolactone and beta-tricalcium phosphate nanocomposites for tissue engineering applications. *Biomaterials* 2008, 29(30):4065-4073.

27. Sharma B, Williams CG, Kim TK, Sun DN, Malik A, Khan M, Leong K, Elisseeff JH: Designing zonal organization into tissue-engineered cartilage. *Tissue Eng* 2007, 13(2):405-414.

28. Bratt-Leal AM, Carpenedo RL, Ungrin MD, Zandstra PW, McDevitt TC: Incorporation of biomaterials in multicellular aggregates modulates pluripotent stem cell differentiation. *Biomaterials* 2011, 32(1):48-56.

29. Engler AJ, Sen S, Sweeney HL, Discher DE: Matrix elasticity directs stem cell lineage specification. *Cell* 2006, 126(4):677-689.

30. Levenberg S, Huang NF, Lavik E, Rogers AB, Itskovitz-Eldor J, Langer R: Differentiation of human embryonic stem cells on three-dimensional polymer scaffolds. *Proc Natl Acad Sci U S A* 2003, 100(22):12741-12746.

Chapter 7

Conclusions and suggestions for future research

Conclusions

In this thesis, the fabrication of bioactive nanofibrous PLLA scaffolds and their tissue engineering applications have been explored, including inhibiting bacterial growth, promoting angiogenesis, chondrogenesis, and osteogenesis.

In the first study, a three-dimensional (3-D) porous tissue engineering scaffold was developed with the ability to release antibiotics in a controlled fashion for long-term inhibition of bacterial growth. The highly soluble antibiotic drug, doxycycline (DOXY), was successfully incorporated into PLGA nanospheres using a modified water-in-oil-in-oil (w/o/o) emulsion method. The PLGA nanospheres (NS) were then incorporated into prefabricated nanofibrous PLLA scaffolds with a well interconnected macro-porous structure. The release kinetics of DOXY from four different PLGA NS formulations on a PLLA scaffold was investigated. DOXY could be released from the NS-scaffolds in a locally and temporally controlled manner. The DOXY release is controlled by DOXY diffusion out of the NS and is strongly dependent upon the physical and chemical properties of the PLGA. While PLGA50-6.5K, PLGA50-64K, and PLGA75-113K NS-scaffolds discharge DOXY rapidly with a high initial burst release, PLGA85-142K NS-

scaffold can extend the release of DOXY to longer than 6 weeks with a low initial burst release. Compared to NS alone, the NS incorporated on a 3-D scaffold significantly reduced the initial burst release. In vitro antibacterial tests of PLGA85 NS-scaffold demonstrated its ability to inhibit common bacterial growth (S. aureus and E. coli) for a prolonged duration.

Next, we developed novel tissue engineering scaffolds capable of serving as both a three-dimensional (3-D) substrate and a localized and temporally controlled delivery vehicle for an angiogenic factor, basic fibroblast growth factor (bFGF) to promote cellular activity and stimulate tissue neogenesis. bFGF was first encapsulated into poly(lactic-co-glycolic acid) (PLGA) nanospheres (NS) with a double emulsion method and then seeded onto a 3-D scaffold. In vitro release results showed that bFGF nanospheres incorporated scaffold (NS-scaffold) released bFGF in a temporally controlled fashion, which was mainly determined by the chemical and degradation properties of the bFGF-containing NS. Results from subcutaneous implantation into mice after 4, 7 and 14 days indicated that bFGF released from NS-scaffolds preserved its bioactivity, improved cell penetration into scaffolds, and enhanced neovascularization. Passive adsorption of bFGF onto the scaffold did not show such positive effects. Results from subcutaneous implantation of scaffolds with different PLGA polymer nanospheres and with different bFGF dosages into mice after 7 days also indicated that bFGF's function depended on its release profile and dosage. The cell penetration and neovascularization inside the scaffolds within 7 days were improved with the increase of bFGF release rate and dosage (up to the optimal dosage).

Then, we developed a novel PLLA nanofibrous scaffold which can achieve localized dual release of BMP-7 and PDGF in a controlled fashion with distinct dosages and release kinetics. Both ectopic bone formation and periodontal fenestration defect regeneration on these scaffolds were significantly improved over a single release system. The improvement was dependent on the dosages, dosage ratio and the release kinetics of the two individual growth factors. This nanofibrous scaffold with its controlled multiple growth factor delivery capacity can likely be applied to the regeneration of various large sized tissue defects.

Last, an anisotropic composite scaffold was fabricated with an upper layer mimicking the cartilage superficial zone and a lower layer mimicking the cartilage middle zone. The thin superficial layer was fabricated using an electrospinning technique to support high density cell growth and more parallel ECM orientation. The lower layer was fabricated using a phase-separation technique combined with a porogen templating technique to support low density cell growth and a more isotropic ECM orientation. *In vitro* chondrogenesis of human bone marrow-derived mesenchymal stem cells (hMSCs) study illustrated the promising application of the composite scaffold to direct the formation of an anisotropic tissue structure that resembles the natural articular cartilage superficial and middle zones.

Future work

There are a number of interesting future directions this research could lead to. This thesis has already showed that nanofibrous PLLA scaffolds with the dual release of BMP-7 and PDGF could synergistically promote neo-bone formation and periodontal defect repair than scaffold with the release of either growth factor alone. It would be

interesting to apply this BMP-7 and PDGF dual release bioactive scaffold system to other bigger bone defect models.

This thesis also showed that nanofibrous PLLA scaffold with the introduction of controlled release of doxycycline could inhibit bacterial growth over a prolonged time period. It would be of interest to combine three biological factor (BMP, PDGF, doxycycline) release systems into PLLA scaffolds. PDGF is capable to promote angiogenesis, BMP-7 is capable to promote osteogenesis and doxycycline is capable to inhibit both bacterial infection and matrix metalloproteinases (MMPs). These three factors with suitable individual release profiles and dosages from PLLA nanofibrous scaffolds could function synergistically and result in improved bone regeneration in defects.

Additionally, this thesis showed that an anisotropic composite scaffold fabricated using the combination of electrospinning and phase separation techniques could mimic the zonal structure of cartilage. The composite scaffold can be further examined for cartilage tissue regeneration using animal models. With further improvement on the fabrication technologies, the composite concept could be extended to regenerate more complex tissues such as osteochondral interface structure.